ANL-6629
Reactor Technology
(TID-4500, 18th Ed.)
AEC Research and
Development Report

ARGONNE NATIONAL LABORATORY
9700 South Cass Avenue
Argonne, Illinois

CORE A CRITICAL STUDIES FOR THE ENRICO FERMI ATOMIC POWER PLANT ON ZPR-III

by

C. E. Branyan*

*On loan to Idaho Division from Atomic Power Development Associates, Inc. during Fermi Critical Studies Program

October 1962

Operated by The University of Chicago
under
Contract W-31-109-eng-38
with the
U. S. Atomic Energy Commission

DISCLAIMER

This report was prepared as an account of work sponsored by an agency of the United States Government. Neither the United States Government nor any agency Thereof, nor any of their employees, makes any warranty, express or implied, or assumes any legal liability or responsibility for the accuracy, completeness, or usefulness of any information, apparatus, product, or process disclosed, or represents that its use would not infringe privately owned rights. Reference herein to any specific commercial product, process, or service by trade name, trademark, manufacturer, or otherwise does not necessarily constitute or imply its endorsement, recommendation, or favoring by the United States Government or any agency thereof. The views and opinions of authors expressed herein do not necessarily state or reflect those of the United States Government or any agency thereof.

DISCLAIMER

Portions of this document may be illegible in electronic image products. Images are produced from the best available original document.

TABLE OF CONTENTS

TABLE OF CONTENTS

TABLE OF CONTENTS

LIST OF FIGURES

LIST OF FIGURES

LIST OF FIGURES

LIST OF FIGURES

LIST OF TABLES

LIST OF TABLES

CORE A CRITICAL STUDIES FOR THE ENRICO FERMI ATOMIC POWER PLANT ON ZPR-III

by

C. E. Branyan

ABSTRACT

A critical studies program for the Enrico Fermi Atomic Power Plant was run with the ZPR-III fast critical facility by the Idaho Division of Argonne National Laboratory at the National Reactor Testing Station in Idaho.

The objectives of this program included determination of the uranium enrichment required for criticality, the effect of minor variations in core and blanket composition, reactivity coefficients, control and safety rod characteristics, power distribution, spectral indices, and the reactivity worth and wave shape of the oscillator rod.

The experimental program was separated into two phases. The first phase involved investigations of a clean assembly, which was a simplified and homogenized core and blanket geometry constructed for ease of experimental manipulation and analysis. The second phase involved experiments on the engineered, or "as-designed," core. This assembly included such engineering details as control and safety rod channels, core end gaps, and a precise reconstruction of the core outline. This provided detailed information on worths of control rods and fuel subassemblies, power distribution, and the effect of variations in core and end-gap dimensions.

The application of critical experiment data to the determination of the Enrico Fermi reactor characteristics has established the U^{235} enrichment for the fuel alloy, worths of fuel subassemblies, and the B^{10} enrichment for the control and safety rods. In addition, material-substitution experiments and fuel-worth measurements have provided the parametric data for the determination of the net temperature coefficient of the Enrico Fermi reactor.

I. INTRODUCTION

The Enrico Fermi Atomic Power Plant is a sodium-cooled fast breeder reactor with intermediate sodium loops, sodium-to-water steam generators, and an associated steam-driven turbine-generator. The reactor and steam-generating portions of the plant have been designed by the Atomic Power Development Associates, Inc., (APDA) and are owned and operated by the Power Reactor Development Company. The Enrico Fermi Atomic Power Plant is located at Lagoona Beach on Lake Erie, approximately 30 miles southwest of Detroit near Monroe, Michigan. Steam produced will be purchased by The Detroit Edison Company for the production of electricity in the adjacent Detroit Edison turbine-generator facility for distribution in the southeastern area of Michigan.

A contract, effective January 1, 1957, between the Power Reactor Development Company and the U.S. Atomic Energy Commission,[1] included provisions for a critical experimental program for the Enrico Fermi reactor to be carried out by the Atomic Energy Commission. This program was conducted with Zero Power Reactor (ZPR-III), Argonne National Laboratory's fast critical facility, located at the National Reactor Testing Station in Idaho. During the course of the experimental work, two APDA personnel were assigned to the ZPR-III facility. This report covers the work done in this program.

II. DESCRIPTION OF THE ENRICO FERMI REACTOR[2,3]

The reactor portion of the Enrico Fermi Atomic Power Plant is a sodium-cooled fast breeder reactor containing U^{235}-enriched uranium in 10 w/o molybdenum alloy fuel pins in subassemblies having a square cross section. The core subassemblies have an upper and lower reflector section of depleted uranium-molybdenum alloy. Additional reflector subassemblies of depleted uranium-molybdenum surround the core radially to produce a fully reflected core. These reflector regions are commonly referred to as the axial and radial blankets. A perspective view of the reactor and associated control and fuel-handling mechanisms is shown in Fig. 1. The core and blanket subassemblies are spaced on matrices of 2.693-in.-square cross section, so that the whole approximates a right circular cylinder, 79 in. in diameter and 69 in. high. The core, containing the enriched fuel alloy, approximates a right circular cylinder 30.5 in. in diameter and 30.5 in. high.

The reactor components are shown diagrammatically in Fig. 2. The core region consists of the central fuel portion of 91 subassemblies plus 10 control-element channels. The fuel is in the form of partially enriched uranium-molybdenum alloy pins, 0.148 in. in diameter and 30.95 in. long, clad by co-extrusion with 0.005 in. of zirconium to produce

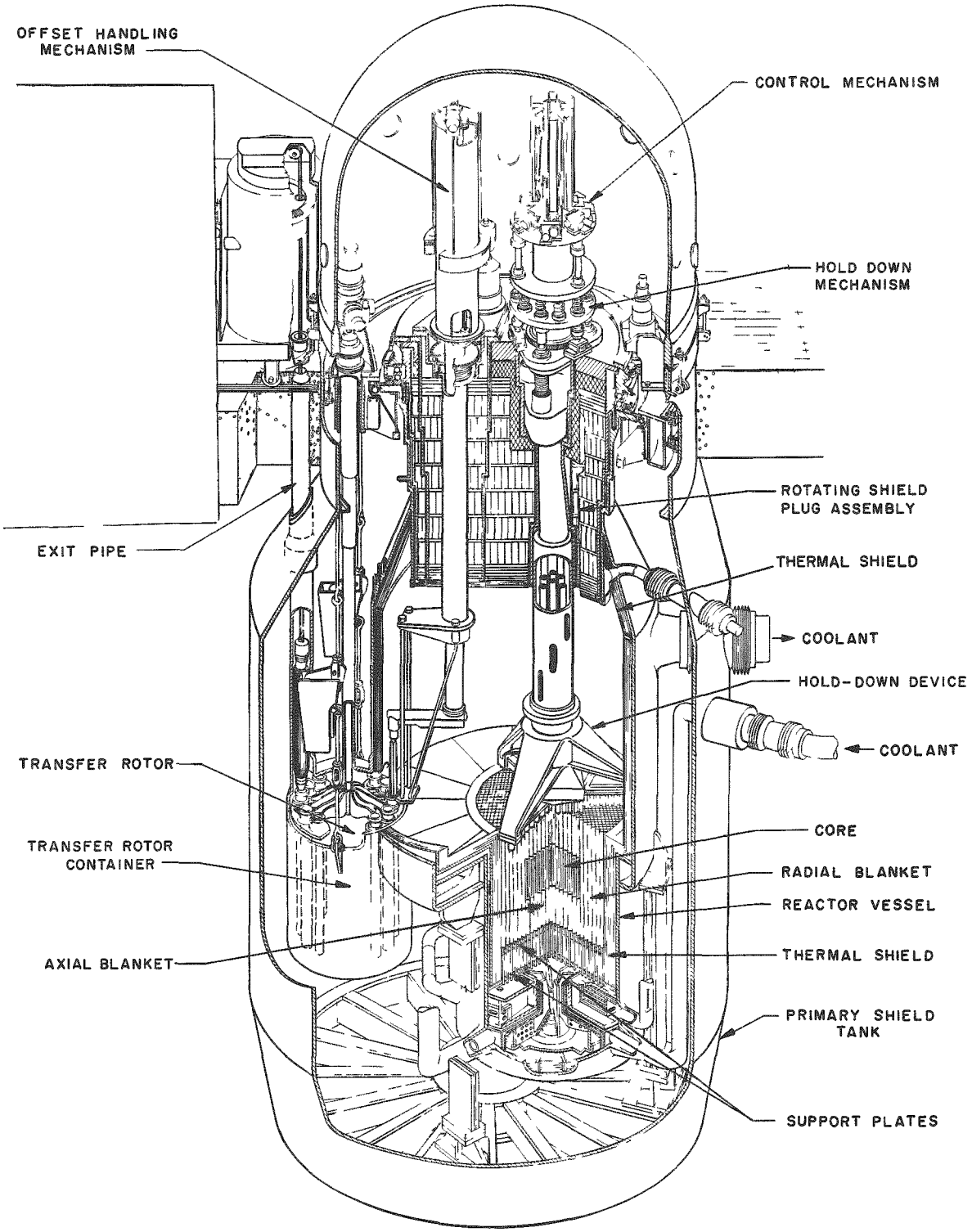

Fig 1 Perspective View of Enrico Fermi Reactor

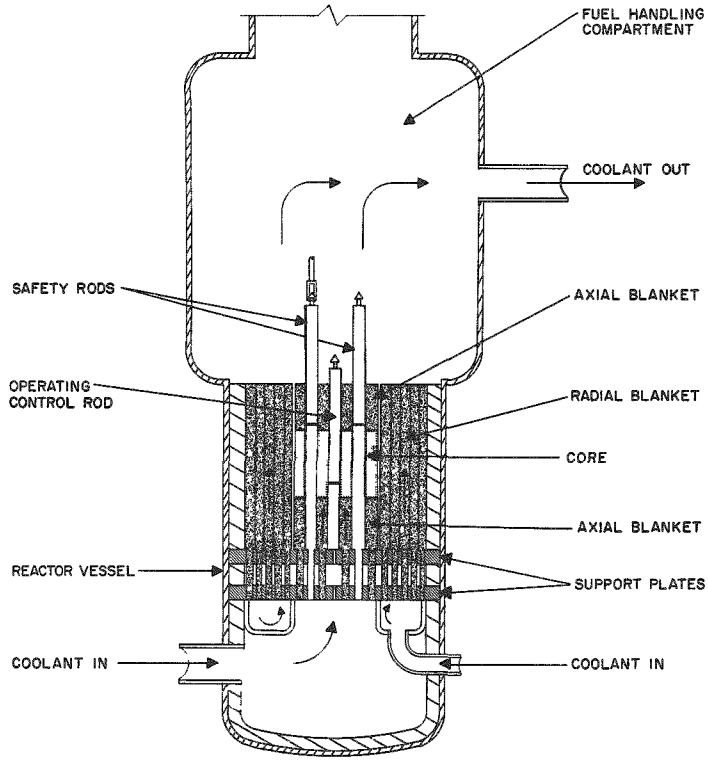

Fig. 2

Fermi Reactor Arrangement

a pin OD of 0.158 in. The fuel pins are arranged in the subassembly on a 0.199-in.-square matrix. Since both ends of the fuel alloy within the pin are swaged to a tapered point over a $\frac{1}{2}$-in. length at either end, an average uniform length of 30.50 in. has been assumed for the purposes of the experimental program. The axial blanket portions of the 91 core subassemblies and the remaining 548 radial blanket subassemblies consist of stainless steel-clad, depleted uranium-molybdenum alloy in the form of 0.443-in.-OD cylindrical rods on a 0.483-in.-square matrix. Plutonium is produced in both the core and blanket. Figure 3 is a cross section of the reactor showing the arrangement of the core and blanket subassemblies and the control element channels.

Boron carbide poison rods in the core provide both regulating and safety control. Regulation is accomplished by two boron carbide rods located near the radial center of the reactor operating over a limited vertical stroke from core center to core edge. Eight safety, or shutdown, boron carbide rods are situated at about half-radius of the core and are fully withdrawn to a point above the upper axial blanket during reactor operation. Rapid shutdown is accomplished by dropping the eight safety rods into the core with an initial spring-assisted acceleration.

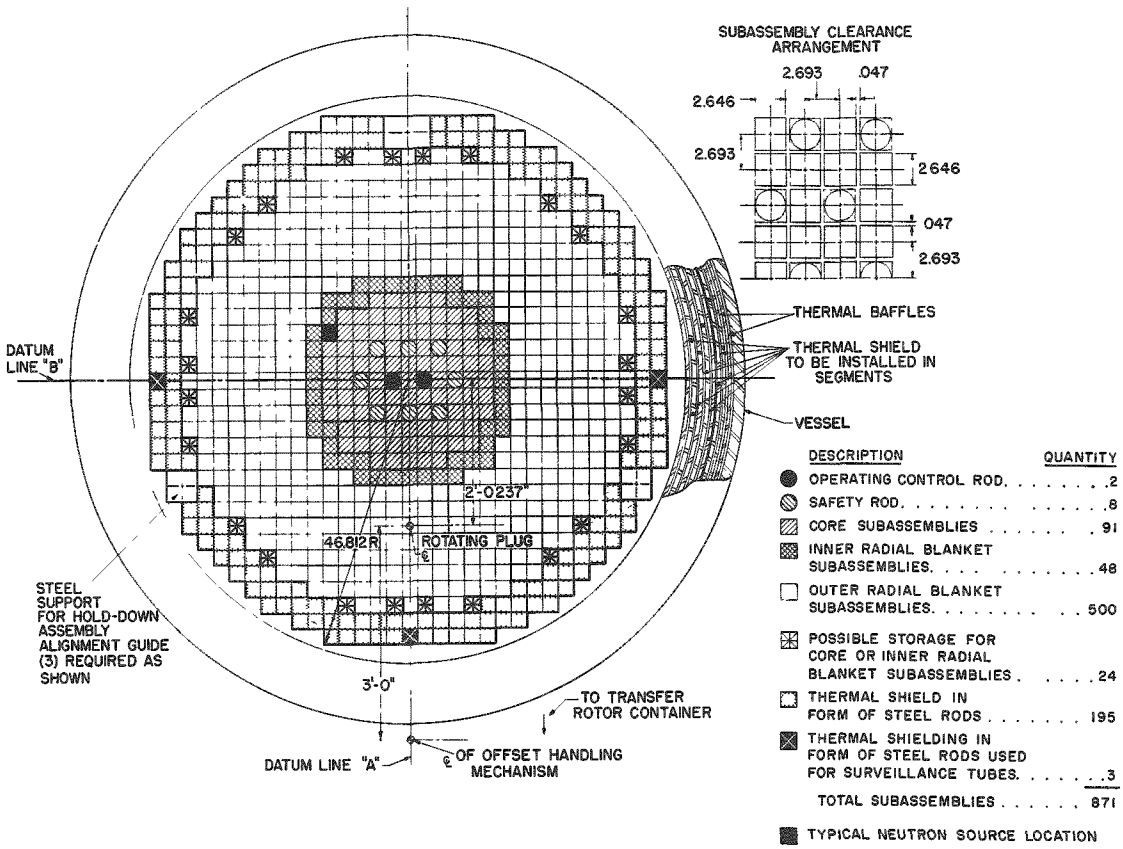

Fig. 3. Fermi Reactor Cross Section

III. DESCRIPTION OF ZPR-III[4,5,6]

The ZPR-III is a fast critical reactor facility constructed and operated by Argonne National Laboratory for the U.S. Atomic Energy Commission at the National Reactor Testing Station in Idaho. The ZPR-III machine is built in two halves, one of which is movable. Each half consists of 961 square tubes, each 2.18 in. on a side and 33 in. long. These tubes are stacked in an array 31 rows high and 31 columns wide to form a square matrix approximately 67 by 67 in., constrained in position by means of I-beam clamps fastened to the platforms. The matrix tubes commonly used are made of stainless steel, but an alternative aluminum set may be substituted. The stainless steel matrix tube array was used throughout the critical experimental program for the Enrico Fermi reactor. The movable half of the machine allows the critical assembly to be separated as a safety measure and for convenience in loading and unloading. Figure 4 shows these features of the machine.

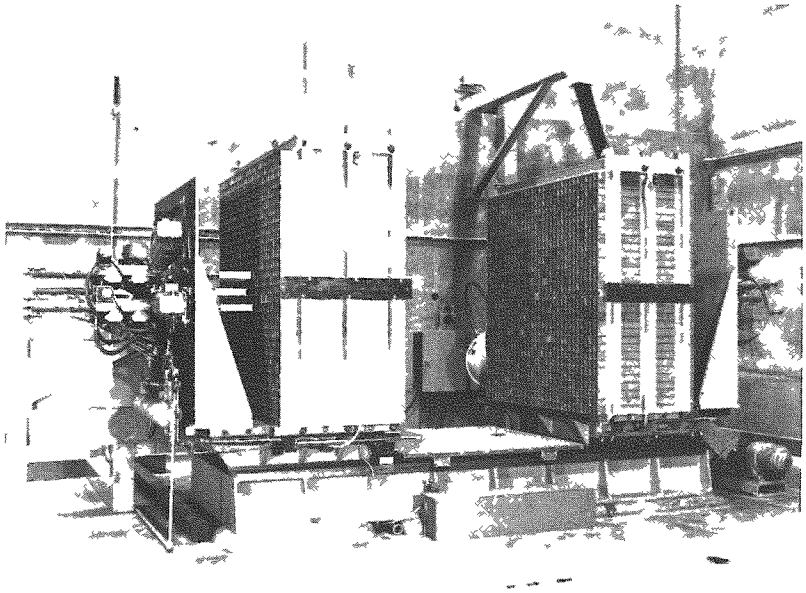

Fig. 4

ZPR-III Critical Assembly Machine

Drawers containing any combination of fissionable, structural, and simulated or canned coolant materials may be inserted into the matrix tubes, thus building a configuration of the desired shape and composition. The drawers themselves are made of aluminum or stainless steel, perforated to reduce density A drawer loaded with typical materials is shown in Fig. 5 A 16-finger steel leaf spring is inserted at the end of

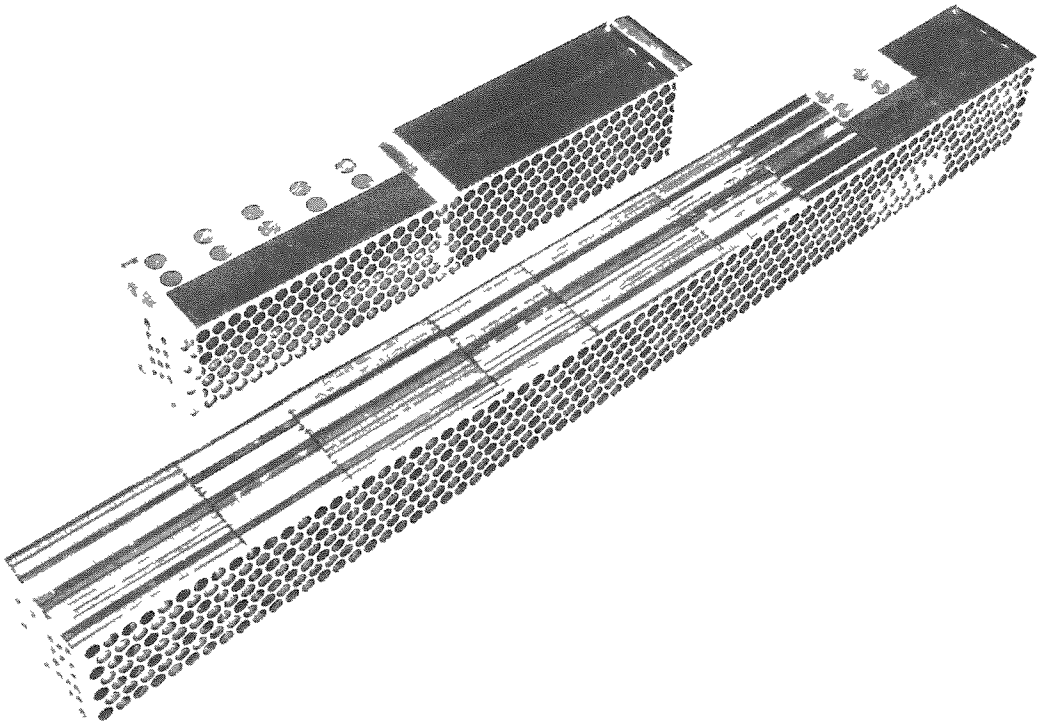

Fig 5 Photograph of Typical ZPR-III Clean Core and Back Blanket Drawer Loadings

each drawer opposite the assembly interface to produce a compact array of materials; the spring allows for axial expansion in the event of an extreme power transient. Stainless steel drawers used for the Fermi critical experiments were 21.25 in. long; thus, the $\frac{3}{16}$-in. spring gap was well removed from the axial ends of the core, which occurred at 15 and 15.5 in. from the assembly interface.

The control and safety mechanisms of the critical assembly consist of 10 stainless steel drawers and drive extensions attached through magnetic clutches to drive motors. The forward portion of these drawers is normally filled with core material. The drawers are driven into the reactor to add reactivity. For rapid shutdown, the magnetic clutches are released, whereupon the control and safety rods are rapidly forced out of the reactor by compressed air.

The combinations of materials and shapes which can be assembled in the machine are extensive. The materials most commonly used are uranium enriched to the extent of 93.2 per cent U^{235}, depleted uranium containing approximately 0.2 per cent U^{235}, natural uranium, stainless steel and zirconium to represent the structural materials of fast reactors, full- and reduced-density aluminum to represent the liquid-metal coolant, and a limited amount of sodium canned in stainless steel. Limited quantities of natural and B^{10}-enriched boron carbide, graphite, and aluminum oxide are available. Samples of many other elements are also available for reactivity coefficient measurements. Most of the materials are in the form of $\frac{1}{8}$-in.-thick plates, 2 in. wide and 1, 2, or 3 in. long. Aluminum is available with perforations approximately $\frac{3}{8}$ in. in diameter, spaced to reduce the density to 63, 56, or 45 per cent of normal. Arranged in the drawers, these materials can simulate a wide variety of fast reactor compositions. The plates are color-coded and normally are loaded in a drawer with the 2-in. dimension vertical to facilitate complete identification of the materials, as shown in Fig. 5.

The neutron instrumentation for the ZPR-III is conventional, although adapted to the low levels of fast-neutron flux involved. Three safety channels with adjustable power level trips, 2 period channels set to trip at 15-sec periods, and 2 recording power-level channels without trips all operate from sensitive ion chambers. Proportional counters, fission counters, and other instruments are used as required in particular experiments. Two retractable polonium-beryllium neutron sources, one in each half of the assembly, are used to insure an adequate neutron flux for startup. Once criticality has been attained, the sources are remotely withdrawn from the reactor to reduce their contribution to the self-sustaining neutron population and for accurate reactivity measurements at the low operating levels involved. After the two halves are loaded manually, the assembly is driven together remotely from behind a 5-ft concrete wall and the necessary measurements of reactivity, etc., obtained. Operating power levels of 0.01 to 10 w are normal.

IV. CRITICAL STUDIES PROGRAM FOR THE ENRICO FERMI REACTOR

A critical studies program for the Enrico Fermi Atomic Power Plant was developed by the Atomic Power Development Associates, Inc., in co-operation with Argonne National Laboratory.(7) This program served as a basis for the experimental work with ZPR-III. The objectives of this program were as follows:

1. to obtain the enrichment required for criticality with a fixed core composition and geometry;
2. to obtain the reactivity effects of a variety of minor size and composition variations in core and blanket;
3. to obtain the reactivity coefficients of various materials in the core and blanket, and to determine the nuclear equivalence between sodium and the aluminum used as a sodium mockup in the critical experiments;
4. to obtain a variety of operational data such as: power distribution, reactivity worths of core versus blanket subassemblies or sodium, and the total and rotational reactivity worths of a boron carbide oscillator rod; and
5. to obtain the necessary B^{10} enrichment and worth characteristics of the boron carbide control and safety rods having a fixed composition and geometry.

In addition to the above objectives, a series of "meltdown" configurations was also to be investigated.(8) These experiments were included to determine criticality and material worths for various hypothetical configurations resulting from assumed accident situations in which the fuel melts and subsequently freezes or otherwise accumulates. This portion of the experimental program has been covered in a separate report(9) and analyzed by others.(10,11)

The experimental program was divided into two primary phases. The first phase involved the construction of a "clean" or homogenized cylindrical core having the same volume and average composition as the Enrico Fermi reactor, but with the control and safety rod channel voids averaged over the entire core region. Also, both the radial and axial blanket or reflector regions were constructed to have a uniform composition corresponding to that of the radial blanket of the Fermi design. This simplified loading was primarily intended to present a simple, two-region system to facilitate analysis of the data obtained. Experiments with the clean core included determination of average density effects on reactivity for the various core and blanket materials, including zirconium, molybdenum, stainless steel, sodium, U^{238}, and U^{235}. These results allowed

minor reactivity corrections to be applied to the critical mass of the engineering core to compensate for the unavoidable mass differences between the engineering critical and the Fermi core design. The density effect on reactivity of aluminum, utilized as a mockup for sodium, was also determined. By means of small samples of Pu^{239}, U^{235}, and B^{10}-enriched and natural boron carbide, reactivity coefficients were also obtained at space points in the core and blanket. Additional experiments were included to determine the heterogeneity introduced by using $\frac{1}{8}$-in.-thick plates of depleted and highly enriched uranium to simulate the fuel alloy pins of lower enrichment uranium in the engineering design.

The second phase of the experimental program involved the detailed assembly of the engineering dimensions and compositions of the core, control, and safety rod channels, core end gaps, and axial blankets of lower density. This engineering design loading, together with the results of the preceding clean-core experiments, provided the data necessary to establish the final enrichment for the Fermi fuel alloy. The engineering core critical also provided additional design and operation information, including B^{10} enrichment, reactivity, and power distribution effects of the control and safety rods, the effects of the addition of fuel subassemblies at the edge of the core, and a measure of the axial expansion coefficient by an effective lengthening of the core.

V. CLEAN-CORE EXPERIMENTS

A. Description of the Enrico Fermi Reactor Core and Blanket

The Enrico Fermi reactor core consists of 91 fuel subassemblies and 10 control and safety rod channels. The inner radial blanket region contains 48 blanket subassemblies which may be replaced with fuel subassemblies. The outer radial blanket contains 500 blanket subassemblies with 24 fuel-storage positions at its outer periphery. The core and blanket subassemblies are square in cross section and are spaced on a 2.693-in.-square matrix (see Fig. 3). The geometry is approximately cylindrical, with an equivalent radius of 15.25 in. for the core and 39.40 in. for the radial blanket. The core is 30.95 in. high. The average uniform height was taken as 30.50 in., the same as that of the fuel pins noted in Section II. Fourteen-in.-long upper and lower axial blanket regions are separated from the core by a 3.713-in. upper axial end gap and a 5.963-in. lower axial end gap. These axial end gap regions are composed of end caps, support grids, and sodium plenum regions. The dimensions of the various regions of the Fermi fuel subassembly are shown in Fig. 6. The compositions of these regions are given in Table I. These compositions are based on the volume defined by the matrix spacing and thus include the spacing between subassemblies to provide an average volume per cent composition. Since the radial blanket composition is uniform over the entire active length of a blanket subassembly, the weights of materials involved are given for a typical one-cm length. A typical control or safety rod channel with the poison section withdrawn consists of 14.46 v/o, Type 304 stainless steel and 85.54 v/o sodium.

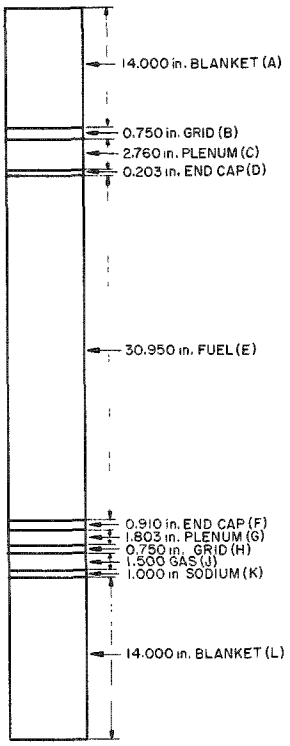

Fig. 6. Regional Dimensions of Fermi Core A Fuel Subassembly

B. Description of the Clean Core Assembly

Geometry and Composition. To determine the average composition in terms of volume per cent for the clean core mockup of the Fermi reactor in ZPR-III, the 10 control and safety rods were assumed to be withdrawn from the core and their channels filled with sodium. The materials in the 10 sodium-filled rod channels and the 91 fuel subassembles were then homogenized over the core volume to obtain average volume fractions. These average compositions for the Fermi reactor are compared in Table II with the average compositions achieved in the clean and engineering criticals in ZPR-III.

Table I

VOLUME PER CENT COMPOSITION AND WEIGHTS OF ENRICO FERMI REACTOR SUBASSEMBLIES*

Core Subassembly

Zone	Volume (cm^3)	Volume %	Density (g/cm^3)	Weight (kg)
Upper Axial Blanket (A)**				
Total	1663.3			
Uranium	470.3	28.3	19.00	8.97
Molybdenum	25.2	1.5	10.20	0.26
Sodium	890.6	53.5	-	-
304 Stainless Steel	277.1	16.7	7.85	2.21
Grid (B)				
Total	89.1			
304 Stainless Steel	39.5	44.3	7.85	0.31
Sodium	49.7	55.7	-	-
Plenum (C)				
Total	327.9			
304 Stainless Steel	44.4	13.5	7.85	0.35
Sodium	283.5	86.5	-	-
End Cap (D)				
Total	24.1			
304 Stainless Steel	3.3	13.5	7.85	0.03
Zirconium	1.5	6.0	6.44	0.01
Sodium	19.4	80.5	-	-
Fuel (E)				
Total	3677.1			
Uranium	1025.8	27.9	19.00	19.56
Molybdenum	213.0	5.8	10.20	2.17
Zirconium	217.5	5.9	6.44	1.42
304 Stainless Steel	486.4	13.2	7.85	3.87
Sodium	1734.4	47.2	-	-

Table I (Cont'd.)

Core Subassembly

Zone	Volume (cm^3)	Volume %	Density (g/cm^3)	Weight (kg)
End Cap (F)				
Total	108.2			
Zirconium	28.2	26.1	6.44	0.18
304 Stainless Steel	22.8	21.0	7.85	0.18
Sodium	57.2	52.9	-	-
Plenum (G)				
Total	220.1			
304 Stainless Steel	35.7	16.2	7.85	0.28
Sodium	184.4	83.8	-	-
Grid (H)				
Total	91.6			
304 Stainless Steel	40.6	44.3	7.85	0.31
Sodium	51.0	55.7	-	-
Gas (J)				
Total	183.2			
304 Stainless Steel	30.6	16.7	7.85	0.24
Gas	56.7	31.0	-	-
Sodium	9.58	52.3	-	-
Sodium (K)				
Total	122.1			
304 Stainless Steel	20.4	16.7	7.85	0.16
Sodium	101.7	83.3	-	-
Lower Axial Blanket (L)				
Total	1709.0			
Uranium	483.2	28.3	19.00	8.97
Molybdenum	25.9	1.5	10.20	0.26
304 Stainless Steel	284.7	16.7	7.85	2.21
Sodium	915.1	53.5	-	-

Table I (Cont'd.)

Radial Blanket (Based on 1-cm length)

	Volume (cm^3)	Volume %	Density (g/cm^3)	Weight (kg)
Total	48.1			
Uranium	21.4	44.6	19.00	0.40
Molybdenum	1.0	2.1	10.20	0.10
304 Stainless Steel	8.9	18.6	7.85	0.15
Sodium	16.7	34.7	-	-

*Compositions are based on unit cell dimensions and thus include the spacing between subassemblies.

**The letters refer to the notations in Fig. 6.

Table II

COMPARISON OF DESIGN AND EXPERIMENTAL CORES

	Enrico Fermi Reactor		Clean Critical ZPR-III		Engineering Critical ZPR-III	
Core Volume, liters	371.5		378.0		367.3	
Core Height, in.	30.95		30.10		30.60	
Equivalent Diameter, in.	30.5		31.3		30.5	
Cold Critical Mass of U^{235}, kg	-		431.5		434.4	
Total Core Composition	v/o[1]	kg[1]	v/o	kg	v/o[1]	kg[1]
U^{235}	25.14	1774.5	6.09	431.5	6.30	434.4
U^{238}			18.97	1362.5	19.54	1363.6
Mo	5.2	198.2	5.0	193.9	4.54	170.0
Zr	5.3	127.0	4.3	104.9	4.49	106.3
SS	13.3	388.7	14.3	424.8	13.97	402.7
Na	51.0	-				
Al	-	-	25.1	256.7	28.94	287.0
Blanket Composition (v/o)	Radial	Axial	Radial[2]	Axial	Radial[2]	Axial
U^{235}	44.6	28.3	0.1	0.1	0.1	0.06
U^{238}			45.6	45.6	45.6	28.3
Mo	2.1	1.5	2.5	2.5	2.5	
SS	18.6	16.7	19.5	19.5	19.5	18.5
Na	34.7	53.5				
Al	-	-	10.1	10.1	18.6	24.1

[1] Includes safety and control rod channels.
[2] Fine radial blanket only.

The densities used to calculate the volume per cent compositions in ZPR-III from the weights of the materials are as follows:

Material	Density (g/cm^3)
U^{235}	18.75
U^{238}	19.00
Aluminum	2.70
Stainless steel (304)	7.85
Molybdenum	10.20
Zirconium	6.44

For ease in analyzing the results of the clean-core experiments, end-gap regions in the Fermi Reactor were omitted from the clean assembly by loading the axial blanket regions adjacent to the cylindrical ends of the core. To simplify the drawer loadings, the core height was fixed at 30 in., thus allowing a uniform loading 15 in. of core material in each half of the assembly. The assembly interface spacing, composed of the perforated steel drawer fronts, adds an additional 0.08 in. to the overall length of the core. A reasonably cylindrical core geometry was achieved by the use of partial edge drawers loaded to contain a representative region of core material over that fraction of the drawer adjacent to, and lying within, the core. The remaining portion of the drawer was loaded with typical blanket material. The locations of the partial edge drawers for the clean-core critical loading are shown in Fig. 7, which represents a cross section of the critical assembly at the cylindrical midplane. The reflector or blanket was loaded in fine, medium, and coarse regions representing increasing heterogeneity. This was necessitated by a limited inventory of $\frac{1}{8}$-in.-thick plates of the various materials required to extend the fine blanket region. The medium blanket region utilized 1 x 1 x 5-in. pieces of U^{238}, aluminum, and stainless steel, whereas the coarse blanket contained 2 x 2 x 5-in. pieces of U^{238} separated by a 1 x 2 x 2-in. region composed of $\frac{1}{4}$ x 2 x 2-in. pieces of Type 304 stainless steel and void. Figure 8 is a cross section of the clean core along the cylindrical axis, showing the radial and axial dimensions of the core and blanket regions of the assembly. The radial and axial dimensions are measured from the cylindrical axis and the core midplane, respectively. The radii shown are the equivalent radii of the various regions.

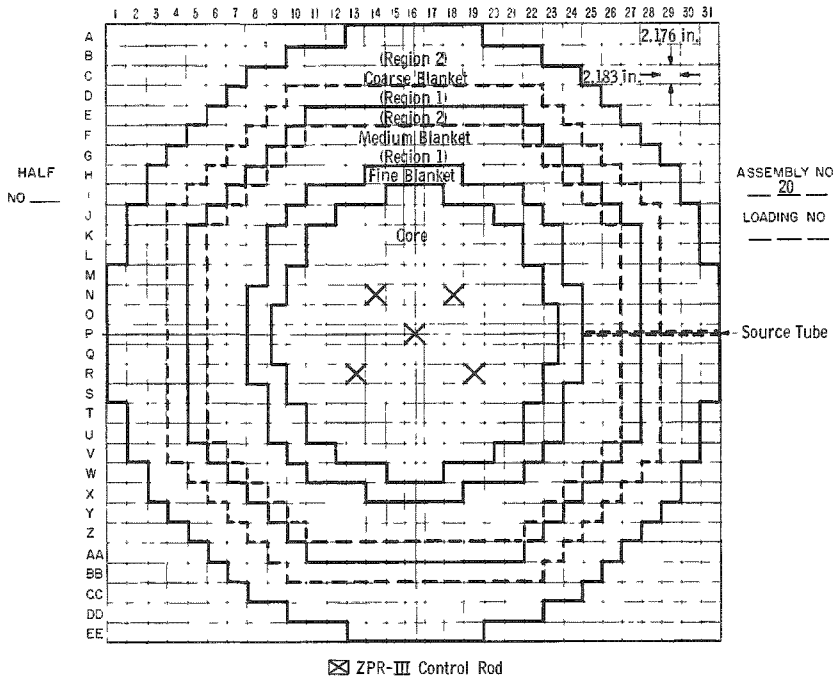

Fig. 7. ZPR-III Assembly Loading Diagram - Clean Core

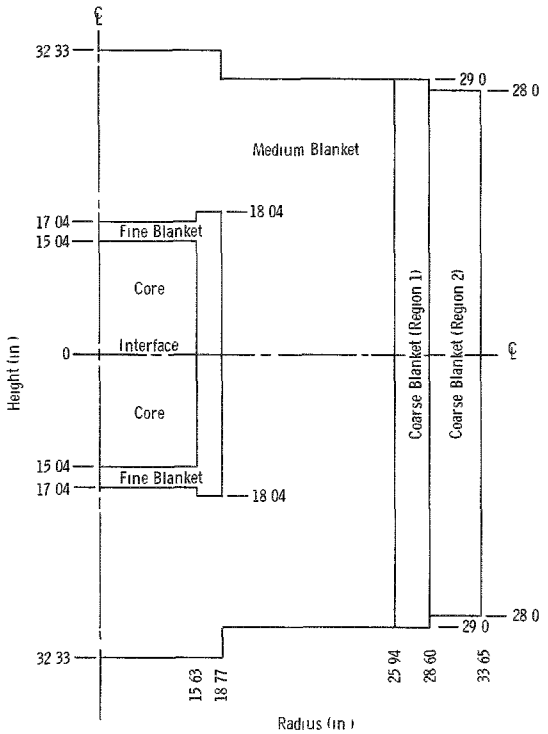

Fig. 8

Longitudinal Cross Section, Clean Core

The requirements of fixed composition imposed on the clean core prohibited the use of a standard core drawer loading without using partial-height axial columns of the various core materials. Since partial columns would have required many more small pieces of the materials than were available, four different drawer loadings were used as a repetitive unit. The order of the materials in the various drawer loadings used in the clean core assembly is given in Table III.

Table III

CLEAN-CORE DRAWER LOADINGS (CORE SECTION)

1/8-in columns, left to right across drawer face

Drawer Loading*	A	B	C	D	E	F	G	H	I	J	K	L	M	N	O	P
No 1	63%	Zr	63%	28	SS	45%	63%	28	25	63%	63%	Mo	63%	28	63%	63%
No 2	63%	Zr	28	63%	28	25	63%	45%	SS	28	63%	63%	Mo	63%	28	63%
No 3	63%	28	25	63%	28	Zr	45%	SS	63%	28	Mo	63%	63%	28	25	63%
No 4	63%	28	Zr	63%	63%	28	63%	SS	45%	63%	28	25	63%	63%	Mo	28
No 5** (1/2 core)	63%	28	25	63%	28	Zr	45%	SS	SS	28	45%	28	28	28	45%	28
No. 6** (1/2 core)	28	45%	28	28	1/2 Mo 1/2 45%	45%	28	SS	63%	28	Mo	63%	63%	28	25	63%
No 7** (3/4 core)	28	45%	28	28	63%	28	63%	SS	45%	63%	28	25	63%	63%	Mo	28
No 8** (3/4 core)	63%	Zr	28	63%	28	25	63%	45%	SS	28	63%	63%	28	28	45%	28
No 9 (seed)	63%	Zr	28	63%	28	25	63%	45%	SS	63%	63%	28	25	63%	Mo	63%
No 10 (seed)	Zr	63%	28	25	63%	63%	63%	SS	45%	63%	28	25	63%	63%	Mo	28
(Only 15 columns in control drawers)																
Control-1	63%	Zr	63%	28	45%	63%	28	25	63%	63%	Mo	63%	28	63%	63%	-
Control-2	63%	Zr	28	63%	28	25	63%	45%	28	63%	63%	Mo	63%	28	63%	-
Control-3	63%	28	25	63%	28	Zr	45%	63%	28	Mo	63%	63%	28	25	63%	-
Control-4	63%	28	Zr	63%	63%	28	63%	45%	63%	28	25	63%	63%	Mo	28	-
Control-5 (seed)	63%	Zr	28	25	45%	63%	63%	63%	63%	Mo	63%	28	25	63%	63%	-

*Typical locations of the drawers are shown in Fig 10
**Core edge drawers

28 - U^{238}
25 - U^{235}
SS - 304 stainless steel
Mo - molybdenum
Zr - zirconium (13-in column)
% refers to aluminum density

A diagram of a typical core drawer loading as portrayed in Fig. 5 is shown in Fig. 9. The zirconium columns were interrupted at different axial points in the various drawer loadings with a 2 x 2 x $\frac{1}{8}$-in. piece of 63% density aluminum to approximate more closely an initial requirement of an average of 4.41 v/o zirconium. Following the critical experimental program, the zirconium v/o for the designed core was increased to 5.31%, with a corresponding reduction in the stainless steel, as shown in Table II.

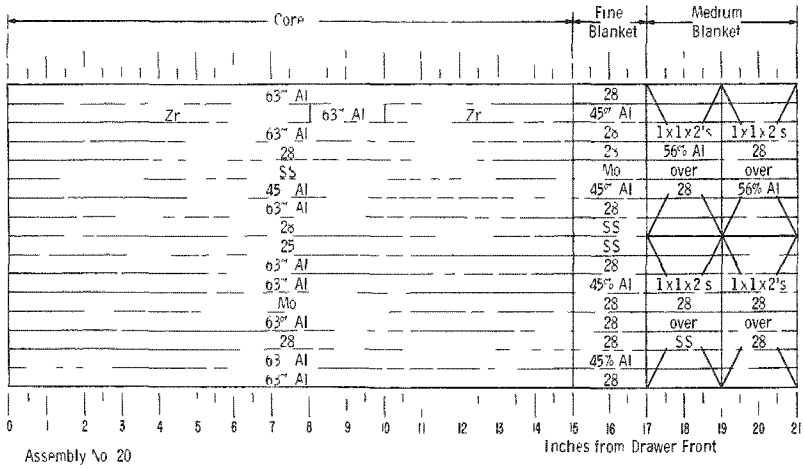

Fig. 9. Clean-core Drawer Loading, Master No. 1

Drawer loadings 9, 10, and C-5 (Control-5) in Table III represent "seeded" drawers in which the U^{235} content was increased by replacing a column of depleted uranium with a column of enriched uranium. Figure 10 is the clean-core loading diagram for half No. 1 of ZPR-III at criticality,

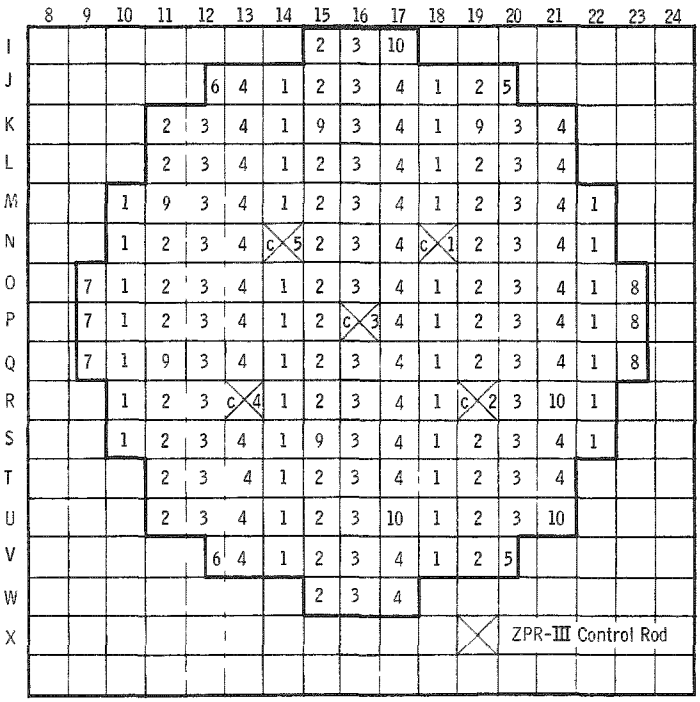

Fig. 10

Clean-core Loading Diagram, Half No. 1 (See Table III for description of drawers)

showing the locations of the seeded drawers. A corresponding array was used for Half No. 2, with different locations for the seeded drawers, to produce a relatively homogeneous distribution. Reactivity effects in excess of that available in the control rods were compensated by the exchange of normal and seeded drawers in the course of the experimental program.

Figure 11 is a diagram of a typical fine radial blanket drawer loading. The $11\frac{1}{4}$-in. axial blanket drawers immediately behind the $21\frac{1}{4}$-in. core drawers continued the medium blanket loading pattern as shown in the last 4 in. of the core drawer loading of Fig. 9. The v/o compositions of the clean critical core and of the various blanket regions are given in Table IV. The dimensions of the assembly are those shown in Fig. 8.

Table IV

COMPOSITION OF VARIOUS REGIONS OF CLEAN-CORE ASSEMBLY

		Blanket			
	Core	Fine	Medium	Coarse I	Coarse II
Outer Radius (in.):	15.63	18.77	25.94	28.60	33.65
Composition (v/o):					
U^{235}	6.09	0.10	0.11	0.11	0.14
U^{238}*	18.97	45.39	48.70	46.35	59.59
Al	25.14	10.08	13.47	0.86	1.10
Stainless Steel (304)	14.32	19.42	21.00	16.65	7.31
Mo	5.03	2.46	-	-	-
Zr	4.32	-	-	-	-

*This also includes U^{234} and U^{236}

Fig. 11. Fine Radial Blanket Drawer Loading Master

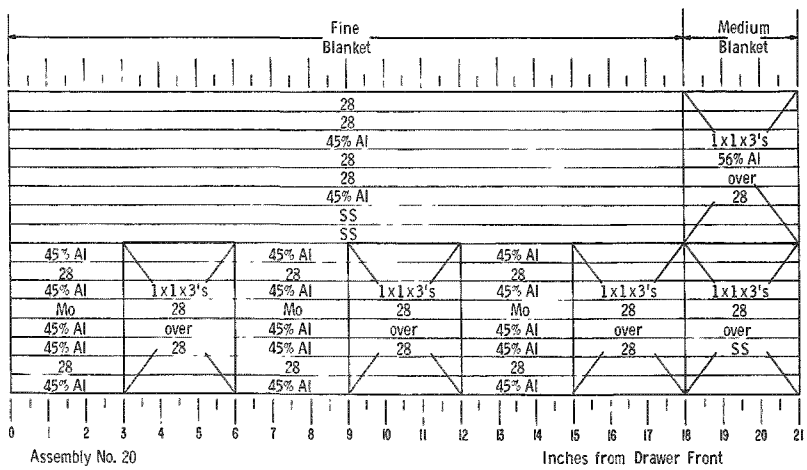

Loading to Critical and Critical Mass. The radial and axial blanket regions were loaded as shown in Figs. 7 and 8. The core was loaded according to Fig. 10 with the repetitive unit drawer sequence, but without seeded drawers. The core drawers were initially loaded with an axial column of 63% density aluminum in place of each column of uranium enriched in U^{235}. A conservative stepwise approach to a critical loading was then accomplished by replacing these aluminum columns with U^{235}. Without seeded drawers, a subcritical loading of 414 kg of U^{235} was attained. Eighteen distributed normal core drawers were then "seeded" by substituting a column of U^{235} for U^{238} to produce a loading of 433.5 kg of U^{235}, which was supercritical by 104.6 inhours.

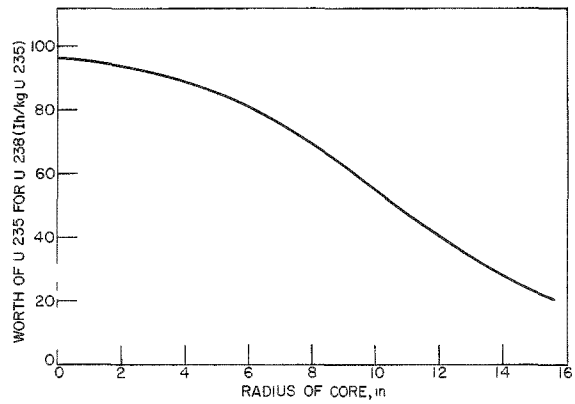

Fig. 12. Radial Worth of an Axial Column of U^{235} Substituted for U^{238}

The worth of an axial column of U^{235} for U^{238} as a function of radius was determined (see Fig. 12), and an average worth was then calculated to be 51.6 Ih/kg U^{235}. Thus, the clean critical mass of this assembly was calculated to be 431.5 kg U^{235} at 28.6 °C. The volume of the core was 378.0 liters with the dimensions as shown in Fig. 8.

Inhour Relation. The period-versus-inhour curve utilized for the positive period measurements of reactivity during this program was calculated from the following data.(7)

Group	λ_i (sec^{-1})	α_i	β_i
1	0.0127	0.033	0.000227
2	0.0318	0.195	0.00134
3	0.112	0.182	0.00125
4	0.301	0.400	0.00275
5	1.33	0.151	0.00104
6	3.85	0.038	0.000261

$$\beta_{eff} = 0.00687$$

$$1\% = 451 \text{ Ih}$$

$$\$1 = 310 \text{ Ih}$$

$$1 \text{ Ih} = 2.2169 \times 10^{-5} \Delta k/k$$

$$1\phi = 6.87 \times 10^{-5} \Delta k/k$$

ZPR-III Temperature Coefficient. A series of reference measurements were conducted on the clean-core loading at various equilibrium temperatures in order to define an average temperature coefficient for the ZPR-III assembly. Measurements over a range covering 8.2°C indicated a net temperature coefficient of -1.5 ± 0.2 Ih/°C ($-3.3 \pm 0.4 \times 10^{-5}$ $\Delta k/k$-°C).

ZPR-III Control Rod Calibration. Two of the ten fuel-containing control rods in ZPR-III were loaded as "seeded" drawers to provide additional reactivity control during the course of the experimental program. A calibration curve for the rod located in position N14 (see Fig. 10), loaded as a seeded drawer C-5 (whose composition is given in Table III), is given in Fig. 13. This curve was generated by determining the positive reactivity changes produced by stepwise rod insertions by means of positive period measurements. The 10-in. position means, for example, that the control rod drawer, which has been loaded in zones to correspond to the core and axial blanket regions, is withdrawn 10 in. from the assembly interface, or core midplane. This produces a 2.10 x 2.10 x 10-in. air-filled "void" region in the core. As indicated in Fig. 13, the insertion of the rod from this point to the "full-in" or zero position represents a reactivity addition of 101 Ih or 2.24×10^{-3} $\Delta k/k$.

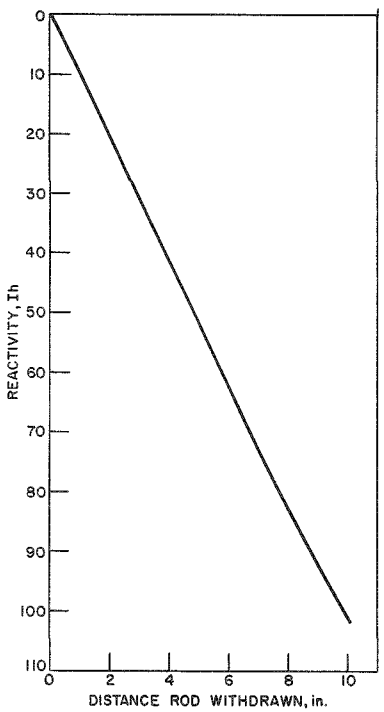

Fig. 13. ZPR-III Control Rod Calibration Curve, Fermi Clean Core.

The 15-in. core region of a "seeded" control drawer, including the steel drawer itself, contained the following weights of materials:

Material	Weight (g)
U^{235}	1033
U^{238}	1178
Mo	606
Zr	329
SS	758
Al	897

C. Reactivity Coefficient Measurements

Danger coefficient or reactivity coefficient measurements were made with the clean-core assembly for a selected group of materials. In general, these measurements involved the insertion of 8 $in.^3$ of the sample material in the form of two blocks of the material, each 1 x 2 x 2 in.

An air-filled void region of this size was initially provided, and the reactivity effect of the sample was then determined with respect to this void. Special drawers were utilized to eliminate any axial shifting of the core material. An accuracy of $\pm$ 0.5 Ih can be assigned to the net reactivity measurement. This accuracy has been repeatedly demonstrated by the reproducibility of these measurements.

Core Center. Measurements at the center of the core were made by removing 4 in.^{3} of core material from the front, or assembly interface end of the center drawer in each half, thus producing an 8-in.^{3} void region at the center of the core with the halves assembled. With this void condition as a reference, various materials were inserted and the resulting reactivity changes noted. The data obtained are given in Table V. In the smaller samples of boron-10 and of boron-10 carbide, the remaining volume was either filled with aluminum or left void, as indicated.

Radial Core-Blanket Interface. Measurements at the core-blanket interface along the core midplane were conducted in a similar manner by providing a 4-in.^{3} void in each of the opposing drawers in V-12 (see Fig. 10). This provided a radial core-blanket interface position which placed half of the sample volume in each region. The data thus obtained are given in Table V.

Table V

CENTRAL AND CORE-EDGE REACTIVITY COEFFICIENTS
(With Respect to Void)

		Core Center			
Sample	Material (Size)	Number of Pieces	Weight (g)	Total Reactivity Effect (Ih)	Ih/kg of Sample[1]
Al	Aluminum (100%) (1 x 1 x 2 in.)	4	350.7	-1.4	-4.0
SS	Stainless Steel (Type 304) (1/8 x 1 x 2 in.)	32	999.8	-4.1	-4.1
Mo	Molybdenum (1 x 2 x 2 in.)	2	1280.5	-13.8	-10.8
Zr	Zirconium (1 x 2 x 2 in.)	2	846.0	-3.1	-3.7
Be	Beryllium (1 x 2 x 2 in.)	2	240.7	8.3	34.5
Depleted Uranium	U^{238} (0.2% U^{235}) (1/8 x 1 x 2 in.)	32	2462.0	-13.6	-5.5
Ph I	Physicum I (oxide)[2] in SS Cans (1/4 x 2 x 2 in. cans)	8	230.0 (of Physicum I) 170.0 (of SS)	-5.4	-20.4
B^{10}	Boron in SS cans (1/8 x 2 x 2 in. cans) Aluminum (45%) (1/8 x 2 x 2 in.)	6 10	23.1[3] (of boron) 205.3 (of SS) 93.9 (of Al)	-42.9	-1800
B_4C[4]	Boron-10 Carbide (1/4 x 1 x 2 in.)	2	32.2	-41.0	-1275
C	Graphite (1 x 2 x 2 in.)	2	196.5	1.3	6.6

Table V (Cont'd.)

Sample	Material (Size)	Number of Pieces	Weight (g)	Total Reactivity Effect (Ih)	Ih/kg of Sample[1]
		Core Center			
Ta	Tantalum (1/8 x 2 x 2 in.)	16	2103.1	-51.9	-24.6
Inconel-X	Inconel-X (2 x 2 x 1/4 in.)	8	1044	-5.2	-5.0
Hg	Mercury in SS Can (2 x 2 x 1 in.)	2	1383.4 (of Hg) 197.3 (of SS)	-7.5	-4.8
		Core-blanket Interface			
Axial					
Al			256.8 (net)	2.3	9.0
	Aluminum (100%) (1 x 1 x 2 in.)	4	350.7		
	Replaced by Aluminum (45%) (1/8 x 2 x 2 in.)	10	93.9		
SS	Stainless Steel (Type 304) (1/8 x 2 x 2 in.)	6	371.6	1.9	5.1
B^{10}	Boron in SS Cans (1/8 x 2 x 2 in. cans)	6	23.1[3] (of boron) 205.3 (of SS)	-7.8	-383
B_4C[4]	Boron-10 Carbide (1/4 x 1 x 2 in.)	2	32.2	-8.3	-258
Radial					
Al	Aluminum (100%) (1 x 1 x 2 in.)	4	350.7	3.6	10.3
SS	Stainless Steel (Type 304) (1 x 1 x 2 in.)	4	1017.4	4.3	4.2
Mo	Molybdenum (1 x 2 x 2 in.)	2	1280.5	3.5	2.7
Zr	Zirconium (1 x 2 x 2 in.)	2	846.0	4.3	5.1
Be	Beryllium (1 x 2 x 2 in.)	2	240.7	5.1	21.2
Depleted Uranium	U^{238} (0.2% U^{235}) (1/8 x 1 x 2 in.)	32	2462.0	2.6	1.1
Ph I	Physicum I (oxide)[2] in SS Cans (1/4 x 2 x 2 in. cans)	8	230.0 (of Physicum I) 170.0 (of SS)	1.9	5.1
Inconel-X	Inconel-X (2 x 2 x 1/4 in.)	8	1044	5.7	5.4

[1] Corrected for canning material and aluminum

[2] Composition given in Reference 6. Molecular weights in Reference 6 are incorrect however. The corrected values are

Formula	Molecular weight
$(Ph\text{-}I)O_{1.519}$	142.2
$(Ph\text{-}II)O_{1.146}$	136.1

In computing the above, 2 atoms of oxygen are substituted for each sulfur atom, and 3/4 atoms oxygen for each carbon atom.

[3] Boron sample contains 94 w/o boron and 6 w/o impurities, and is enriched to 92 atom % B^{10}.

[4] Boron carbide sample contains 69.34 w/o boron and 27.68 w/o carbon. The boron is enriched to 90.7 atom % B^{10}.

Axial Core-Blanket Interface. The measurements at the axial core-blanket interface were similarly obtained by providing an 8-in.^{3} void region extending 1 in. into the core and 1 in. into the axial blanket. This was located on the cylindrical axis at one end of the core. The data for this location are given in Table V.

D. Reactivity Worths of Plutonium and U^{235}

Axial and radial traverses of the reactivity worth of plutonium and U^{235}, as well as radial traverses of the worth of an axial column of these materials, were conducted with the clean-core assembly. An initial

reference loading was established for both materials by loading a $\frac{1}{8}$-in.-thick column of 63% density aluminum adjacent to a $\frac{1}{8}$-in.-thick column of 45%-density aluminum at the locations where sample materials were to be placed. In the case of the $\frac{1}{4}$-in.-thick ($\frac{1}{4}$ x 2 x 2-in. and $\frac{1}{4}$ x 2 x 3-in.) aluminum-clad, aluminum-alloyed plutonium samples, the removal of the two aluminum columns and the substitution of the plutonium sample resulted in a negligible change of aluminum mass. For the U^{235} sample, the two partial-density aluminum columns were replaced by a $\frac{1}{8}$-in.-thick U^{235} sample plus two $\frac{1}{16}$-in.-thick plates of 100% density aluminum to produce again a negligible change of aluminum mass. Thus, the observed reactivity changes in all cases are directly attributed to the presence of the sample material versus void.

The two, $\frac{1}{4}$ x 2 x 2-in. plutonium samples used for the radial and axial traverses contained 185.99 g plutonium, of which 175.78 g were Pu^{239}. The two $\frac{1}{8}$ x 2 x 2-in. U^{235} samples contained 287.36 g uranium, of which 267.84 g were U^{235}.

The axial sample column contained 464.96 g plutonium, of which 439.43 g were Pu^{239}, and 729.60 g of uranium, of which 680.14 g were U^{235}.

The reactivity values given in Table VI assume a negligible reactivity contribution from the U^{234}, U^{236}, and U^{238} in the uranium sample.

Table VI

WORTHS OF PLUTONIUM AND U^{235}

Radial Traverse at Midplane (0 - 2 in. in drawer)

Radius (in.)	Worth (Ih/kg) U^{235}	Worth (Ih/kg) Pu*
0	135.0	223.0
8.73	85.2	138.8
15.28	31.0	45.2

Axial Traverse Along Cylindrical Axis of Core

Position in Drawer (in.)	Worth (Ih/kg) U^{235}	Worth (Ih/kg) Pu*
0 - 2	135.0	223.0
6 - 8	105.3	172.0
13 - 15	43.7	66.2

Axial Column as Function of Radius

Radius (in.)	Worth (Ih/kg) U^{235}	Worth (Ih/kg) Pu*
0	95.1	156.0
4.74	82.7	134.0
8.73	59.7	98.5
10.79	46.5	74.6
13.47	29.7	46.6
15.28	20.6	31.4
17.71	11.2	13.8
19.90	4.7	6.2
22.08	2.5	2.2

*Isotopic analysis of Pu in a/o:

Pu^{239}	94.51 ± 0.08 a/o
Pu^{240}	5.11 ± 0.07 a/o
Pu^{241}	0.38 ± 0.03 a/o

Radial Traverse. The radial traverse was conducted at the core midplane by locating the sample material at a point from 0 to 2 in. in opposing drawers on either side of the core midplane. A core center, core edge, and intermediate location were utilized. These data are shown in Table VI.

Axial Traverse. The axial traverse was conducted in the two opposing central drawers along the cylindrical axis (P-16) at 0 to 2 in., 6 to 8 in., and 13 to 15 in. from the core midplane. These data are shown in Table VI.

Radial Traverse of Axial Column. Since only four samples, representing a total of 10 in. of plutonium, were available for these measurements, a comparable amount of U^{235} was also used. The samples were located from 1 to 3 in., 4 to 7 in., 8 to 10 in., and 11 to 14 in. These data are included with the axial and radial traverse numbers in Table VI.

E. Material Substitutions

Two separate series of material-substitution experiments were conducted with the Fermi clean-core loading to determine average reactivity coefficients in the core and fine radial blanket. The materials studied were aluminum, molybdenum, zirconium, sodium, oxygen in the form of aluminum oxide, Type 304 stainless steel, and depleted uranium (containing ~0.2% U^{235}). The fine radial blanket substitutions were restricted to aluminum, sodium, and stainless steel. Additional measurements of average reactivity coefficient for aluminum and depleted uranium in the radial and axial blankets were conducted with the Fermi engineering core loading and are included with the engineering core data.

The first series of material substitutions were conducted with the clean-core loading. Inasmuch as anomalous data resulted from the depleted-uranium substitutions in the core, a modified clean-core loading was assembled following the engineering-core experiments. The purpose of this modified loading was to investigate the reactivity effects produced by small local variations in density for the aluminum and depleted uranium over the entire core.

Distributed Worths in Core and Fine Blanket. Each drawer has seven symmetrical counterparts in other parts of the core, one in each of the three other quadrants in its one half and four more in the opposite half. By selecting a group of drawers each of which is the symmetrical counterpart of a different drawer in one quadrant, a sample consisting of only one-eighth of the total drawers can be obtained such that its radial distribution is characteristic of the whole core. At the same time, the sample can

be chosen so that it is fairly uniformly distributed over the entire core. Such a sample is identified in this report as a distributed eighth of the core. A distributed quarter or other fraction can be chosen in a similar manner. These distributed patterns of drawers have been used for determination of the worth of materials distributed uniformly throughout the core. Several such distributed patterns which have been used are illustrated in Fig. 14, where the circled numbers represent drawers in Half No. 2, while the uncircled numbers are for Half No. 1.

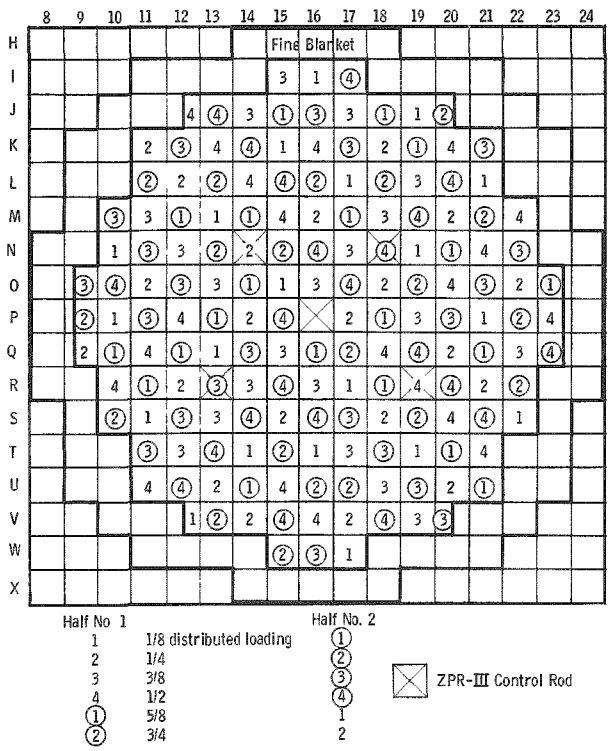

Fig. 14. Distributed Loading Scheme for Both Halves in the Material-substitution Measurements

Drawers indicated as No. 1 correspond to a $\frac{1}{8}$ distributed loading; No. 2 correspond to $\frac{2}{8}$ loading; etc. When the loading involved more than half the core, the same sequence was used except that the circled numbers in Fig. 14 then correspond to Half No. 1 and the uncircled numbers to Half No. 2. The measurements of the worths of stainless steel, molybdenum, zirconium, and U^{238} were done with a fraction of the core involving 38 drawers rather than the 41 drawers making up a full quarter. This represented the omission of the partial edge drawers and control drawers.

The volume of the core was not changed at any time from the 378-liter reference core volume. When additional reactivity was required to compensate for the reactivity change resulting from a material substitution, additional seeded drawers were substituted for standard drawers. This was the same procedure as was used in making the reactor critical. An effort was made to distribute the additional fuel uniformly.

The reference loadings for the four typical core drawers and the fine blanket drawer are those given for the clean-core loading (see Table III and Figs. 10 and 11). Substitutions were made for materials within these drawers as well as in the partial, control, and seeded drawers, with no change in material location. Exceptions to this occurred in the U^{238} and sodium-substitution experiments, in which aluminum columns were moved

to avoid placing two columns of U^{238} adjacent to each other, or where double columns of aluminum were not present for sodium replacement. In these cases, a reference measurement was made for the revised loading before the substitutions were undertaken.

1. Aluminum, Full-drawer Substitution

Full-density aluminum pieces were substituted for all of the 63% density aluminum in a given drawer. This substitution was repeated stepwise in other core drawers so that changes varied from $\frac{1}{16}$ to $\frac{1}{2}$ of the core. The manner of substitution is shown in Fig. 14, except that the $\frac{1}{16}$-core loading was accomplished by loading the drawers indicated for the $\frac{1}{8}$-loading in only one half of the assembly. The weight of aluminum substituted, the reactivity change, and the average and incremental worths of aluminum are presented in Table VII. The changes in the average volume per cent of aluminum are also given.

Table VII

ALUMINUM DENSITY COEFFICIENT, FULL-DRAWER SUBSTITUTION

	Distributed Fraction of Core Drawers			
Core Composition (v/o):	1/16	1/4	3/8	1/2
U^{235}	6.09	6.09	6.06	6.06
U^{238}	18.97	18.97	19.00	19.00
Al	25.91	28.33	29.92	31.54
Stainless Steel	14.32	14.32	14.32	14.32
Mo	5.03	5.03	5.03	5.03
Zr	4.32	4.32	4.32	4.32
Number of drawers changed	20	81	122	164
Reference Al added (w/o)	3.05	12.68	19.02	25.45
Weight of Al added (kg)	7.8	32.5	48.8	65.3
Reactivity change (Ih)	29.3	123.5	186.8	248.2
Average worth of Al (Ih/kg)	3.75	3.80	3.83	3.80
Incremental worth of Al (Ih/kg)	3.81	3.89	3.72	

Subsequent work on the depleted-uranium substitutions suggested the possibility that the aluminum worth per kilogram obtained by changing all the aluminum in one drawer would not correspond to the value obtained by varying the density of a single column in every drawer. This prompted the following partial-drawer substitutions of aluminum in a modified clean-core loading.

2. Aluminum, Partial-drawer Substitution

The modified clean core was a reloading of the clean core after completion of the engineering-core experiments. The four basic core drawer loadings were modified as shown in Table VIII, such that

three columns of 63%-density aluminum were bunched in each drawer with no change in drawer composition. The special drawers were similarly loaded. This allowed the subsequent substitution of a column of depleted uranium for aluminum with adequate separation from any other U^{235} or depleted uranium in the drawer. The fine radial blanket drawers and the 11-in. end-blanket drawers remained as loaded for the engineering-core mockup as described in a subsequent section. The 5 in. of end blanket immediately adjacent to the cylindrical ends of the core contained three 1 x 1 x 5-in. pieces of U^{238} and one 1 x 1 x 5-in. piece of 56% density aluminum with two pieces of $\frac{1}{4}$ x 2 x 2-in. stainless steel and two pieces of $\frac{1}{4}$ x 2 x 2-in. 100% density aluminum extending from 5 to 6 in. behind the core-end blanket interface in each drawer.

Table VIII

BASIC DRAWER LOADING FOR MODIFIED CLEAN-CORE EXPERIMENTS
1/8-in. Columns, Left to Right Across Drawer Face

Master No.	Assembly	Drawer Column A	B	C	D	E	F	G	H	I	J	K	L	M	N	O	P
1	Clean Core	63%	Zr	63%	28	SS	45%	63%	28	25	63%	63%	Mo	63%	28	63%	63%
1	Modified Clean Core	63%	Zr	63%	28	SS	45%	63%	28	25	63%	63%	63%	Mo	63%	28	63%
2	Clean Core	63%	Zr	28	63%	28	25	63%	45%	SS	28	63%	63%	Mo	63%	28	63%
2	Modified Clean Core	63%	Zr	28	63%	28	25	63%	45%	SS	28	63%	63%	63%	Mo	28	63%
3	Clean Core	63%	28	25	63%	28	Zr	45%	SS	63%	28	Mo	63%	63%	28	25	63%
3	Modified Clean Core	63%	28	25	63%	28	Zr	45%	SS	28	Mo	63%	63%	63%	28	25	63%
4	Clean Core	63%	28	Zr	63%	63%	28	63%	SS	45%	63%	28	25	63%	63%	Mo	28
4	Modified Clean Core	63%	28	Zr	63%	63%	63%	28	SS	45%	63%	28	25	63%	63%	Mo	28

25 - U^{235}-enriched uranium
28 - Depleted uranium
SS - Stainless Steel
Mo - Molybdenum
Zr - Zirconium
45% - 45% density aluminum
63% - 63% density aluminum

Four basic aluminum density changes were conducted within the three bunched columns of aluminum in each drawer:

a. One column of 45% density aluminum was substituted for one column of 63% density aluminum per drawer over a distributed half of the core and then over the remaining half to effect a full core change. This resulted in a change of the three-column bunch from 63%-63%-63% to 63%-45%-63% in each drawer.

b. Two additional columns of 45% density aluminum were substituted for the two remaining 63% density columns per drawer over a distributed half of the core, thus producing a 45%-45%-45% array in half of the drawers with a 63%-45%-63% array in the remaining half.

c. Three 100% density aluminum columns were substituted for three columns of 45% density aluminum per drawer over $\frac{1}{8}$ of the core and then over an additional $\frac{1}{8}$ core to provide a $\frac{1}{4}$-core substitution with a three-column 100%-100%-100% array. Of the remaining drawers, $\frac{1}{4}$ of the core contained the three-column 45%-45%-45% bunched array and $\frac{1}{2}$ of the core contained the three-column 63%-45%-63% array.

d. One column of 100% density aluminum was substituted for one column of 63% density aluminum over one-half of the core to produce a three-column 63%-100%-63% array in one-half of the core drawers with the three-column 63%-63%-63% density array in the remaining half.

The results of the above substitutions are shown in Table IX.

Table IX

ALUMINUM DENSITY COEFFICIENT, PARTIAL DRAWER SUBSTITUTION*
(Ih/kg)

Distributed fraction of core drawers	1/8	1/4	1/2	1
(a) 1 column of 45% for 63% Al/drawer			4.50	4.43
(b) 2 columns of 45% for 63% Al/drawer			4.39	
(c) 3 columns of 100% for 45% Al/drawer	4.18	4.18		
(d) 1 column of 100% for 63% Al/drawer			4.24	

*The aluminum density changes were all made within the three bunched columns of aluminum as shown in the initial drawer loadings (see Table VIII).

3. Stainless Steel (Type 304), Molybdenum, Zirconium, and Oxygen (Al_2O_3)

Tests to determine average core worths were run for Type 304 stainless steel, molybdenum, zirconium, and oxygen by substituting aluminum for these materials over a distributed quarter of the core (38 drawers). Partial core-edge drawers and control drawers were not altered (see Fig. 14).

Stainless steel and molybdenum worths were determined by substituting 100% density aluminum for these materials and noting the net reactivity change. By using the aluminum worth as determined from the preceding measurements by partial drawer substitution of the aluminum density, the worth of the material in question can be determined. In the case of zirconium, the 13 in. of material in each drawer were replaced by

an equal amount of 100% density aluminum. For the oxygen measurement, two 14-in. columns of 63% density aluminum and one 14-in. column of 45% density aluminum were replaced by three 14-in. columns of aluminum oxide (Al_2O_3) to provide an oxygen addition with a negligible change in aluminum.

Substitution of 45% density aluminum for stainless steel in a distributed $\frac{1}{8}$ of the fine blanket drawers resulted in a value of +1.035 Ih/kg for stainless steel in this region. The value of +2.53 Ih/kg of aluminum as shown in Table XIX was used to correct for the aluminum addition.

An alternative technique for material-substitution measurements of materials other than aluminum and sodium has also been employed on ZPR-III, but was not used in this series of measurements. This involves compensating for the aluminum inserted in place of the sample material by reducing the density of the remaining aluminum columns in the drawer to produce a negligible net change in aluminum. This method eliminates the necessity for an aluminum reactivity correction and thus allows a direct determination of the sample material worth with respect to void. This technique was used, however, in a portion of the material-substitution measurements with depleted uranium and is described in a subsequent section.

The data resulting from the above measurements with stainless steel, molybdenum, zirconium and oxygen are presented in Table X.

Table X

WORTHS OF VARIOUS CORE MATERIALS FOR A DISTRIBUTED LOADING

	SS			Mo			Zr	O
Core Composition	38 Drawers		76 Drawers	38 Drawers		76 Drawers	76 Drawers	38 Drawers
U^{235}		6.09			6.09		6.09	6.09
U^{238}		18.97			18.97		18.97	18.97
Al	25.73		26.34	25.73		26.34	26.17	25.17
SS	13.72		13.13		14.32		14.32	14.32
Mo		5.03		4.43		3.83	5.03	5.03
Zr		4.32			4.32		3.29	4.32
Percentage of material changed	4.17		8.33	11.91		23.82	23.82	-
Weight of material changed (kg)	-17.7		-35.4	-23.0		-46.1	-24.9	8.00
Weight of aluminum changed (kg)	6.1		12.1	6.1		12.1	10.5	.31
Reactivity (Ih):								
relative to reference	6.3		13.1	50.9		104.7	-16.8	83.1
of aluminum*	25.9		51.3	25.9		51.3	44.5	1.3
of material	-19.6		-38.2	25.0		53.4	-61.3	81.8
Worth of material (Ih/kg)	1.107		1.079	-1.087		-1.158	2.462	10.23

* Aluminum worth assumed to be + 4.24 Ih/kg.

4. Sodium

Sodium in stainless steel cans of dimensions 8 x 2 x $\frac{1}{4}$ in., 7 x 2 x $\frac{1}{4}$ in., 4 x 2 x $\frac{1}{4}$ in., and 3 x 2 x $\frac{1}{4}$ in. was substituted for aluminum and stainless steel in the core and fine blanket. Since the sodium cans were $\frac{1}{4}$-in. thick, it was necessary to remove two columns of material for for each column of sodium inserted. Therefore, 63% density aluminum columns were bunched in pairs as a reference loading. The column order for these experiments is given in Table XI.

Table XI

DRAWER LOADINGS FOR SODIUM-SUBSTITUTION MEASUREMENTS
1/8-in. Columns, Left to Right Across Drawer Face

Master No.	Drawer Type	Drawer Column A	B	C	D	E	F	G	H	I	J	K	L	M	N	O	P
Core																	
1	Reference	63%	63%	Zr	28	SS	45%	63%	28	25	63%	63%	Mo	63%	28	63%	63%
1	Test	Na		Zr	28	Na		63%	28	25	Na		Mo	63%	28	Na	
2	Reference	63%	63%	28	Zr	28	25	63%	45%	SS	28	63%	63%	Mo	28	63%	63%
2	Test	Na		28	Zr	28	25	63%	Na		28	Na		Mo	28	Na	
3	Reference	28	25	63%	63%	28	Zr	45%	SS	28	Mo	63%	63%	28	25	63%	63%
3	Test	28	25	Na		28	Zr	Na		28	Mo	Na		28	25	Na	
4	Reference	63%	28	Zr	63%	63%	28	63%	SS	45%	63%	28	25	63%	63%	Mo	28
4	Test	63%	28	Zr	Na		28	Na		Na		28	25	Na		Mo	28
Core Edge																	
5[1]	Reference	28	25	63%	63%	28	Mo	45%	SS	SS	28	28	28	45%	45%	28	28
5	Test	28	25	Na		28	Mo	Na		SS	28	28	28	Na		28	28
6[1]	Reference	28	45%	45%	28	(1/2 45% 1/2 Mo)	28	28	SS	28	Mo	63%	63%	28	25	63%	63%
6	Test	28	Na		28	(1/2 45% 1/2 Mo)	28	28	SS	28	Mo	Na		28	25	Na	
7[2]	Reference	28	45%	28	28	63%	28	63%	SS	45%	63%	28	25	63%	63%	Mo	28
7	Test	28	45%	28	28	63%	28	Na		Na		28	25	Na		Mo	28
8[2]	Reference	63%	63%	28	Zr	28	25	63%	45%	SS	28	63%	63%	28	28	45%	28
8	Test	Na		28	Zr	28	25	63%	Na		28	Na		28	28	45%	28
Seed																	
9	Reference	63%	63%	28	Zr	28	25	63%	SS	45%	63%	63%	28	25	63%	63%	Mo
9	Test	Na		28	Zr	28	25	Na		Na		63%	28	25	Na		Mo
10	Reference	Zr	63%	28	25	63%	63%	63%	SS	45%	63%	28	25	63%	63%	Mo	28
10	Test	Zr	63%	28	25	Na		Na		Na		28	25	Na		Mo	28
Fine Blanket[3]																	
B-1 or B-2	Reference	28	28	45%	45%	28	28	SS	SS	Unchanged, see Fig. 11							
B-1 or B-2	Test	28	28	Na		28	28	SS	SS								
B-1'	Reference	28	28	45%	28	28	45%	SS	SS								
B-1'	Test	28	28	45%	28	28	Na		SS								

[1] Half of drawer is core and half is blanket
[2] 3/4 of drawer is core and 1/4 is fine blanket (not changed)
[3] 1/2 of the B-1 drawers were loaded as B-1' to compensate for SS in Na cans

CODE: 25 U^{235}-Enriched Uranium
28 Depleted Uranium
Zr Zirconium
Mo Molybdenum
SS Stainless Steel
% Per cent Density Al

Two cans of sodium (one 7-in. and one 8-in.) replaced the 15-in. aluminum and stainless steel columns, as indicated, in the core drawers. Three cans (one 3-in., one 7-in., and one 8-in.; or one 4-in. and two 7-in.) replaced the 45% density aluminum and stainless steel columns indicated in the fine blanket drawers, i.e., 15 in. in the core and 18 in. in the fine blanket drawers. The void end of each can was placed toward the reactor interface. The smaller cans in each case were placed in the front of the drawer, nearest the core interface. This was done on the assumption that the worth of sodium is less near the core center, thereby minimizing the heterogeneity effect introduced by the small void region in each can.

Table XII presents the data relating to the sodium worth experiments. The core data were obtained with no sodium in the fine blanket. The fine blanket data were obtained with a $\frac{5}{8}$-distributed sodium loading in the core. The density coefficient of reactivity for aluminum utilized in

Table XII

DISTRIBUTED WORTH OF SODIUM IN THE CORE AND FINE BLANKET

Composition	1/8[1]	1/4[1]	1/2[1]	5/8[1]	3/4[1]	F.B.[2]
U^{235}	6.09	6.09	6.09	6.09	6.09	0.10
U^{238}	18.97	18.97	18.97	18.97	18.97	45.39
Al	22.54	19.88	14.66	12.06	9.47	6.38
SS	14.60	14.89	15.49	15.76	15.88	19.46
Mo	5.03	5.03	5.03	5.03	5.03	2.46
Zr	4.32	4.32	4.32	4.32	4.32	-
Na	3.94	7.96	15.82	19.76	23.69	8.12
Number of drawers changed	40	81	181	204	241	142
Weight of Na added (kg)	14.5	29.2	58.0	72.5	86.8	15.7
Weight of Al added (kg)	-26.6	-53.7	-106.0	-133.6	-159.9	-20.2
Weight of SS added (kg)	8.2	16.9	35.6	43.8	47.3	1.14
Reactivity (Ih):						
relative to reference	12.4	20.7	30.0	26.1	17.6	-1.2
of Al[3]	-101.0	-204.2	-406.5	-507.5	-607.7	-56.3
of SS[3]	8.8	18.2	38.4	47.3	51.0	-1.2
of Na	104.6	206.7	398.1	486.3	574.3	56.3
Worth of Na (Ih/kg)	7.21	7.08	6.86	6.71	6.62	3.59
Incremental Worth of Na (Ih/kg)	6.95	6.65	6.08	6.15		

(1) Four columns of Na substituted for 6 columns of 63% Al, 1 column of 45% Al and 1 column of SS in the core.

(2) Four columns of Na substituted for 7 columns of 45% Al and 1 column of SS in the fine blanket.

(3) The worths of Al and SS used here:
Al (core) 3.80 Ih/kg; Al (F.B.) 2.53 Ih/kg
SS (core) 1.079 Ih/kg; SS (F.B.) 1.035 Ih/kg

Table XII to correct for the aluminum removed is the value obtained from the full drawer substitutions (see Table VII). The full-drawer results were thought to resemble more nearly the situation that is produced when the majority of the available aluminum is removed and replaced by an equivalent amount of sodium. A precise substitution of sodium for aluminum would have resulted in no reactivity change. The small positive reactivity changes are assumed to have resulted from the uncompensated addition of sodium and stainless steel.

The limited inventory of sodium restricted these measurements to a total insertion of approximately 90 kg sodium, or 25 v/o of the core at room temperature. The maximum amount of sodium that could be loaded into the clean core assembly with all the available aluminum removed was 32.5 v/o, whereas the sodium in the Enrico Fermi reactor core is 50.99 v/o with the control rod channels averaged over the entire core, or 47.2 v/o in the fuel region only.

The total sodium content of the Fermi core is approximately 184 kg at 20°C (density 0.97 g/cm^3) decreasing to 166 kg at 300°C (density 0.87 g/cm^3). By linear extrapolation of the sodium-substitution data, the average sodium worth is estimated to be 6.1 Ih/kg at 300°C, decreasing to 5.9 Ih/kg at 20°C.

By comparing the sodium worth of 5.9 Ih/kg and the minimum perturbation aluminum worth of 4.3 Ih/kg, one obtains an average core reactivity equivalence between equal volumes of sodium and 49.3% density aluminum. Since there is approximately 11 v/o void in the ZPR-III assembly in drawer clearances, etc., which is unavailable for loading, this corresponds to the use of an average aluminum density of 63%.

Utilizing the full-drawer aluminum substitution value of 3.8 Ih/kg, the equivalent aluminum density becomes 55.8%, corresponding to the use in ZPR-III of aluminum having an average density of 71%. This was approximated in the engineering-core loading by a combination of 63% and 100% density aluminum to provide an average aluminum density of 73% as noted in the subsequent engineering core description.

5. Depleted Uranium

Two separate series of substitutions were undertaken to determine the average worth of depleted uranium in the clean-core assembly. Columns of depleted uranium were both added and removed in various distributed fractions over the core. Also, the effect of actual placement of material within a drawer was investigated. The total amount of the U^{238} isotope in the reference core loading for these measurements was 1362.4 kg.

It should be noted that all of these substitutions involved the measurement of the worth of depleted uranium. No correction has been made for the contained U^{235}. The amount of the U^{235} isotope in the depleted uranium used in these tests is approximately one part in 500, while the distributed worth of U^{235} in the clean core is 51.6 Ih/kg. Therefore, the reactivity effect of the contained U^{235} is +0.10 Ih for each distributed kilogram of depleted uranium.

a. Initial Clean-core Assembly

In removing depleted uranium for this set of measurements, the general procedure was to replace a column of depleted uranium with a column of 100% density aluminum. Depleted uranium was added by removing a column of 63% density aluminum. In all cases, the relocation of other materials within a drawer was kept to a minimum. The locations for the addition and removal of depleted uranium were chosen on the basis of maximum physical separation from other columns of enriched or depleted uranium. Table XIII gives the sample column locations for each drawer type. The reference loadings for these drawer types are given Table III.

Table XIII

ADDED AND REMOVED COLUMNS OF DEPLETED URANIUM
(Letters indicated column identification, see Table III)

Drawer Loading No. (See Table III)	Added Uranium(1)	Removed Uranium(2)	Added Uranium(1) Adjacent to 25
1	P	D	J
2	M(3)	C	G
3	L	J	P
4	I(3)	F	M
5	Not changed	Not changed	Not changed
6	L	J	Not changed
7	I(3)	F	Not changed
8	A	Not changed	Not changed
9	P	C	G
10	G	P	M

(1)Removed one 15-in. column of 63% density Al.

(2)Added one 15-in. column of 100% density Al.

(3)Original material at this position exchanged with adjacent column of 63% density Al to enable U-for-63% Al substitutions.

The first series of substitutions consisted of four independent measurements in the same distributed eighth of the core, each with respect to the reference loading:

Test 4) removal of a column of depleted uranium at a position remote from a U^{235} column;

Test 5) addition of a column of depleted uranium at a position remote from a U^{235} column;

Test 8) addition of a column of depleted uranium adjacent to a U^{235} column; and

Test 9) a combination of 5) and 8).

A second series was undertaken to increase the observed reactivity effect by the removal of a column of depleted uranium over a distributed $\frac{1}{4}$ of the core, Test 3, and the addition of a column of depleted uranium over a distributed $\frac{1}{4}$ and $\frac{1}{2}$ of the core, Tests 6 and 7, respectively. The results of this and the preceding series are combined in Table XIV, Test Nos. 3-9, which also includes data on the composition, material change, reactivity change, and the resulting calculated worth of depleted uranium.

Table XIV

DISTRIBUTED WORTH OF DEPLETED URANIUM CONTAINING (~0 2% U^{235}) IN THE CLEAN CORE

Test No		1	2	3	4	5	6	7	8	9
Composition (Volume %)	Ref	-1/2	-1/4	-1/4	-1/8	+1/8	+1/4	+1/2	+1/8[1]	(+1/4)[2]
U^{235}	6 09	6 09	6 09	6 09	6 09	6 09	6 09	6 09	6 09	6 09
U^{238}	18 97	16 64	17 74	17 77	18 43	19 51	20 17	21 37	19 51	20 17
Al	25 14	25 29	25 21	26 36	25 73	24 76	24 36	23 60	24 76	24 36
SS	14 32	14 32	14 32	14 32	14 32	14 32	14 32	14 32	14 32	14 32
Mo	5 03	5 03	5 03	5 03	5 03	5 03	5 03	5 03	5 03	5 03
Zr	4 32	4 32	4 32	4 32	4 32	4 32	4 32	4 32	4 32	4 32
Number of drawers changed		158	80	78	38	38	78	155	38	38
% of Material added		-12 88	-6 34	6 34	3 09	3 09	6 34	12 63	3 09	6 18
Wt of depleted U added (kg)		-175 25	-88 75	86 283	42 036	42 036	86 304	171 806	42 036	84 072
Wt of Al added (kg)		1 46	0 74	12 433	6 058	-3 857	7 917	-15 733	-3 857	7 714
Reactivity (Ih) relative to ref		14 2	8 5	62 4	34 1	-30 4	59 8	-117 6	20 0	-52 2
of Al[3]		6 2	3 1	52 7	25 7	-17 1	35 1	69 7	17 1	-34 2
of depleted U		8 0	5 4	9 7	8 4	-13 3	-24 7	-47 9	-2 9	18 0
Worth of depleted U (Ih / kg)		-0 046	-0 061	-0 112	0 200	-0 316	0 286	-0 279	0 069	-0 214

(1) Column of depleted adjacent to U^{235}

(2) Combination of Runs No 5 and No 8

(3) Worth of Al taken as +4 43 Ih kg when the Al density decreases and +4 24 Ih / kg when the Al density increases

From Table XIV, it can be noted that, in the above runs, the aluminum worth represents from $\frac{1}{2}$ to $\frac{3}{4}$ of the total reactivity change. A third series was then arranged to reduce the aluminum correction by replacing a column of depleted uranium and two columns of 63% density aluminum with 3 columns of 45% density aluminum in a distributed $\frac{1}{4}$ and $\frac{1}{2}$ of the drawer. These data also appear in Table XIV for Tests No. 1 and No. 2. The aluminum worths used in Table XIV to determine the depleted uranium worth are the values resulting from the partial-drawer

aluminum substitutions as described in Section V,E,2. These values more nearly represent the local changes of aluminum density resulting from the addition or removal of a single column of aluminum per drawer.

b. Modified Clean-core Assembly

The modified clean-core assembly as described in Section V,E,2, was utilized to conduct a series of depleted uranium substitutions in which the average reactivity coefficient for depleted uranium upon addition or removal from the core could be determined as a function of the local aluminum density. The neighboring aluminum columns were adjusted in each loading to minimize the net variation in aluminum and the consequent aluminum correction. Although not in precise agreement with the preceding depleted uranium substitutions, these results show comparable trends.

Two experiments were run in which the depleted uranium density in the core was decreased, each with a different amount of aluminum present. One other experiment was run in which the depleted uranium density was increased. The drawer changes for each experiment are given in Table XV and summarized below.

Table XV

BASIC DRAWER LOADINGS, MODIFIED CLEAN CORE, DEPLETED URANIUM SUBSTITUTIONS

1/8-in. Columns, Left to Right Across Drawer Face

Experiment No.	Drawer Master No.	Drawer Column A	B	C	D	E	F	G	H	I	J	K	L	M	N	O	P
1	1 Reference	63%	Zr	63%	28	SS	45%	63%	28	25	63%	63%	63%	Mo	63%	28	63%
	1 Test	63%	Zr	63%	28	SS	45%	63%	28	25	45%	45%	63%	Mo	63%	45%	63%
	2 Reference	63%	Zr	28	63%	28	25	63%	45%	SS	28	63%	63%	63%	Mo	28	63%
	2 Test	63%	Zr	28	63%	28	25	63%	45%	SS	45%	63%	45%	45%	Mo	28	63%
	3 Reference	63%	28	25	63%	28	Zr	45%	SS	28	Mo	63%	63%	63%	28	25	63%
	3 Test	63%	28	25	63%	28	Zr	45%	SS	45%	Mo	63%	45%	45%	28	25	63%
	4 Reference	63%	28	Zr	63%	63%	63%	28	SS	45%	63%	28	25	63%	63%	Mo	28
	4 Test	63%	28	Zr	45%	45%	63%	45%	SS	45%	63%	28	25	63%	63%	Mo	28
2	1 Reference	63%	Zr	63%	28	SS	45%	63%	28	25	100%	100%	100%	Mo	63%	28	63%
	1 Test	63%	Zr	63%	28	SS	45%	63%	28	25	100%	100%	63%	Mo	63%	45%	63%
	2 Reference	63%	Zr	28	63%	28	25	63%	45%	SS	28	100%	100%	100%	Mo	28	63%
	2 Test	63%	Zr	28	63%	28	25	63%	45%	SS	45%	63%	100%	100%	Mo	28	63%
	3 Reference	63%	28	25	63%	28	Zr	45%	SS	28	Mo	100%	100%	100%	28	25	63%
	3 Test	63%	28	25	63%	28	Zr	45%	SS	45%	Mo	63%	100%	100%	28	25	63%
	4 Reference	63%	28	Zr	100%	100%	100%	28	SS	45%	63%	28	25	63%	63%	Mo	28
	4 Test	63%	28	Zr	100%	100%	63%	45%	SS	45%	63%	28	25	63%	63%	Mo	28
3	1 Reference	63%	Zr	63%	28	SS	45%	63%	28	25	63%	45%	63%	Mo	63%	28	63%
	1 Test	63%	Zr	63%	28	SS	45%	63%	28	25	63%	100%	28	Mo	63%	28	63%
	2 Reference	63%	Zr	28	63%	28	25	63%	45%	SS	28	63%	45%	63%	Mo	28	63%
	2 Test	63%	Zr	28	63%	28	25	63%	45%	SS	28	63%	100%	28	Mo	28	63%
	3 Reference	63%	28	25	63%	28	Zr	45%	SS	28	Mo	63%	45%	63%	28	25	63%
	3 Test	63%	28	25	63%	28	Zr	45%	SS	28	Mo	28	100%	63%	28	25	63%
	4 Reference	63%	28	Zr	63%	45%	63%	28	SS	45%	63%	28	25	63%	63%	Mo	28
	4 Test	63%	28	Zr	28	100%	63%	28	SS	45%	63%	28	25	63%	63%	Mo	28

Code: 25 - U^{235}-enriched Uranium
28 - Depleted Uranium
Zr - Zirconium
Mo - Molybdenum
SS - Stainless Steel
% - Per Cent Density Al

Experiment No.	Columns Removed	Columns Added
1	1 - U^{238} 2 - 63% Al	3 - 45% Al
2	1 - U^{238} 1 - 100% Al	1 - 63% Al 1 - 45% Al
3	1 - 63% Al 1 - 45% Al	1 - U^{238} 1 - 100% Al

The results of the three experiments are given in Table XVI.

Table XVI

DISTRIBUTED WORTH OF DEPLETED URANIUM IN THE CLEAN CORE

	Experiment No. 1			Experiment No. 2			Experiment No. 3		
Composition	Ref.	A**	B**	Ref.	A**	B**	Ref.	A**	B**
U^{235}	6.08	6.08	6.08	6.05	6.05	6.05	6.10	6.10	6.10
U^{238}	18.88	17.58	16.33	18.85	17.62	16.37	18.80	20.03	21.28
Al	24.63	24.75	24.80	27.42	27.53	27.63	24.18	24.06	23.98
SS	14.32	14.32	14.32	14.32	14.32	14.32	14.32	14.32	14.32
Mo	5.03	5.03	5.03	5.03	5.03	5.03	5.03	5.03	5.03
Zr	4.32	4.32	4.32	4.32	4.32	4.32	4.32	4.32	4.32
Number of drawers changed		81	162		81	162		81	162
Wt of depleted U added (kg)		-89.60	-179.20		-89.60	-179.20		89.66	179.32
Wt of Al added (kg)		0.89	1.78		1.03	2.06		-1.03	-2.03
Reactivity (Ih):									
relative to reference		11.85	20.70		26.65	50.95		-32.50	-69.10
of Al*		3.77	7.55		4.36	8.73		-4.56	-9.00
of depleted U		8.08	13.15		22.29	42.22		-27.94	-60.10
Worth of depleted U (Ih/kg)		-0.090	-0.073		-0.249	-0.236		-0.312	-0.335
Incremental worth of depleted U		-0.057			-0.223			-0.360	

*Worth of Al taken as 4.43 Ih/kg when Al is removed and 4.24 Ih/kg when Al is added.

**Test A was done with a distributed quarter of the core, Test B with a distributed half of the core.

6. Stainless Steel for Depleted Uranium

A direct substitution of stainless steel for depleted uranium was made in a distributed $\frac{1}{8}$ and $\frac{1}{4}$ of the core during the initial clean core experiments. In drawers loaded as type 1 and 2 (see Table III), a direct substitution of two columns of stainless steel for two columns of depleted uranium was affected; in drawers of type 3 and 4, two columns of stainless steel were substituted for two columns of depleted uranium with an accompanying shift of one column of aluminum by one position; in drawers of types 9 and 10 (seeded drawers), only one column of depleted uranium was replaced by stainless steel. The drawer types were arranged for these measurements as shown in Fig. 10. In all cases, no depleted uranium was removed if adjacent to enriched uranium. The results of the substitution are given in Table XVII.

Table XVII

RELATIVE WORTH OF DEPLETED URANIUM VS. STAINLESS STEEL DISTRIBUTED IN CLEAN CORE

	Drawer Loading Type	No. of Drawers	No. of Columns	Wt of Depleted (kg)	Wt of SS (kg)	Reactivity (Ih)
$\frac{1}{8}$ of Core*	1	11	22			
	2	9	18			
	3	7	14			
	4	10	20			
	9	1	1			
	10	0	0			
			75	-83.0	35.1	58.8
Additional $\frac{1}{8}$ of Core*	1	11	22			
	2	8	16			
	3	7	14			
	4	8	16			
	9	1	1			
	10	2	2			
			71	-78.6	33.2	58.1
Total $\frac{1}{4}$ Core*			146	-161.6	68.3	116.9

*Distributed fraction of the core as shown in Fig. 14.

Mid-radius Annular Ring in Core. An annular ring of 28 core drawers in each half located at an average radius of 11.2 in. was utilized for a series of substitution measurements. These drawers are identified in Fig. 15 by the small circles. The substitutions were made in the front 5 in. of the drawer in each half of the assembly, thus producing an annular test region in the core, approximately 2 in. thick and 10 in. high, centered about the midplane of the core at an average radius of 11.2 in. A second column of stainless steel was inserted in each of the 56 test drawers, replacing a column of 45% density aluminum. This was used as the reference loading to allow a larger variation in the stainless steel than would have been available with the single column of steel per drawer.

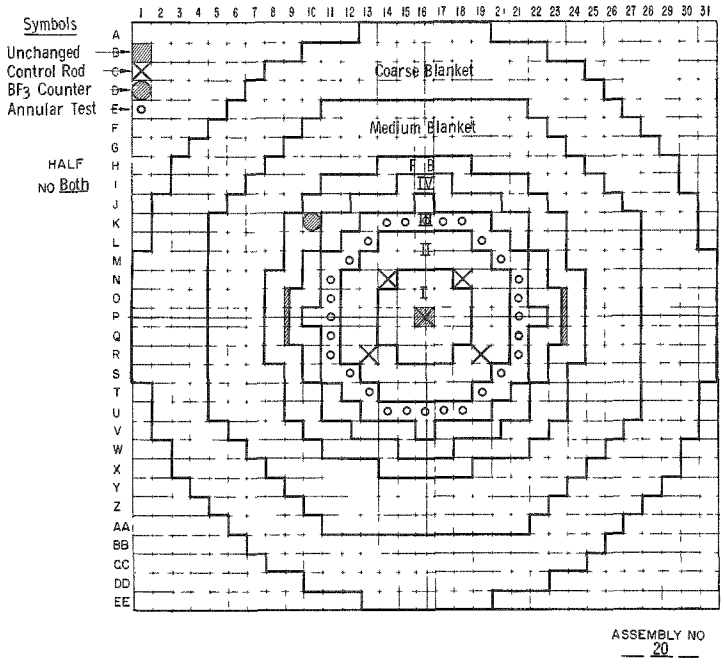

Fig. 15. Material-substitution Test Regions, Interface View of Clean Core.

An average of 7 columns of 100% density aluminum were substituted for a like number of columns of 63% density aluminum in the front 5 in. of each test drawer to obtain the aluminum worth. Stainless steel, molybdenum, and zirconium were each replaced by 45% density aluminum. For each substitution, the remaining materials in the drawer were those of the reference loading. Table XVIII gives the results of these tests.

Table XVIII

WORTHS OF VARIOUS CORE MATERIALS IN ANNULAR RING AT 11.2-IN. RADIUS

	Al	SS	Mo	Zr
Number of 5-in. Columns Changed	388	112	56	56
Material change	100% Al for 63% Al	45% Al for SS	45% Al for Mo	45% Al for Zr
Weight of material (kg)	-13.12	-17.42	-11.72	-7.07
Weight of aluminum (kg)	20.61	2.64	1.32	1.32
Reactivity (Ih):				
relative to reference	35.0	-2.8	23.1	-12.7
of aluminum	0	12.32	6.16	6.16
of material	35.0	-15.1	16.9	-18.9
Worth of material (Ih/kg)	4.67	0.867	-1.44	2.67

Radial Dependence of Aluminum Worth in Core and Fine Blanket. At the conclusion of the full-drawer aluminum-substitution measurements as described in Section V,E,1, half of the core drawers contained 100% density aluminum with the reference combination of 63 and 45% density aluminum in the remaining half of the core. With this loading as a new reference, the core was divided into four radial regions (see Fig. 15), and measurements of the aluminum worth were made as a function of radial position by substituting 45% density aluminum for the 100% density aluminum.

During this series of measurements, the reactivity lost by removing aluminum was compensated by the addition of seeded drawers and by substitution of 100% density aluminum for the 45% density aluminum in the fine blanket. This provided a measurement of the aluminum worth as well as the necessary compensating reactivity. However, this procedure may have introduced an additional effect that modified the experimental values for aluminum worth in the core, as evidenced by the higher average core worth obtained in these measurements compared with the value obtained from the full-drawer aluminum-substitution measurements described in Section V,E,1. The results of these substitutions are given in Table XIX. Since region IV involved a large net reactivity change, this substitution was done in two steps, first Half No. 2 and then Half No. 1; then the average value obtained.

Table XIX

ALUMINUM DENSITY COEFFICIENT AS FUNCTION OF RADIUS

Region[1]	Core[2] I	Core[2] II	Core[2] III	Core[2] IV	Fine[3] Blanket	
Average radius (in.):	3.90	8.19	11.72	14.50	17.83	
Inner-Outer (in.)	1.23-5.64	5.64-10.22	10.22-13.07	13.07-15.63	15.63-18.77	
Number of drawers changed	20	49	43	52	71	71
Weight of Al added (kg)	-12.6	-30.2	-26.5	-31.1	33.0	33.0
Reactivity change (Ih)	-22.2	-94.9	-125.6	-157.4	80.5	86.9
Worth of Al (Ih/kg)	1.76	3.15	4.75	5.07	2.43	2.63
Average worth of Al (Ih/kg)		4.00			2.53	

(1) See Fig. 15 for location of regions.
(2) 45% Al was substituted for 100% Al in the core.
(3) 100% Al was substituted for 45% Al in the fine blanket.

F. Inhomogeneity Effects

The use of $\frac{1}{8}$-in.-thick columns of highly enriched and depleted uranium in ZPR-III represents an inherent limitation of this facility in simulating a large, homogeneous, low-enrichment core. Therefore, limited quantities of partially enriched uranium (31.3% U^{235}) in the form of $\frac{1}{8}$-in.-thick plates and highly enriched uranium (93.2% U^{235}) in the form of $\frac{1}{16}$-in.-thick plates were obtained to determine the reactivity effects introduced by the use of relatively thick pieces of highly enriched and depleted uranium.

Two series of experiments were conducted to define these effects. The first series involved establishing a reference with a uniform drawer loading. In this loading, two adjacent $\frac{1}{16}$-in. columns of U^{235} replaced the $\frac{1}{8}$-in. column of U^{235}. Subsequent measurements were then made with the $\frac{1}{16}$-in. columns separated and bunched ($\frac{3}{16}$-in.) with no net change in core materials. The data obtained allowed extrapolation to zero thickness U^{235}, which then represents a completely homogeneous system.

The second series provided for the direct substitution of three adjacent columns of 31.3% enriched U^{235} for a three-column sandwich of $\frac{1}{8}$-in. columns, formed by two limiting columns of U^{238} and one center column of U^{235}. A uniform drawer loading was also used in the test region for this series. The 31.3% enrichment was chosen to duplicate precisely the average enrichment of the combination of the two columns of depleted

uranium and one column of enriched uranium. A subsequent measurement was also made with the three columns of 31.3% enriched material separated or "unbunched." A comparison between the "bunched" U^{238}, U^{235}, U^{238} and the "bunched" 31.3% enriched uranium provides the necessary correction to compensate for the use of highly enriched material.

Detailed U^{235} and U^{238} fission foil traverses were conducted over a region of minimum flux gradient during each of the above series of measurements to determine the fine structure of the fission distribution in the region of the uranium columns. Special $\frac{1}{8}$-in. plates of U^{238} with provisions for the insertion of foils enabled foil traverses to be made within a plate as well as between plates.

Enrichment and Bunching Effects. A wedge-shaped portion of the core extending along the full axial length of the core was loaded with a uniform drawer loading as a reference. This region, containing 32 drawers in each half, is shown in Fig. 16. The drawers around the periphery of the test region were loaded with the uniform reference drawer loading over the full length of the core region and were not changed during the test measurements. These "buffer" drawers were utilized to minimize undesirable reactivity changes due to the interaction of core material in the bunched drawers with the remainder of the clean-core loading.

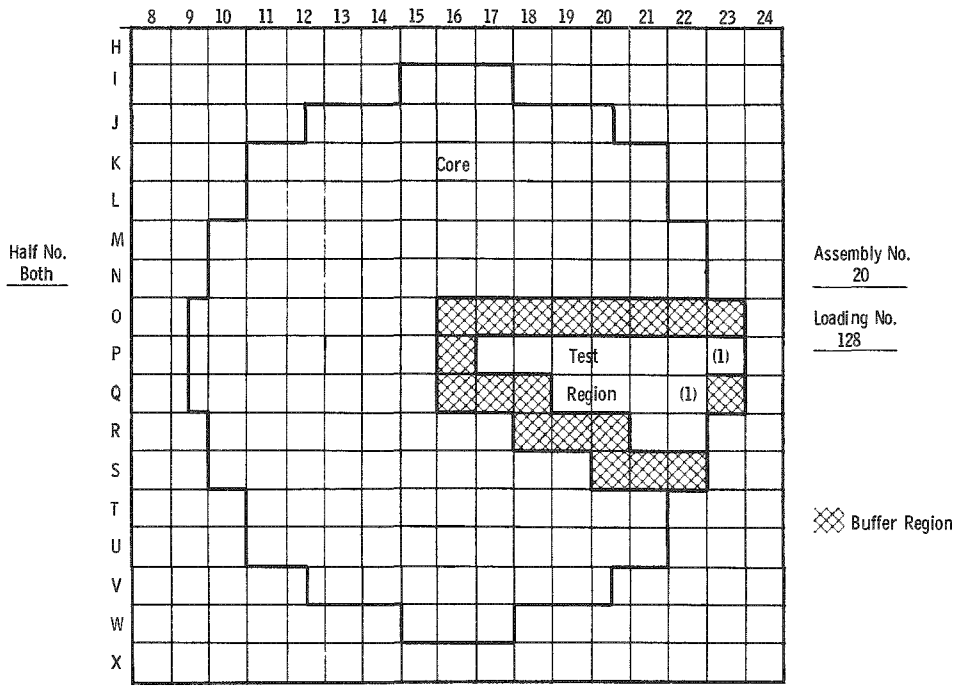

Fig. 16. Test Region for Inhomogeneity Effects

(1) indicates test drawers in Half No. 1 only, Buffer drawers in this position in Half No. 2.

The uniform reference drawer loading is shown in cross section as configuration A in Fig. 17. The requirement of loading the buffer and test regions with a uniform drawer configuration resulted in a somewhat lower uranium density in this region than in the remainder of the core. Table XX is a comparison of the v/o composition of the test region with the composition of the remaining core drawers.

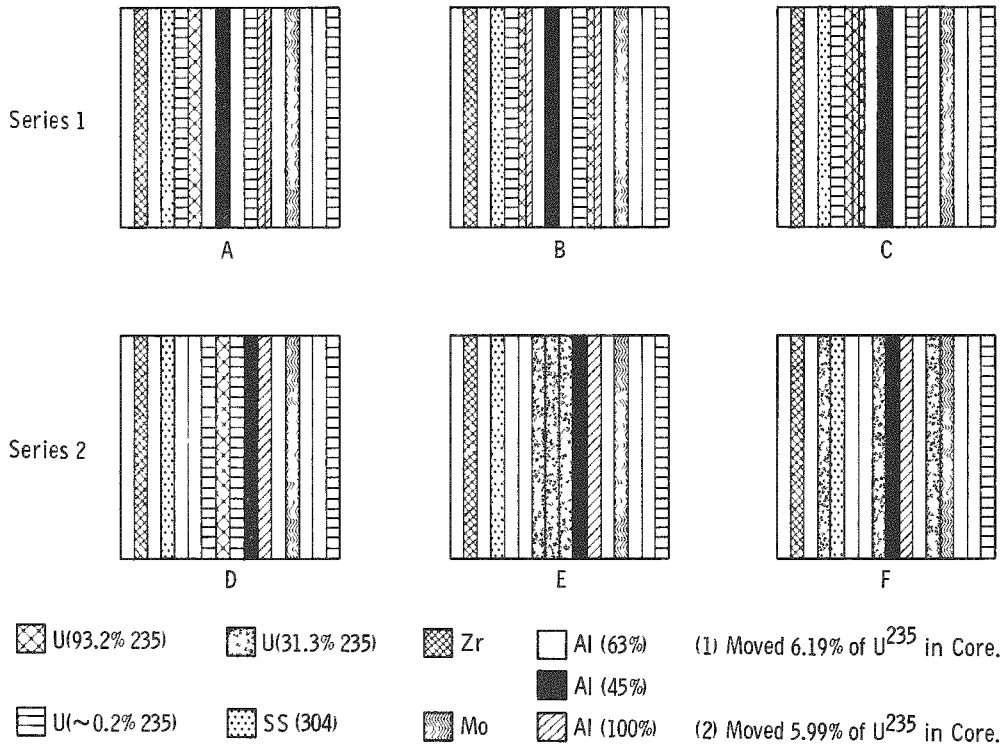

Fig. 17. Drawer Loadings for Inhomogeneity Experiments.

Table XX

COMPARISON OF MATERIALS IN TEST REGION AND REMAINDER OF CLEAN CORE FOR INHOMOGENEITY EXPERIMENTS

Material	Composition of Test Region (v/o)	Composition of Remainder of Clean Core (v/o)
U^{235}	4.70	6.09
U^{238}	15.19	18.97
Aluminum	31.30	25.14
Stainless Steel	14.32	14.32
Molybdenum	5.03	5.03
Zirconium	4.32	4.32

The various loadings are enumerated and the resulting test data given in Table XXI. The radial movement of U^{235} in the transition from configuration A to configuration B (see Fig. 17) in one half was compensated by the opposite displacement of the U^{235} in the opposing half. This is a consequence of the use of the same drawer loading in both halves rather than having the drawers in one half the mirror image of the drawers in the opposing half. Configuration C, however, involved the shifting of the $\frac{1}{16}$-in. columns of U^{235} to neighboring drawers. The pattern utilized was chosen to minimize the reactivity effect of the net radial movement of fuel and is shown in Fig. 18. The net effect of this radial movement was not determined experimentally and could conceivably represent as much as a 70% increase in the positive reactivity effect of the $\frac{3}{16}$-in. bunching. A correction of this magnitude would linearize the data resulting from configurations A, B, and C.

Table XXI

RESULTS OF INHOMOGENEITY EXPERIMENTS

Type Loading	Test Configuration (see Fig. 17)	Reactivity Change with Respect to Reference Loading, Ih	Test Fraction[2] of Clean-core Critical Mass, %
$\frac{2}{16}$-in. U^{235} bunched (reference)	A	0	6.15
$\frac{2}{16}$-in. U^{235} unbunched	B	-11.8	6.15
$\frac{3}{16}$-in. U^{235} bunched	C	+21.6	6.15
238-235-238 sandwich	D	+5.0	5.95
$\frac{3}{8}$-in. 31.3% bunched	E	-11.6[1]	5.95
31.3% unbunched	F	-27.1[1]	5.95

[1] Corrected for increase of 164 g U^{235} with respect to reference. Utilized average clean core worth of 51.6 Ih/kg U^{235}.

[2] Clean-core Critical Mass = 431.5 kg U^{235}. Critical Mass of As-Loaded Test core is 434 kg U^{235}, resulting from lower density of uranium in test region.

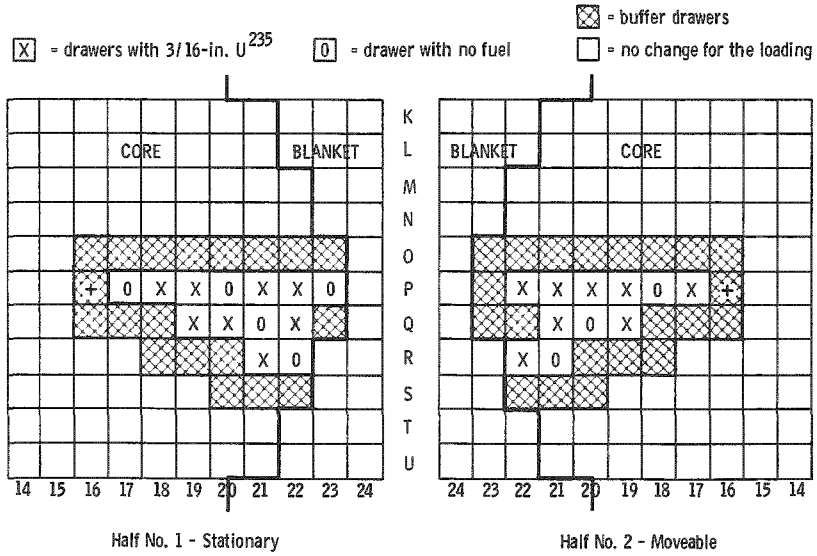

Fig. 18

Pattern for $\frac{3}{16}$-in. Bunching in Full-Length Wedge of Core.

The substitution of 31.3% enriched U^{235} columns involved a slight mass change (less than 0.1%) in loadings E and F with respect to D, resulting from the use of differing plate sizes. The data shown in Table XXI have been corrected for this U^{235} increase as noted.

Foil Traverses through Test Drawer Loadings. A 21-drawer test region, 7 in. deep in each half, was constructed at the core center in a manner similar to the preceding axial wedge. The drawers were loaded in the various configurations with numerous U^{235} and U^{238} foils located 1 in. back from the assembly interface across the width of the central drawers. Irradiation and counting of these foils provided a detailed mapping of the relative U^{235} and U^{238} fission rates across a single drawer. These traverses are shown in Figs. 19-23. The U^{235} and U^{238} data have been arbitrarily normalized at one point and show relative rates only. The U^{235} fission rate is not comparable with the U^{238} rate.

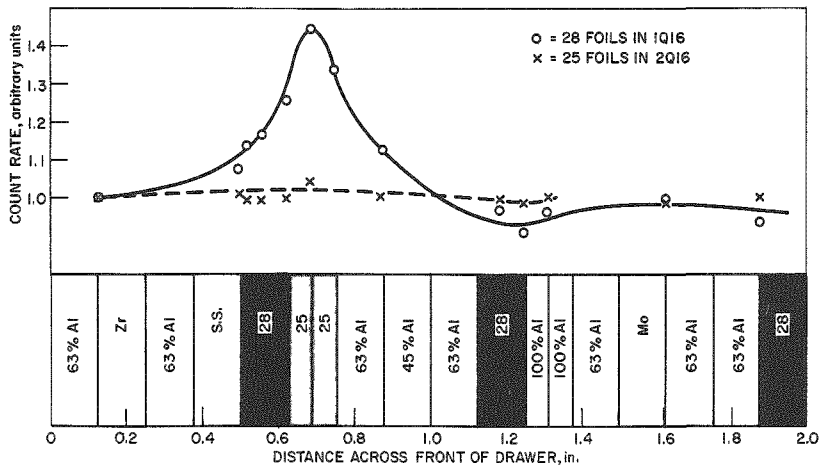

Fig. 19. Single-drawer Fission Rate Distribution, Configuration A

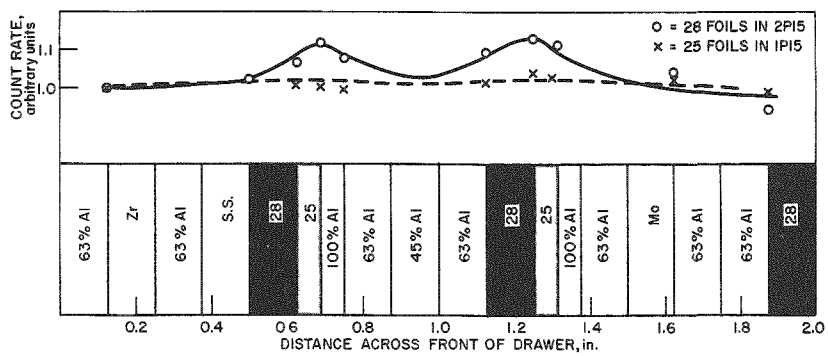

Fig. 20. Single-drawer Fission Rate Distribution, Configuration B

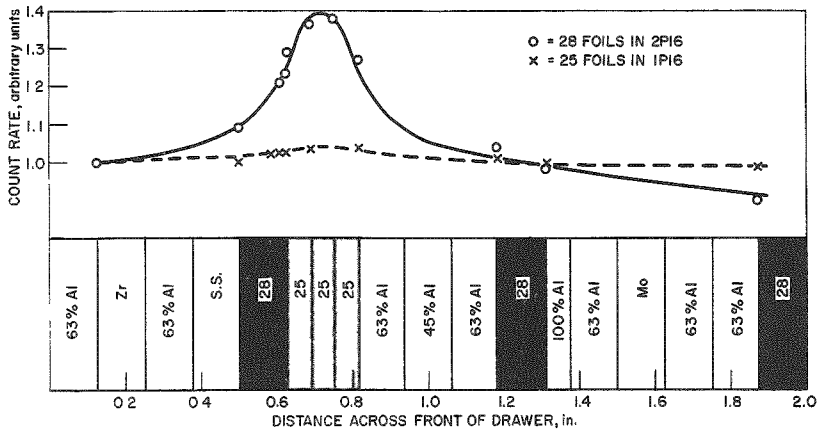

Fig. 21. Single-drawer Fission Rate Distribution, Configuration C

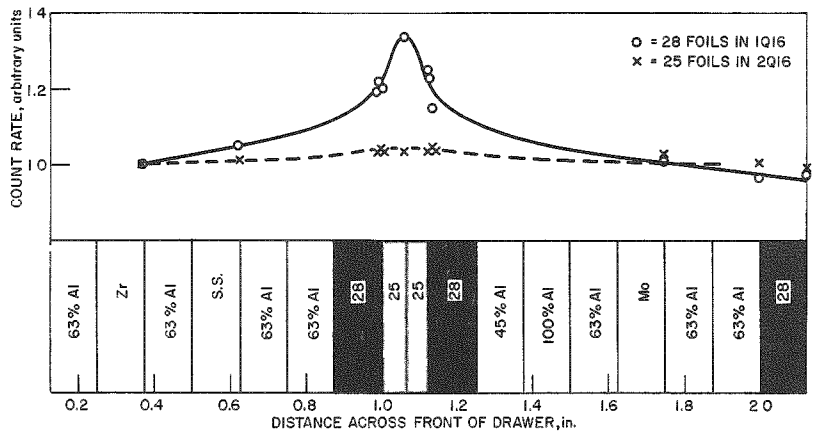

Fig. 22. Single-drawer Fission Rate Distribution, Configuration D

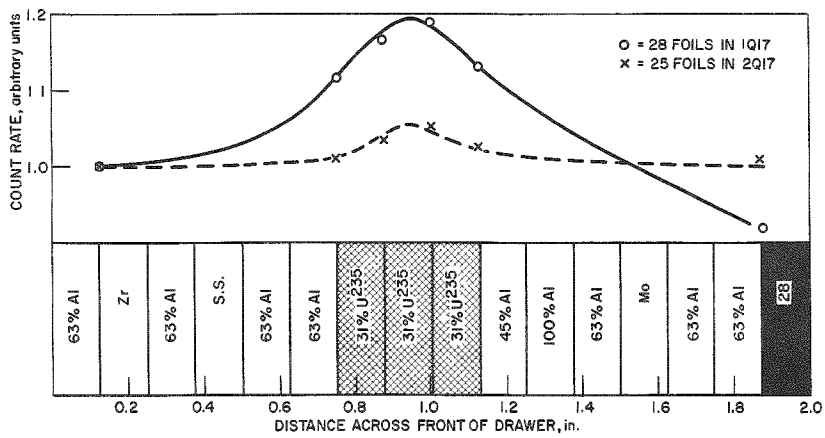

Fig. 23. Single-drawer Fission Rate Distribution, Configuration E

G. Spectral Indices

Central Fission Ratios. A series of central-core fission ratios were obtained on the clean-core loading with absolute-type fission chambers containing a known quantity of the test material. These detectors have been described in detail by F. S. Kirn[12] and the method evaluated by W. G. Davey and R. N. Curran.[13]

Two detectors, one of which contained a known quantity of U^{235}, were inserted at the center of the core for each measurement. The second detector contained a known quantity of the test material, thereby providing a direct measurement of the fission ratio. The detectors each occupied a volume, 1 in. deep by 2 $in.^2$, at the front of the two central drawers (P-16). The leads were brought out axially with the remaining drawer composition unchanged from the clean core loading. The data obtained from these measurements are given in Table XXII.

Table XXII

FISSION RATIOS AT CENTER OF CLEAN-CORE ASSEMBLY

Material	Counter	$\frac{\sigma_f(\text{Material})}{\sigma_f(U^{235})}$ [1]	Average
U^{238}	2	0.0356[2]	0.0351[2]
U^{238}	3	0.0345[2]	
U^{234}	8	0.296[2]	0.288[2]
U^{234}	11	0.280[2]	
U^{233}	16	1.517	1.517
Pu^{239}	20	1.149	1.147
Pu^{239}	21	1.145	
Pu^{240}	12	0.319[2]	0.319[2]

[1] All ratios determined with respect to counter No. 5 (U^{235}).

[2] These ratios have been adjusted to include the following absolute fission counter wall corrections implied by Ref. 13:

U^{238}	0.92
U^{234}	0.96
Pu^{240}	0.96

U^{238} Capture Rate. Radiochemical analyses of irradiated U^{235}-enriched and depleted-uranium foils by S. Skladzien provided radial and axial traverses of the relative U^{238} capture rates in the clean-core

assembly, as shown in Fig. 24, along with a measurement of the U^{238} capture to U^{235} fission ratio at the core center.(14) This value was determined radiochemically to be

$$\left[\frac{\sigma_c(28)}{\sigma_f(25)}\right]_{\text{core center}} = 0.100 \pm 0.004$$

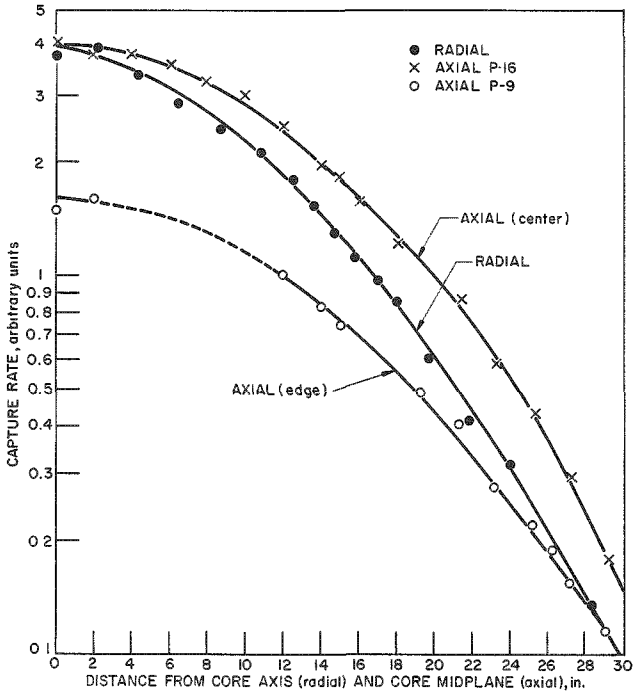

Fig. 24

U^{238} Capture Rates in Clean-core Assembly (Radiochemical Analysis of Irradiated Foils)

Nuclear Track Plate Irradiations. Four types of nuclear track emulsions were irradiated at the core center and at the axial core blanket interface on the core axis. Three plates of each type were irradiated at both locations. The plates were prepared and developed by J. H. Roberts of Northwestern University.(15) The emulsion types and estimated exposures are as follows:

Emulsion Type	Emulsion Thickness, μ	nvt, neutrons/cm-sec
L-1	200	0.27×10^9
E-1	200	7.2×10^9
E-1 (Li-6 loaded)	200	1.9×10^9
C-2	400	1.1×10^9

H. U^{238} and U^{235} Fission Rate Traverses

Enriched and depleted uranium foils were irradiated in the clean core along a radius at the core midplane.(16) The 1-in.-diameter, 20-mil-thick U^{238} and 5-mil-thick U^{235} foils were wrapped in thin aluminum foil

and inserted inside the drawer fronts such that the plane of the foil was parallel to the assembly interface. This provided an integration of the local flux distribution in a single drawer over the area of the foils. Similar foils placed near the radial core-blanket interface were inserted between columns of material to obtain a better resolution of the gradient in this region. As a result of the local flux perturbations in a core drawer, some variation from a smooth fission rate curve is to be expected in the core region. However, the fine radial blanket in this immediate region was reloaded in a relatively homogeneous manner with $\frac{1}{8}$-in. columns of depleted uranium, aluminum, and stainless steel to produce a smooth local flux gradient for these measurements.

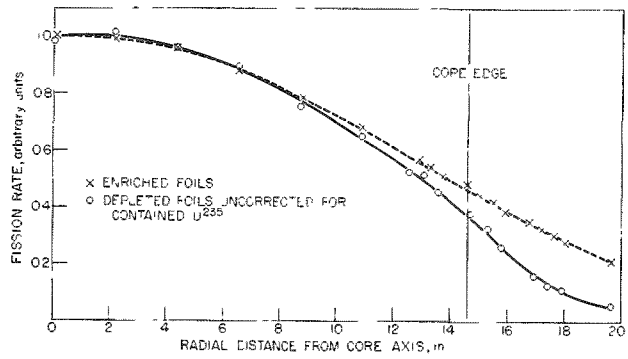

Fig. 25. Radial Fission Rates in Clean Core at Midplane (Through P-Row at Interface) (Foils)

The data obtained from these measurements are shown graphically in Fig. 25. Both curves are normalized to unity at the core center. The U^{238} curve has not been corrected for the U^{235} content (~0.2% U^{235}) in the depleted uranium foil.

Figure 26 is a plot of the ratio $\sigma_f(U^{238})/\sigma_f(U^{235})$ obtained by using the smoothed curves of Fig. 25 and correcting for the fraction of U^{235} in the depleted foils by utilizing the measured value* $\sigma_f(U^{238})/\sigma_f(U^{235}) = 0.0381$ at the core center and the relation:

$$\text{Count rate (CR) (depleted foils)} \propto 0.998\ \sigma_f(U^{238}) + 0.002\ \sigma_f(U^{235}) \quad .$$

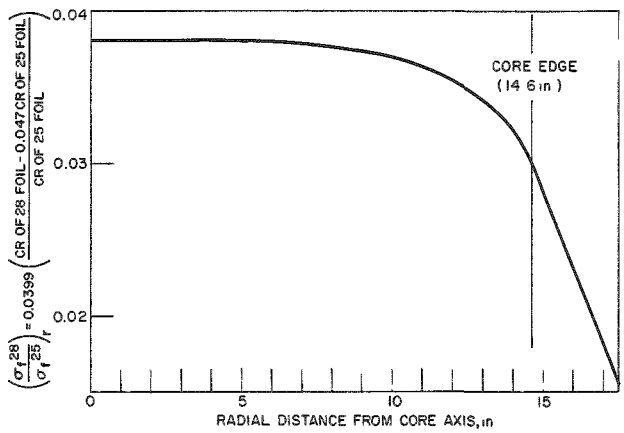

Fig. 26

Radial Variation of $\sigma_f(U^{238})/\sigma_f(U^{235})$ at Midplane of Clean Core

*The absolute fission counter wall correction given in Table XXII has not been included here.

Thus, one obtains

$$\frac{\sigma_f(U^{238})}{\sigma_f(U^{235})} = 0.0399 \left[\frac{\text{CR (depleted foils)} - 0.047\ \text{CR (enriched foils)}}{\text{CR (enriched foils)}} \right]$$

I. Reactivity Worth of Hydrogen

A hypothetical accident in which hydrogenous material is admitted to the primary sodium coolant of the Fermi reactor was simulated in the clean-core assembly. Measurements were performed by producing a mockup of a diffused "front" of hydrogenous material progressing axially through the core and fine blanket in much the same manner as it would in the sodium stream in the actual reactor. Thin, 2-by-5-in. strips of polyethylene $(CH_2)_n$ weighing an average of 0.777 g each were laid on the tops of the ZPR-III drawers, with the exception of the 5 control and safety rod drawers. A total of 155.5 core drawers and 71.5 fine blanket drawers were involved (see Fig. 7).

The first loading involved placing the 5-in. strips of polyethylene in the region extending from 15 to 20 in. from the core midplane in one half of the assembly. This represents a 5-in.-deep region in the radial and axial blanket immediately adjacent to the cylindrical end of the core. Subsequent loadings represented 5-in. additions to the hydrogenous front as it approached the core midplane through the core and fine blanket. The reactivity effect was assumed to be symmetrical about the core midplane; thus, the measurement was terminated when half of the assembly was loaded with polyethylene from the midplane (0-in.) to 5 in. beyond the core end (20 in.). The data resulting from these loadings are given in Table XXIII.

Table XXIII

REACTIVITY EFFECT OF POLYETHYLENE IN CORE AND FINE BLANKET

Distance of Polyethylene from Midplane (in.)	Total Weight of Polyethylene in Reactor (g)	Reactivity Change due to Polyethylene (Ih)
20 - 15	176.2	-6.1
20 - 10	354.5	+3.2
20 - 5	527.7	26.4
20 - 0	704.7	60.7

A negative reactivity effect of the polyethylene in the radial and axial end blanket was observed. The polyethylene was removed from the radial fine blanket, which resulted in a reactivity increase of 37.1 Ih for

the removal of 221 g polyethylene from the 71.5 fine blanket drawers in half of the assembly. The worth of the polyethylene in half of the core and one axial end blanket was therefore +97.8 Ih for 483.7 g polyethylene. This would be expected to increase to +103.9 Ih for the 362.7 g polyethylene in one half of the core alone by removing the 5 in. in the axial end blanket, neglecting corner effects.

J. Rossi-alpha Measurement for Neutron Lifetime

A measurement[17] of the value of the Rossi alpha for the Fermi clean-core assembly was obtained in six runs which yielded the following results:

Run	Rossi Alpha, 10^4 sec^{-1}
1	4.61
2	4.65
3	4.44
4	4.55
5	4.52
6	4.46
Average	4.55

Since these runs were all made at 5.5-Ih subcritical, a correction of -1.8% must be applied to the value of alpha to obtain the delayed critical value. The uncertainty of the above average is estimated to be ±2%. Therefore, the best value for alpha is

$$4.47 \pm 0.09 \times 10^4 \text{ sec}^{-1} \quad .$$

At delayed critical, the neutron lifetime ℓ is

$$\ell = \beta/\alpha \quad ,$$

where β is the delayed-neutron fraction and α is the measured Rossi alpha. Utilizing the value of 0.00687 for β with an uncertainty of at least 4%, resulting from a 3% uncertainty in the absolute delayed-neutron yield and an uncertainty of 2% in ν, one obtains a value for the neutron lifetime of

$$\ell = 15.35 \pm 0.80 \times 10^{-8} \text{ sec} \quad .$$

VI. ENGINEERING-CORE EXPERIMENTS

A. Description of the Engineering-core Mockup

The construction of the engineering-core mockup of the Fermi reactor involved the use of the radial blanket loading of the clean core as described in Section V,B. The core and axial blanket regions were reloaded to duplicate the geometry and composition of the Fermi reactor. The core geometry was mocked up by loading 15.5 in. of core material in Half No. 1 and 15.0 in. in Half No. 2. These partial core lengths, together with the interface dimension, gave a core height of 30.60 in., thus placing the core midplane 0.250 in. from the interface in Half No. 1. The 3.713-in. upper and 5.963-in. lower axial end gaps in the Fermi design were simulated in the ZPR-III loading by a 3.500-in. end gap in Half No. 1 and a 6.000-in. end gap in Half No. 2. Measurements were made during the course of the experimental work to determine the effect of increasing the 3.500-in. end gap in Half No. 1 to 4.000 in. to bracket the design dimension of 3.713 in. The composition of the axial core end blanket was also revised over the clean-core loading better to approximate that of the Fermi design. The control and safety rod channels within the core and axial blanket were initially loaded in slightly off-design compensating positions to simplify the individual, adjacent ZPR-III drawer loadings. Relocating these channels in subsequent experiments provided the necessary reactivity correction on the critical mass.

With the exception of those for measuring the reactivity worth of the oscillator rod and wave shape, all the experiments conducted with the engineering core utilized a clean loading, i.e., the mockup control and safety rod channels contained low-density aluminum only. The presence of boron carbide in the two central shim and regulating rod channels would be expected to affect only the local fission rate distribution and the worths of the mockup fuel subassembly in the central region.

Figure 27 shows the ZPR-III assembly loading through the midplane of the reactor. Figure 28 is an overlay of the ZPR-III loading on the Fermi reactor geometry. It should be noted that the radial core boundaries of both the Fermi core and the ZPR-III core mockup are identical. It was possible to duplicate the cross-sectional area of the Fermi core in ZPR-III to within $\frac{1}{4}$ in.^{2}. The area of the Fermi 91-subassembly core with 10 control channels is 732.48 in.^{2} compared with the ZPR-III mockup core area of 732.72 in.^{2}. The total area (72.50 in.^{2}) of the mocked-up core devoted to control and safety rod channels was within 0.02 in.^{2} of the total area of the Fermi channels. Figure 29 shows a detailed comparison of the positioning of the ZPR-III mocked-up control channels and the Fermi control channels.

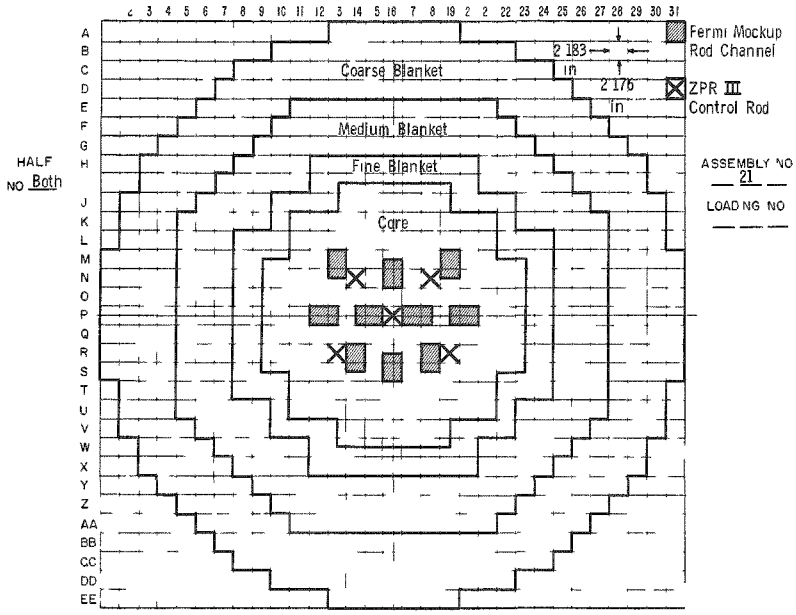

Fig. 27

ZPR-III Loading for Fermi Engineering-core Assembly

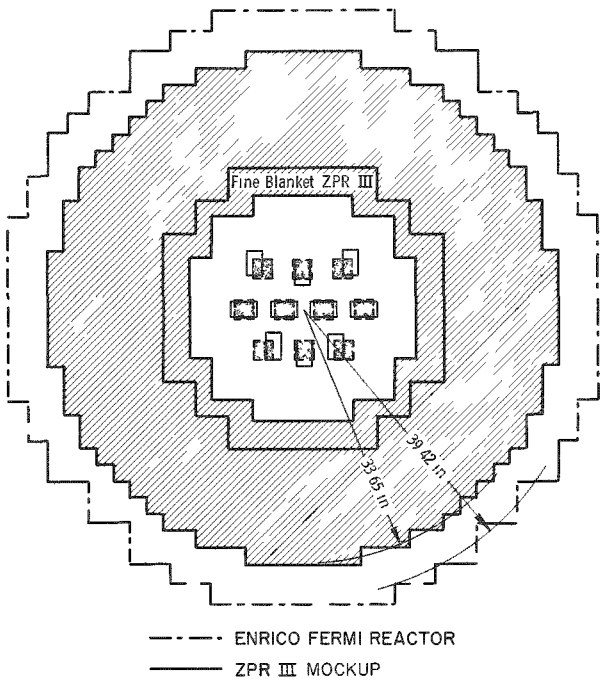

Fig 28 Comparison of ZPR-III Engineering Mockup and Fermi Reactor Cross Sections

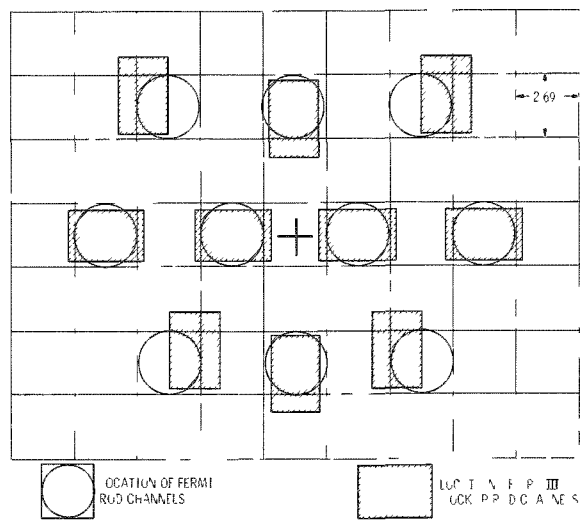

Fig 29 Mockup and Design Control Channel Locations on Fermi Matrix

The average dimensions of the matrix cell of the ZPR-III machine are 2.176 in. vertically by 2.183 in. horizontally, compared with the unit cell dimension of 2.693 in.[2] for the Fermi reactor.

Core Composition and Critical Mass. As in the clean-core loading, the v/o composition of the Fermi reactor did not easily allow a uniform single-drawer type of loading for ZPR-III. Consequently, it was necessary to devise a multidrawer unit cell having an average composition as close as possible to that of the fuel region of the Fermi core. A four-drawer unit cell was selected, consisting of the drawer master sequence Nos. 1-2-3-2, as shown in Table XXIV. This average composition was also distributed as uniformly as possible over the partial core edge drawers and in the partial core drawers bordering the mocked-up rod channels. Figure 30 shows the array of these normal drawers as they were loaded in the assembly. The average aluminum density in the core

Table XXIV

BASIC DRAWER LOADINGS FOR ENGINEERING-CORE ASSEMBLY

1/8-in. Columns Left to Right Across Drawer Face

Drawer Loading	A	B	C	D	E	F	G	H	I	J	K	L	M	N	O	P
1	28	63%	100%	Zr	28	63%	63%	28	25	63%	SS	100%	Mo	63%	28	63%
2	63%	28	25	100%	Zr	28	63%	SS	63%	28	Mo	100%	28	25	63%	63%
3	28	63%	100%	Zr	28	63%	63%	28	25	100%	SS	28	Mo	63%	28	63%
4 (Seed)	28	100%	Zr	28	25	63%	63%	SS	28	63%	100%	28	25	63%	Mo	63%

Normal Unit Cell No. 1 - No. 2 - No. 3 - No. 2

Seeded Unit Cell No. 1 - No. 2 - No. 4 - No. 2

Code: 28 - U^{238}
25 - U^{235}
SS - Stainless Steel
Mo - Molybdenum
Zr - Zirconium
% - Refers to aluminum density

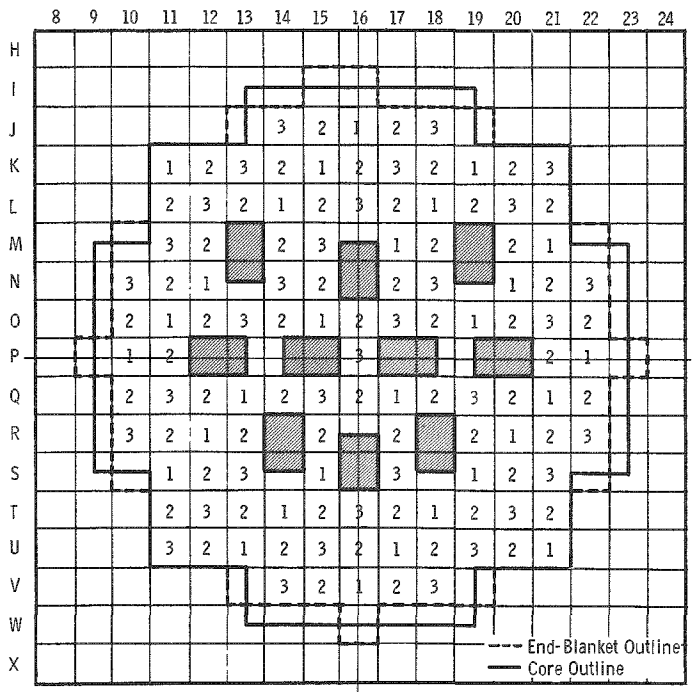

Fig. 30

Engineering-core Drawer Masters and End Blanket Outline

and fine blanket of the engineering-core mockup was increased over that used for the clean-core experiments as a result of the full-drawer aluminum-substitution and sodium-substitution experiments with the clean core. These measurements indicated an equivalence between sodium and an average aluminum piece density of 71%. An average density of 73% was achieved at pieces in the engineering-core loading.

In order to alter the available reactivity without changing either the geometry or the total uranium in the core, it was necessary to use "seeded" drawers, as was done in the Fermi clean-core experiment. Seeding was accomplished by replacing a column of depleted uranium in a No. 3 drawer with a column of enriched uranium, thus making it a No. 4 drawer. The "seeded" four-drawer unit cell has the sequence Nos. 1-2-4-2. The core, as originally planned with no seeded drawers, shown in Fig. 30, contained 430.0 kg U^{235} and was subcritical by 233.9 Ih. This was determined by adding 4 seeded drawers worth 257.7 Ih to produce a clean core which was 23.8 Ih supercritical. By means of the distributed worth of U^{235} as determined for the clean core of 51.6 Ih/kg, a clean cold (17.0°C) critical mass of 434.4 kg U^{235} is obtained for the loading as described. The volume of the engineering-core mockup was 367.3 liters as compared with the Fermi core volume of 371.5 liters. This resulted primarily from the reduced height (30.60 in.) of the mockup. Figure 31 is a horizontal cross section of the ZPR-III loading showing the dimensions associated with the axial end gaps and the axial end blanket. The detailed compositions of the core, control rod channels, end gaps, etc., are given in Table XXV. A comparison of the Fermi engineering-core design composition and the critical ZPR-III engineering mockup is given in Table II. Because of the inventory limitation on the smaller-sized pieces of depleted uranium, it was not possible to load sufficient blanket material into the core region to enable the approach to criticality by replacing blanket material with core material at increasing radii. Instead, the entire core region was initially loaded with core material, except that aluminum replaced the U^{235} in a one-drawer annular rectangular section through the K and U horizontal rows and the No. 11 and No. 21 vertical columns in both

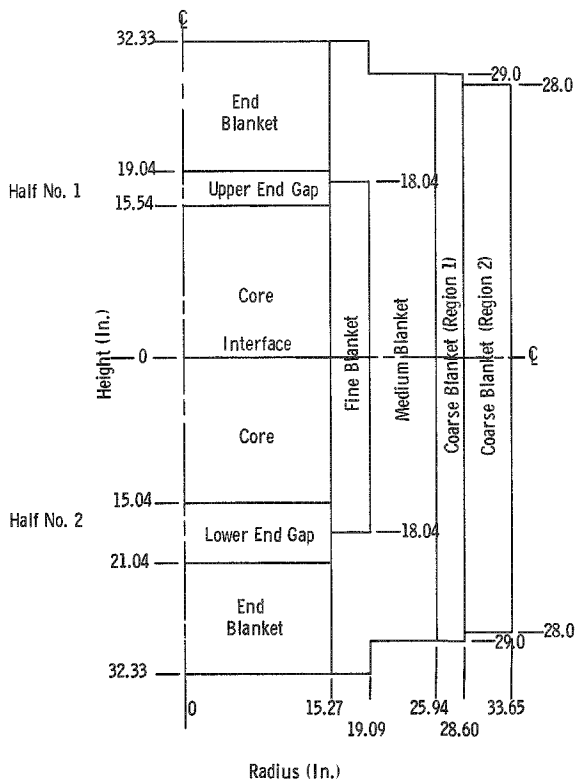

Fig. 31. Dimensions of Fermi Core A Engineering Mockup

halves (see Fig. 27). This produced an initial loading of 311.8 kg U^{235}. The loading progressed by the substitution of enriched uranium for this aluminum and the subsequent addition of seeded drawers. This method provided a reasonably linear inverse count-rate curve allowing accurate extrapolation to criticality.

Table XXV

VOLUME PER CENT COMPOSITIONS OF FERMI ENGINEERING-CORE MOCKUP

	U^{235}	U^{238}	Mo	Zr	S.S.	Al
Core[1]	7.01	21.58	5.04	4.99	14.17	26.93
Safety and Control Rod Channels	-	-	-	-	12.38	49.04
Upper End Gap (3.5 in.)	-	-	-	-	23.79 (Avg)	40.76 (Avg)
0[2] - 0.5 in.					9.01	58.37
0.5 - 2.5 in.					14.06	45.26
2.5 - 3.5 in.					50.61	22.98
Lower End Gap (6 in.)	-	-	-	-	21.99 (Avg)	40.07 (Avg)
0[2] - 1 in.					19.13	53.89
1 - 3 in.					19.50	42.04
3 - 4 in.					45.66	25.24
4 - 6 in.					14.06	38.63
Axial (End) Blanket	0.06	28.30	-	-	18.50	24.14
Fine Blanket	0.10	45.59	2.55	-	19.50	18.55
Medium Blanket	0.11	48.70	-	-	21.00	13.47
Coarse Blanket (Region No. 1)	0.11	46.35	-	-	16.65	0.86
Coarse Blanket (Region No. 2)	0.14	59.59	-	-	7.31	1.10

(1) Does not include safety and control rod channels.

(2) Zero in. is taken at axial end of core.

End Gap and Blanket Composition. The end gaps between the core and axial end blanket in the Fermi fuel-subassembly design were included in considerable detail in the ZPR-III engineering-core mockup. Figure 32 shows the details of a typical 15.5-in. core section and the 3.5-in. end gap in Half No. 1. This represents the upper half of the Fermi core and upper end gap, plus a portion (19 to 21 in.) of the axial end blanket. Figure 33 is the detail of the lower 15 in. of the core and the lower 6-in. end gap. The v/o compositions of both end gaps, neglecting the drawer-end spring gap, are included in Table XXV.

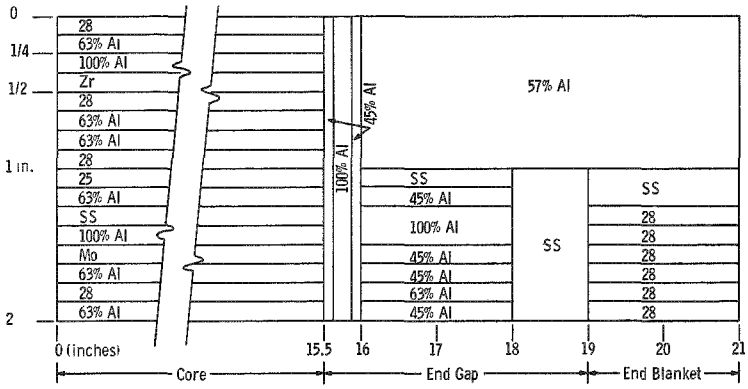

Fig. 32

Upper End Gap and Portion of End Blanket, Half No. 1

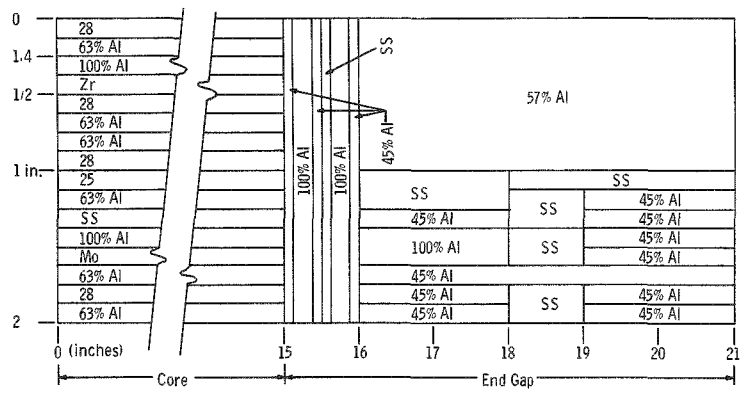

Fig. 33

Lower End Gap, Half No. 2

Aluminum was used to simulate the zirconium end cap on both ends of the Fermi fuel pin. It was assumed that 100% density aluminum was equivalent to the same volume per cent of zirconium in the region immediately adjacent to the core.

The axial end blankets were loaded into the 11-in. back drawers of ZPR-III. Since both core end blankets have the same geometry and composition in the Fermi reactor, the same back drawer loading was used in both halves of ZPR-III. A typical loading of a core end blanket drawer is shown in Fig. 34. The two adjacent 1 x 1 x 5-in. pieces of 56% density aluminum in this loading represent the 2.25-in.^{2}, sodium-filled flow channel in each Fermi fuel subassembly. There are 139 of these mockup flow channels; in other words, 278 in.^{2} were provided in the ZPR-III mockup, compared with 91 channels, or 205 in.^{2}, in the Fermi reactor. A subsequent experiment will be described, which supplied the necessary

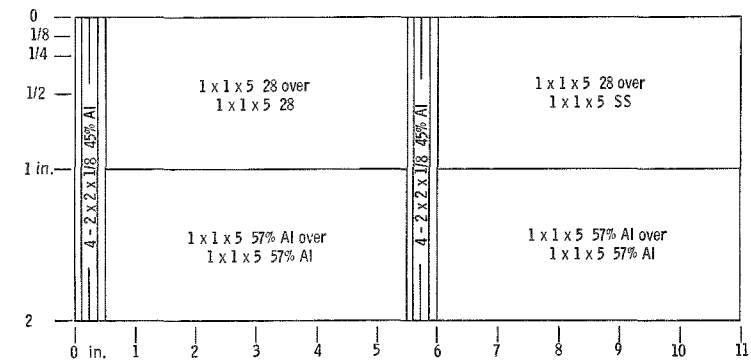

Fig. 34

End Blanket Drawer Loading, Top View

correction for this increased streaming area included in the ZPR-III mockup. Figure 35 is a typical array of the 2-in.^{2} streaming channels as they were loaded in the mockup. The streaming channels formed by the two 1 x 1 x 5-in., 57% density aluminum pieces in the end-gap section of the core drawers were aligned with the corresponding 57% density aluminum channels in the 11-in. back drawers to produce a straight line channel from the end of the core to the outer end of the assembly. The 1 x 1 x 5-in. pieces of stainless steel were alternately placed in the front and the back of the 11-in. back drawer to provide a more homogeneous distribution.

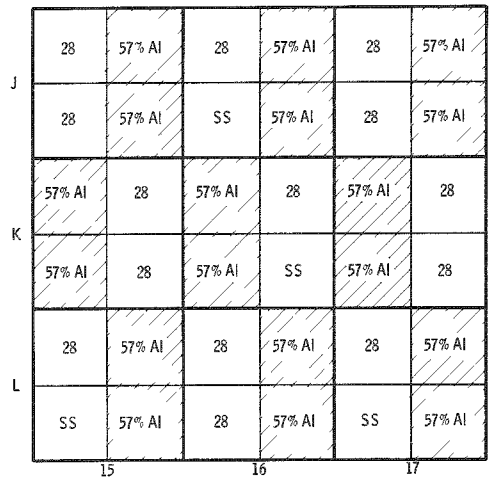

Fig. 35. Arrangement of End Blanket Streaming Channels

As a result of the aluminum substitutions in the fine blanket of the clean core, the aluminum density in the fine radial blanket was also increased over that in the clean-core experiments better to simulate sodium in this region Figure 36 shows the detailed loading of a typical fine radial blanket drawer. This is to be compared with the clean-core fine blanket loading as shown in Fig. 11. The extent of the fine radial blanket region is shown in Figs. 27 and 31. The remaining radial blanket regions were unchanged as compared with those described for the clean-core loading.

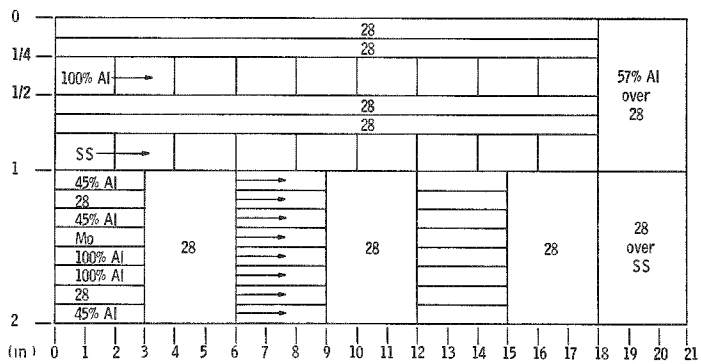

Fig 36

Typical Fine Radial Blanket Drawer Loading

Radial Worth of Seeded Drawers For purposes of experiment and critical-mass determination, it was necessary to obtain a radial worth curve for the substitution of a seeded drawer (No. 4) for a normal drawer (No. 3). This is effectively the substitution of a column of enriched uranium for a column of depleted uranium, corresponding to a net change of 1.051 kg U^{235} in Half No. 1 (15.5-in column), or 1.021 kg in Half No. 2 (15.0-in column). There was also a slight redistribution of the material

in the drawer, as seen in Table XXIV. The results of these measurements are listed in Table XXVI and plotted in Fig. 37 as a function of the average radial position of the drawer.

Table XXVI

RADIAL WORTH OF HALF-CORE AXIAL COLUMNS, U^{235} FOR U^{238}

Drawer Number (See Fig. 27)	Average Radius (in.)	Net Worth (Ih)
1O17 (15.5 in.)	2.916	93.5
1L16	8.704	74.2
1T20	12.324	40.7
1K21	15.411	22.2
2P16 (15.0 in.)	0	90.8
2O15	2.916	88.2
2M17	6.883	79.5
2L16	8.714	70.2
2K15	11.097	53.0
2T12	12.329	39.0
2N10	13.802	29.6
2K11	15.411	21.7

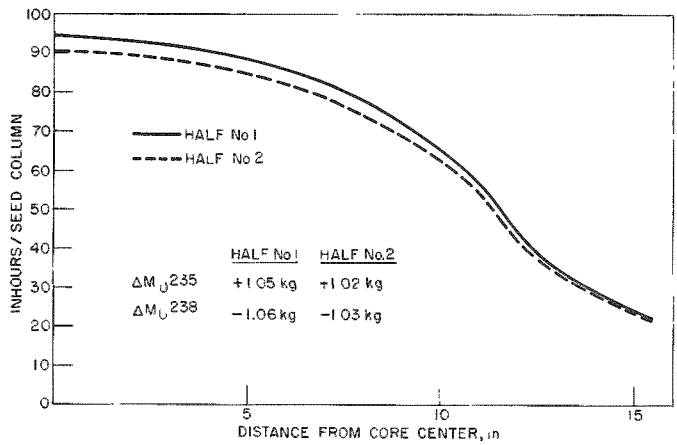

Fig. 37. Radial Worth of Seeded Drawers in Fermi Engineering-core Loading

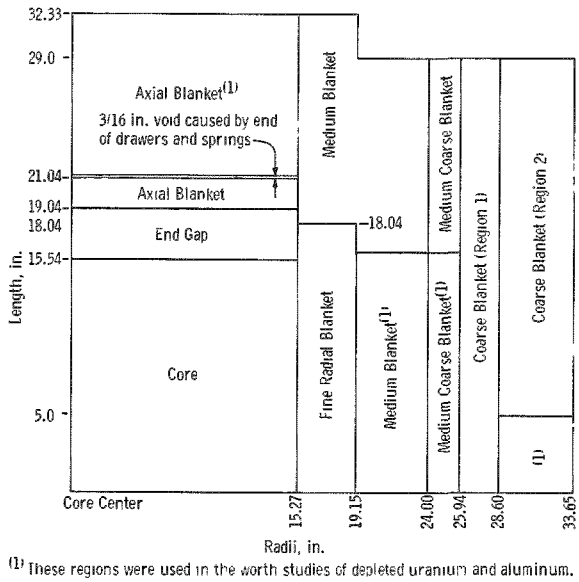

(1) These regions were used in the worth studies of depleted uranium and aluminum.

Fig. 38. Dimensions of Blanket and Fermi Engineering-core Mockup for Blanket and End-gap Substitutions

B. Material Substitutions in Blanket and End Gaps

The worths of aluminum and depleted uranium were determined for the Fermi Engineering Core Mockup in ZPR-III. The regions concerned in this study, as shown in Fig. 38, were:

1. An axial blanket consisting of a region 11 in. in depth separated from the core by a 3.5-in. end gap, 2 in. of unaltered axial blanket and $\frac{3}{16}$ in. of void and spring;

2. A fine radial blanket 36.08 in. long, encompassing an annular region 15.27 to 19.15 in. from the core center line;

3. A medium radial blanket 32.0 in. long in an annular region 19.15 to 24.0 in. from the core center;

4. A medium coarse radial blanket 32.0 in. long in an annular region 24.0 to 25.94 in. from the core center;

5. An outer coarse radial blanket 10.0 in. long in an outer radial region 26.0 to 33.6 in. from the core center.

The radial blanket regions were all concentric with the core and centered about the core midplane. The results of these loadings are given in Table XXVII. The locations of the selected drawers are shown in Fig. 39. The values presented in Table XXVII are based on a comparison with an equal volume of void.

Table XXVII

WORTHS OF DEPLETED URANIUM AND ALUMINUM IN BLANKET OF ENGINEERING-CORE MOCKUP

Loading No.	Blanket	Material	Composition Change (v/o)	Weight Change (kg)	Reactivity Change (Ih)	Worth (Ih/kg)
53	Initial Reference Loading		50.5 Ih (Reference)		0	
54	Axial of Half No. 1[1]	Depleted U	28.3 to 25.9	- 52.8	- 4.8	+0.091
55	Axial of Half No. 1[1]	Depleted U	25.9 to 23.6	- 52.8	- 4.8	+0.091
56	Axial of Half No. 1[1]	Aluminum	24.1 to 28.8	+ 14.94	+ 8.2	+0.548
57	Repeat Reference Loading		49.7 Ih (Reference)		0	
58	Fine Radial[2]	Depleted U	45.6 to 42.7	-116	-49.3	+0.425
59	Fine Radial[2]	Depleted U	42.7 to 40.2	-116	-43.8	+0.378
60	Fine Radial[2]	Depleted U	40.2 to 36.8	-160.2	-45.1	+0.281
61	Medium Radial[3]	Depleted U	48.7 to 46.3	-147.6	-14.1	+0.0955
62	Medium Radial[3]	Aluminum	14.7 to 17.0	+ 21.1	+14.3	+0.678
63	Medium Coarse[3]	Depleted U	48.8 to 45.7	- 93.2	- 2.3	+0.0247
64	Medium Coarse[3]	Aluminum	14.7 to 17.8	+ 13.18	+ 2.3	+0.175
65	Coarse[4]	Depleted U	Negligible	-197.4	- 1.5	+0.0076
66	Repeat Reference Loading		49.0 Ih (Reference)			

[1]There is a 3.5-in. end gap plus 2 in. of unaltered axial blanket between the core and this region.

[2]The fine radial blanket test region is 36.08 in. long.

[3]The medium and medium coarse radial blanket test regions are 32.00 in. long.

[4]This loading was taken over the center 10.0 in. axially of the outside edge of the coarse blanket.

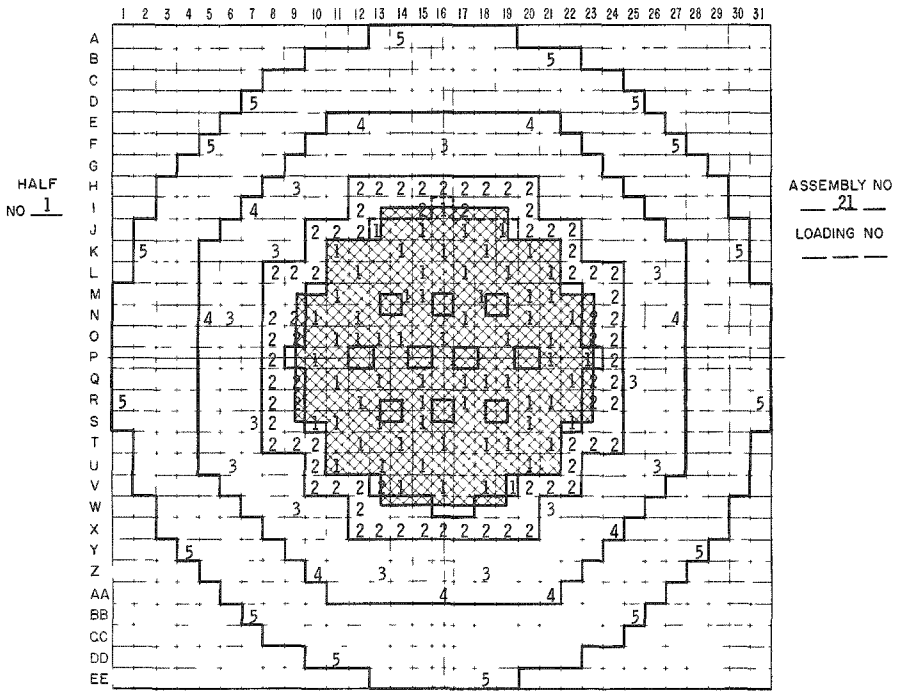

Fig. 39. Location of Altered Drawers for Blanket and End-gap Substitutions

1. Axial Blanket
2. Fine Radial Blanket
3. Medium Radial Blanket
4. Medium Coarse Radial Blanket
5. Coarse Radial Blanket

The engineering-core mockup utilized for these substitutions consisted of 141 full drawers and 36 partial drawers, making an equivalent of 154 full drawers. The axial blanket, which was separated from the core by a 3.5-in. end gap, consisted of 154 drawers, of which 15 were control rod channels containing only aluminum and stainless steel. The fine radial blanket included 64 full drawers and 36 partial drawers. The medium blanket, which included the medium coarse region, was contained in 204 matrix channels and the coarse blanket, in 304 matrix channels.

The core volume was 367.3 liters; height, 30.60 in.; equivalent diameter, 30.5 in.; and the cold critical mass was 434.4 kg U^{235}. The core and blanket compositions are given in Table XXV. Figure 38 indicates the blanket lengths and radii in Half No. 1 of ZPR-III. The core region in Half No. 2 was 15 in. in length with a 6-in. end gap between it and its axial end blanket. This was the only difference over the core and blanket dimensions shown for Half No. 1.

Measurements of Blanket Worth. Measurements of the worths of depleted uranium and aluminum were conducted by removing the material in question and observing the reactivity effect of the remaining void with respect to a previous reference measurement. Both depleted-uranium and aluminum worths were determined in the axial and radial blankets. The aluminum worth was determined by the addition of aluminum in the voids produced by removing uranium. These results are shown in Table XXVII. An initial reference measurement and two subsequent ones agreed to within 1.5 Ih, indicating the overall accuracy of these and other substitution measurements.

1. Axial Blanket

Only the back blanket drawers were used to make the axial blanket studies. The axial blanket in Half No. 1 extends 2 in. into the back of the front core drawers, separated from the core by a 3.5-in. end gap. During the axial blanket substitutions, this 2-in. section remained unaltered. A typical loading of the 11-in. back blanket drawers used in these studies is shown in Fig. 34. The locations of these drawers are shown in Fig. 39. To measure the worth of depleted uranium, one 1 x 1 x 5-in. piece was removed from the double column from selected drawers (No. 1's in Fig. 39), alternating between the front and the back of the 11-in. drawer. The worth of depleted uranium in the axial blanket, 0.091 Ih/kg, did not change as additional material was removed. The blanket composition was changed from 28.3 to 25.9 v/o when 52.8 kg were removed in loading No. 54 (see Table XXVII). The reactivity change was a loss of 4.8 Ih, which was the same as the reactivity loss for the subsequent loading (No. 55) when an additional 52.8 kg were removed.

The worth of aluminum in the axial blanket was determined in a separate measurement by filling the voids created by the removal of depleted uranium in the previous loadings. With the addition of 14.94 kg of aluminum, the reactivity increased by 8.2 Ih, indicating a worth of 0.548 Ih/kg, as shown in Table XXVII. This addition resulted in a composition change from 24.1 to 28.8 v/o of aluminum. On this basis, aluminum is worth slightly less than depleted uranium in the axial blanket, since, for a composition change of 4.7 v/o, aluminum is worth 8.2 Ih versus 9.6 Ih for depleted uranium. The axial blanket was restored to the original loading before the measurements were made on the radial blanket.

2. Radial Blanket

The fine radial blanket extends from 15.25 in. to 19.15 in. from the core center and is adjacent to the core (see Fig. 38). Figure 36 shows a typical drawer loading for this region. The worth of depleted uranium was determined by removing the top 1 x 1 x 3-in. pieces from selected drawers as shown in Fig. 39 (No. 2's). Alternate drawers had the 1 x 1 x 3-in. depleted-uranium pieces at 0-3, 6-9, 12-15 and 18-21 in. By removing

a total of 392.6 kg in increments of 116, 116, and 160.2 kg, the composition of depleted uranium was decreased from 45.6 to 42.7 to 36 v/o, respectively. The loss of reactivity was 49.3, 43.8, and 45.1 Ih, respectively, indicating a worth for the first loading of 0.425 Ih/kg; of 0.378 Ih/kg for the second; and of 0.281 Ih/kg for the third. It is evident that the worth of depleted uranium in this region is strongly dependent upon the uranium composition.

Both depleted-uranium and aluminum worths were determined in the medium and medium coarse blankets. The composition of these two regions was essentially the same. A slight difference in loading resulted from the use of 2 x 2 x 5-in. pieces of depleted uranium instead of four 1 x 1 x 5-in. pieces in the medium coarse blanket. Only the first 16 in. of each half were altered in these studies. A total of 147.6 kg of depleted uranium was removed from the medium blanket to effect a reactivity loss of 14.1 Ih. This yields a worth of 0.0955 Ih/kg of depleted uranium in this portion of the blanket.

With the addition of 21.1 kg of aluminum in the voids formed by the removal of the depleted uranium, the reactivity increased 14.3 Ih, or 0.678 Ih/kg. On a comparative v/o basis, aluminum then has essentially the same worth as depleted uranium; 3.4 change in v/o produces 14.3 Ih versus a 14.1-Ih change for depleted uranium.

The worth of either aluminum or depleted uranium decreases rapidly toward the outer edge of the medium blanket which is the medium coarse blanket region (see Fig. 38). In the medium coarse blanket, the depleted uranium is worth 0.0247 Ih/kg versus 0.0955 Ih/kg in the medium blanket. Aluminum is worth 0.175 Ih/kg versus 0.678 Ih/kg in the medium blanket.

The studies in the coarse blanket were limited to the region extending over the first 5 in. from the interface in each half. The worth of depleted uranium was determined by removing 2 x 2 x 5-in. pieces from each half in selected matrix channels, as shown in Fig. 39. The experimental worth of depleted uranium was found to be 0.0076 Ih/kg in this portion of the coarse blanket.

Measurements of End-gap Material Worths. To verify the correct density of aluminum for mocking up sodium in the end-gap regions, aluminum density experiments were conducted over the 3.5-in. end gap in Half No. 1. The average v/o of aluminum in this region for a normally loaded drawer, as shown in Fig. 32, is 40.8%. This is to be compared with an average of 80.0 v/o sodium occurring in this region of the Fermi fuel subassembly. The aluminum density in this region was increased by substituting 100% density aluminum for the 45 and 57% density aluminum normally occurring in this end gap. Figure 40 (which may be compared with the normal loading in Fig. 32) shows the manner in which this increased density aluminum was loaded in a drawer. The negligible reactivity

effect of the 2-in.^{2} streaming channels, as described later, was justification for the use of increased-density aluminum in the streaming channels rather than replacing the adjacent $\frac{1}{8}$-in. plates of low-density aluminum. This substitution resulted in the net addition of 9.08 kg aluminum with a corresponding reactivity increase of 32.1 Ih, or + 3.53 Ih/kg aluminum. This indicates a volume-for-volume equivalence of 51% density aluminum for room-temperature sodium (0.97 g/cm^3) in this region. This is identical with the average aluminum density that was attained in the normal loading of the 3.5-in. end gap. Thus, no reactivity correction for aluminum density in the end gaps is required.

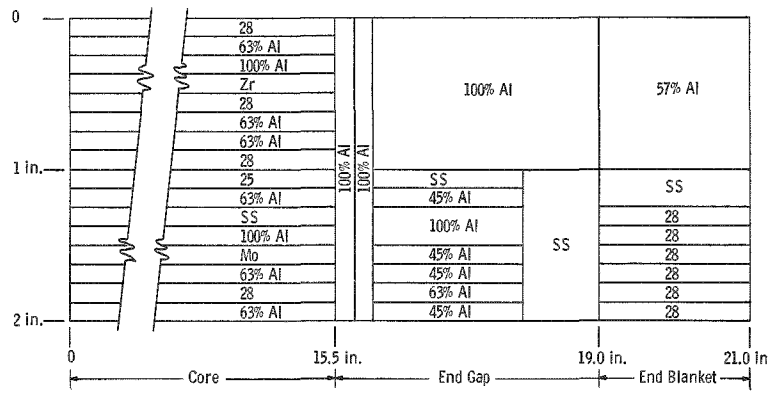

Fig. 40. Increased Aluminum Density in 3.5-in. Upper End Gap (Half No. 1)

C. Spectral Indices

Central Fission Ratios. A series of central-core fission ratio measurements, similar to those obtained with the clean core, were conducted with the Fermi engineering-core loading. The measuring techniques and the detectors utilized have been described in Section V,G. The data from the engineering-core loading, as shown in Table XXVIII, were obtained with the identical detectors used for the clean-core measurements.

Table XXVIII

FISSION RATIOS AT CENTER OF ENGINEERING-CORE ASSEMBLY

Material	Counter	$\left(\frac{\sigma_f \text{Material}}{\sigma_f(25)}\right)^{(1)}$	Average	Material	Counter	$\left(\frac{\sigma_f \text{Material}}{\sigma_f(25)}\right)^{(1)}$	Average
U^{238}	2	0.0327(2)	0.0324(2)	U^{233}	16	1.505	1.505
U^{238}	3	0.0321(2)		Pu^{239}	20	1.133	1.137
U^{234}	8	0.274(2)	0.270(2)	Pu^{239}	21	1.141	
U^{234}	11	0.266(2)		Pu^{240}	12	0.275(2)	0.275(2)

(1) All ratios determined with respect to counter No. 5 (U^{235})

(2) These ratios have been adjusted to include the following absolute fission counter wall corrections implied by Ref. 13:

U^{238}	0.92
U^{234}	0.96
Pu^{240}	0.96

U^{238} Capture Rate. Radiochemical analyses[10] of U^{235}-enriched and depleted uranium foils irradiated at the center of the engineering-core assembly yielded the following:

$$\left[\frac{\sigma_c(28)}{\sigma_f(25)}\right]_{\text{core center}} = 0.100 \pm 0.003$$

and

$$\left[\frac{\sigma_f(28)}{\sigma_f(25)}\right]_{\text{core center}} = 0.038 \pm 0.001 \quad .$$

D. Fission Rate Traverses

Fission rate traverses were conducted with the engineering-core assembly by means of small fission counters[12] containing U^{234}, U^{235}, and Pu^{239}, which were inserted and remotely positioned in the assembly. These counters were approximately 2 in. long by $\frac{3}{8}$ in. in diameter. Unobstructed travel of the counters was facilitated by inserting a $\frac{1}{2}$-in.-diameter thin-walled stainless steel tube through the ZPR-III assembly, either axially or radially, at the location desired. The materials surrounding the traverse tube were loaded to retain the average composition of the local region by means of small pieces. The outer blanket regions immediately adjacent to the traverse tube were reloaded with $\frac{1}{8}$-in.-thick pieces of uranium, aluminum, and stainless steel to provide a more homogeneous environment. The counter to be used for the traverse was remotely selected and positioned along the traverse tube by means of an automatic counter changer and drive mechanism. This allowed a large number of points to be taken during a single run. Each count rate of the sample counter in a given traverse was normalized to the count rate of a fixed detector in the core to eliminate any dependence upon power variation during the traverse.

Radial Fission Rates, Horizontally. The $\frac{1}{2}$-in. traverse tube was loaded horizontally through the P-row parallel to the core midplane in Half No. 1, 1 in. behind the interface, i.e., $\frac{3}{4}$-in. from the core midplane. This location allowed the traverse to be made through the mockup safety rod channel in P-12, 13, and the mockup control rod channel in P-14, 15, to the core center and beyond (see Fig. 27). Figures 41 through 44 show the results of these traverses. Figure 45 is a comparison of the smoothed curves of these various traverses normalized to the uncorrected fission ratios at the core center as determined with the absolute counters.

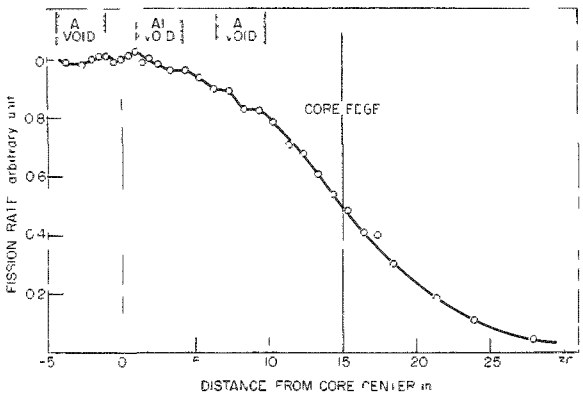

Fig. 41. U^{235} Radial Traverse, P-Row, Engineering-core Assembly

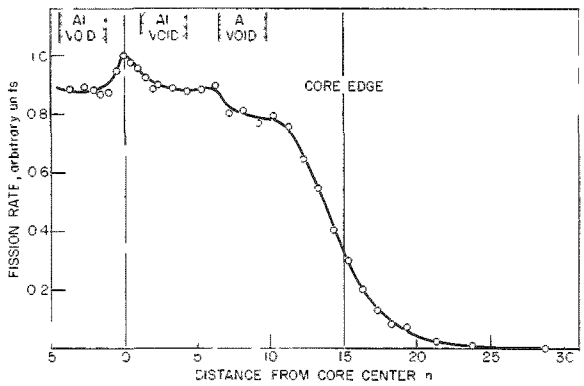

Fig. 42. U^{238} Radial Traverse, P-Row, Engineering-core Assembly

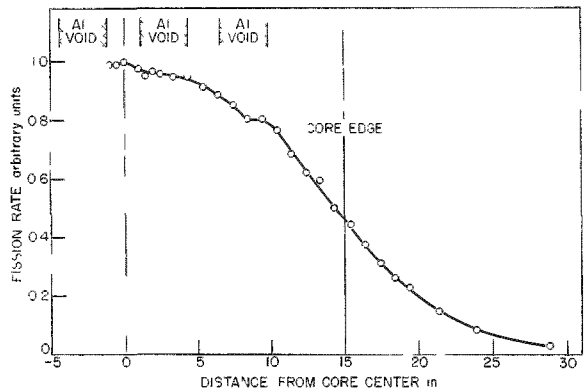

Fig. 43. U^{239} Radial Traverse, P-Row, Engineering-core Assembly

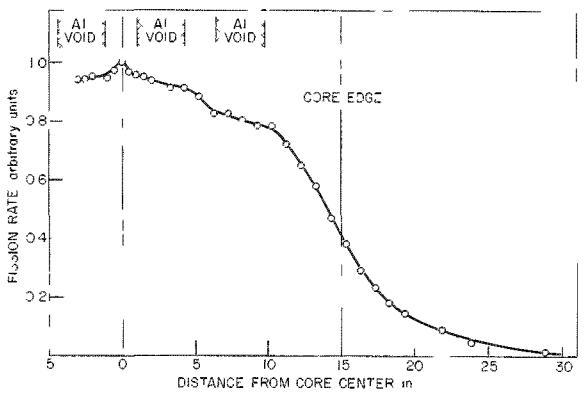

Fig. 44. U^{234} Radial Traverse, P-Row, Engineering-core Assembly

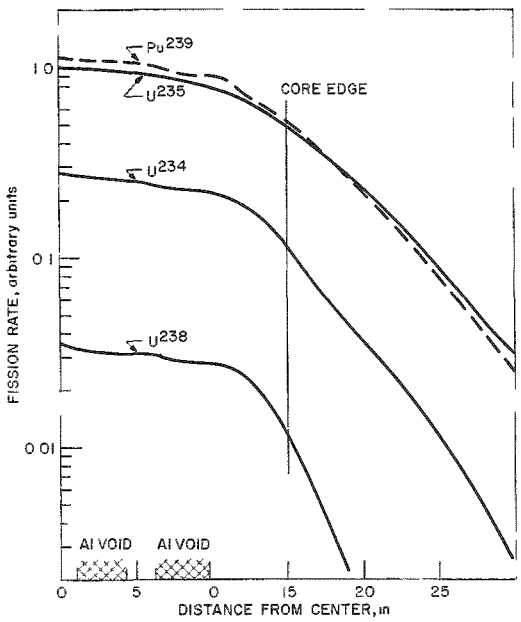

Fig. 45

Comparison of Radial Fission Rates, P-Row, Engineering-core Assembly

Radial Fission Rates, Vertically. These traverses were made by inserting the $\frac{1}{2}$-in.-diameter stainless steel guide tube in a similar manner vertically down through the No. 16 matrix column in Half No. 2, at a point $\frac{1}{2}$ in. from the interface, i.e., $\frac{3}{4}$ in. from the core midplane. This traverse thus includes the mocked-up safety rod channel in M-16 and N-16 and extends beyond the center of the core. Figures 46 through 49 are plots of the individual traverses. Figure 50 compares the smoothed curves of these individual traverses normalized to the uncorrected fission ratios at the core center.

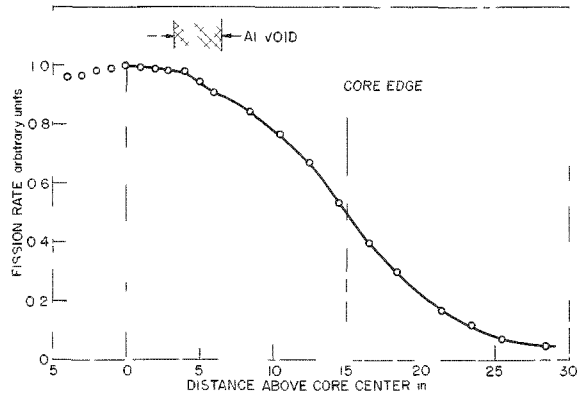

Fig. 46. U^{235} Radial Traverse, Number-16 Column, Engineering-core Assembly

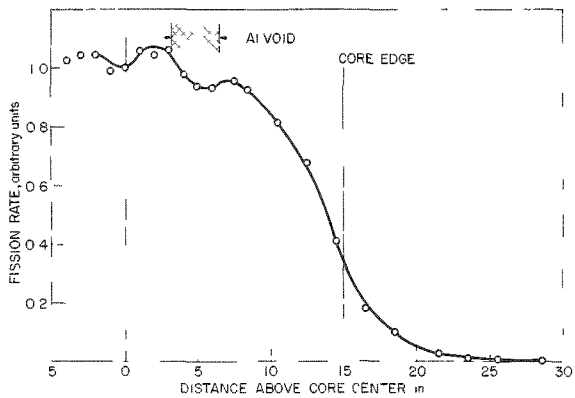

Fig. 47. U^{238} Radial Traverse, Number-16 Column, Engineering-core Assembly

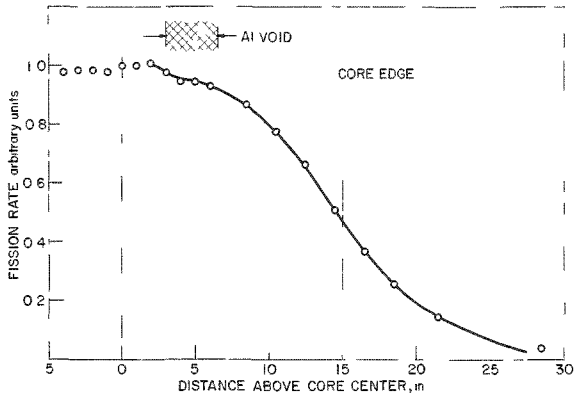

Fig. 48. Pu^{239} Radial Traverse, Number-16 Column, Engineering-core Assembly

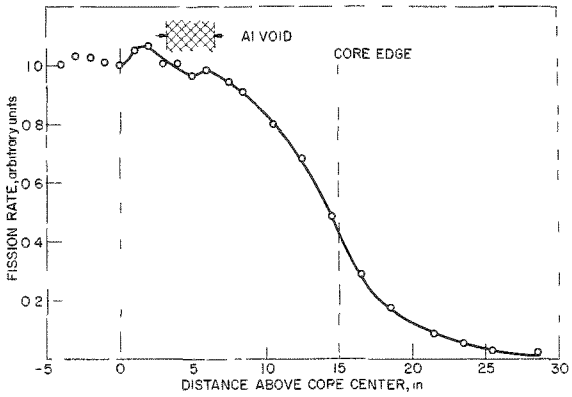

Fig. 49. U^{234} Radial Traverse, Number-16 Column, Engineering-core Assembly

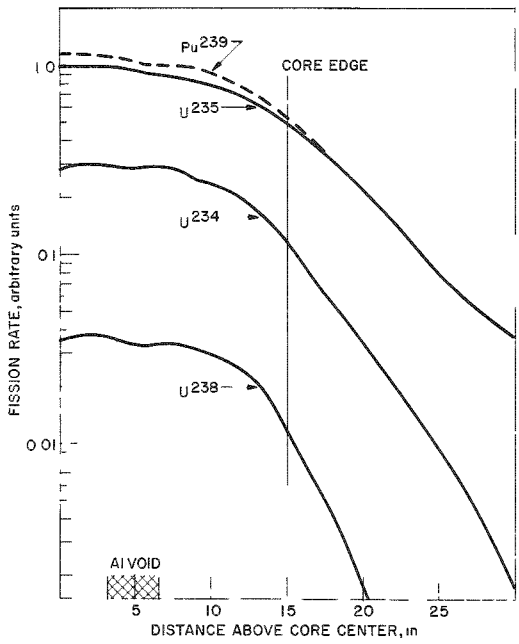

Fig. 50

Comparison of Radial Fission Rates, Number-16 Column, Engineering-core Assembly

Axial Fission Rates, Core Axis. These traverses were made by locating the stainless steel guide tube along the axis of the P-16 drawers in both halves. This allowed the traverse to be conducted through the lower end blanket, lower 6-in. end gap, and core. Figures 51 through 54 are plots of the individual traverses. Figure 55 compares the smoothed curves of these individual traverses normalized to the uncorrected fission ratios at the core center.

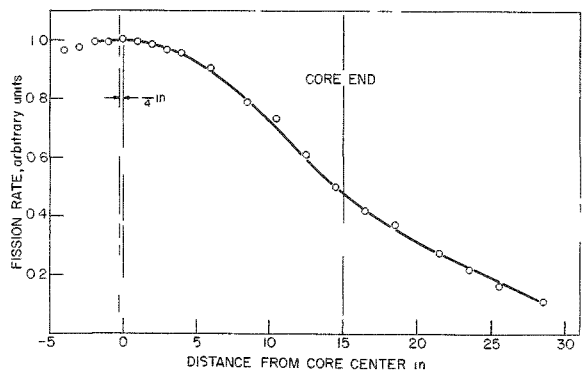

Fig. 51 U^{235} Axial Traverse, P-16 Channel, Engineering-core Assembly

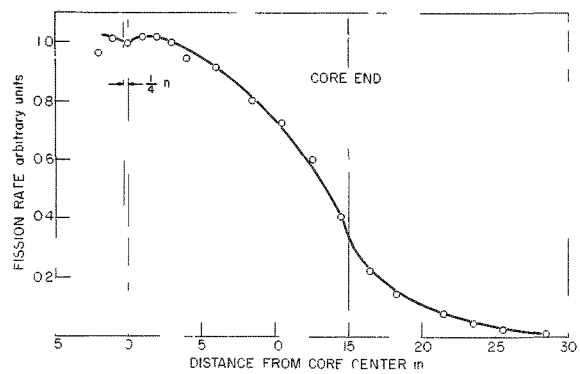

Fig. 52. U^{238} Axial Traverse, P-16 Channel, Engineering-core Assembly

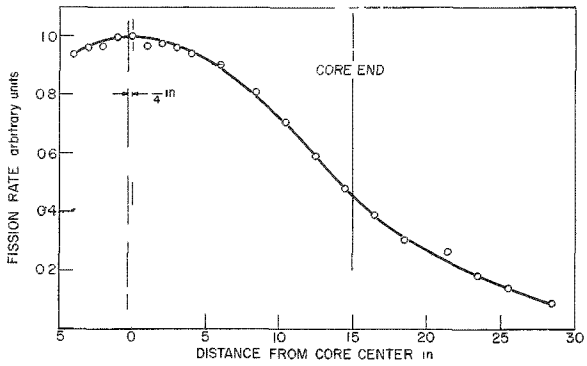

Fig. 53. Pu^{239} Axial Traverse, P-16 Channel, Engineering-core Assembly

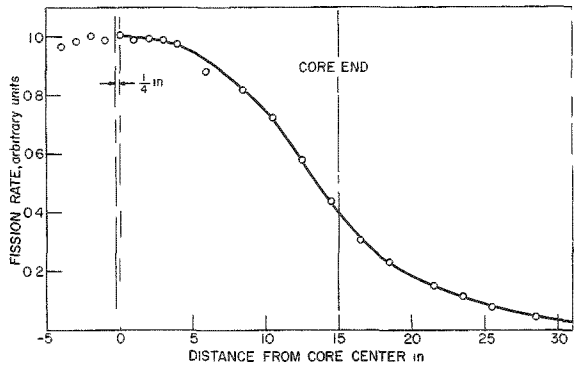

Fig. 54. U^{234} Axial Traverse, P-16 Channel, Engineering-core Assembly

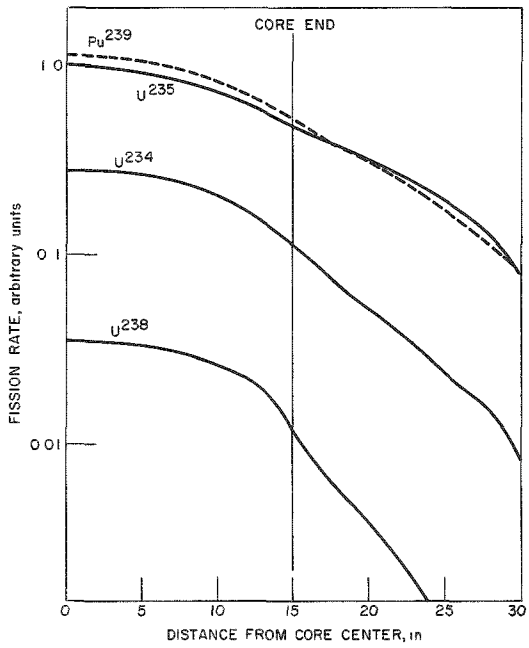

Fig. 55

Comparison of Axial Fission Rates, P-16 Channel, Engineering-core Assembly

Axial Fission Rates, Core Edge. These traverses were made by inserting the $\frac{1}{2}$-in. stainless steel guide tube along the axis of the I-16 drawers in both halves. This placed the fission counters precisely at the core-radial blanket interface and allowed the traverse to be conducted along the interface of the radial blanket and the lower axial blanket, the lower 6-in. end gap, and the core. Figures 56 through 59 are plots of the individual traverses. Figure 60 compares the smoothed curves of the individual traverses on the basis of the fission ratios estimated at the core edge on the midplane from the curves in Fig. 50.

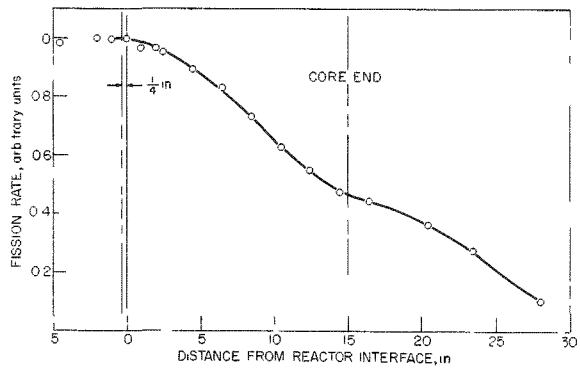

Fig. 56. U^{235} Axial Traverse, I-16 Channel, Engineering-core Assembly

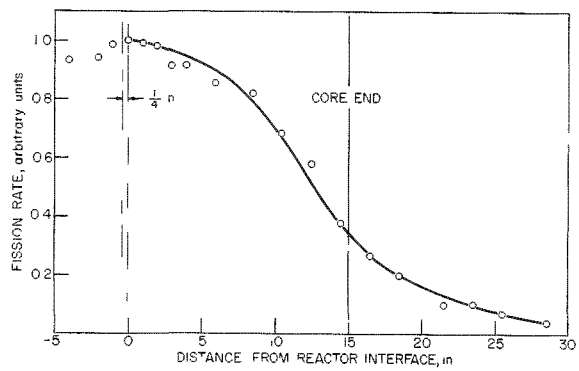

Fig. 57. U^{238} Axial Traverse, I-16 Channel, Engineering-core Assembly

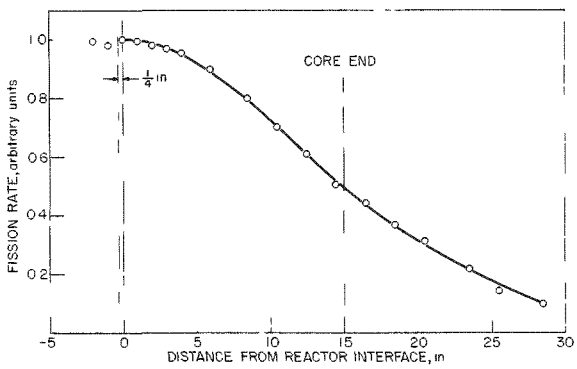

Fig. 58. Pu^{239} Axial Traverse, I-16 Channel, Engineering-core Assembly

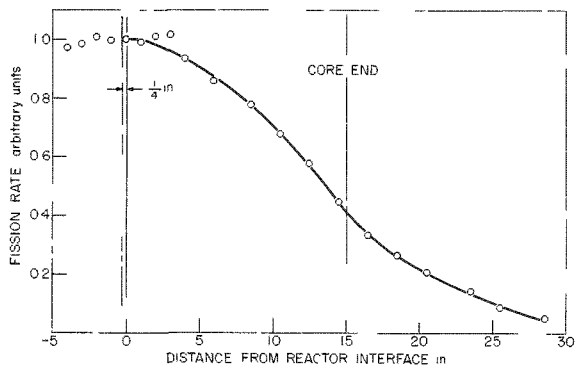

Fig. 59. U^{234} Axial Traverse, I-16 Channel, Engineering-core Assembly

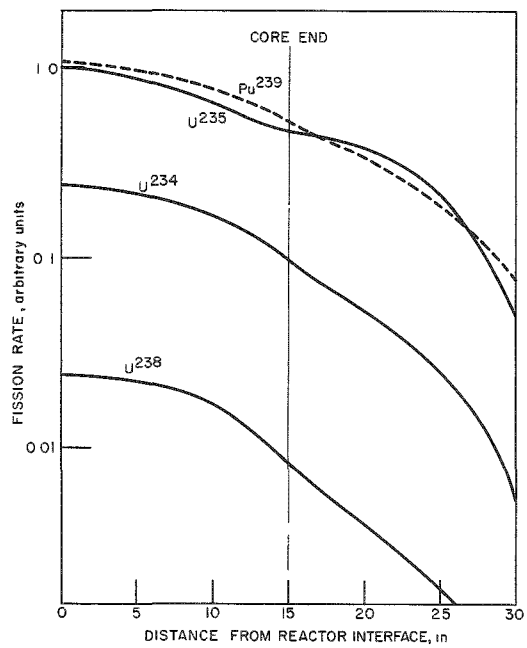

Fig. 60

Comparison of Axial Fission Rates, I-16 Channel, Engineering-core Assembly

E. Variation of End-gap Length

The geometry of the Fermi fuel subassembly includes an end-gap or plenum region at either end of the core, separating the fuel and end-blanket regions. The lower end gap of 5.963 in. was simulated in Half No. 2 of ZPR-III by means of a 6.00-in. region plus the $\frac{3}{16}$-in. spring gap normally occurring at the end of the 21-in. drawer, as shown in Fig. 33. This was considered to be a satisfactory representation as a result of the following variation in end-gap length.

The upper Fermi end gap of 3.713 in. was simulated by means of a 3.5-in. region at the end of the 15.5-in. core section in Half No. 1, as shown in Fig. 32. To evaluate the reactivity effect of increasing the length of this region to represent more correctly the engineering design, the entire end gap in Half No. 1 was increased to 4.00 in. by replacing the first $\frac{1}{2}$ in. of depleted uranium representing the axial end blanket with an equal volume of aluminum having an average density of 67%. The total reactivity change was the loss of one Ih, a negligible result. Consequently, the end-gap length was returned to 3.5 in. for subsequent experiments to facilitate drawer handling and loading.

F. Streaming Effect of End Blanket Flow Channels

As noted in Section VI,A, the mocked-up core and blankets provided an excess of 73 in.^{2} of flow channel over that in the Fermi reactor design. To determine the necessary reactivity correction for this increase in the neutron-streaming area, one-quarter of the mockup flow channels (69.5 in.^{2}) was eliminated by staggering the loading of the uranium and aluminum, as shown in Figs. 61 and 62. These loadings are to be compared with the normal end-blanket loadings shown in Figs. 32 and 34. The elimination of the excess streaming channels in one end blanket resulted in a gain of 2.3 Ih, or approximately a 5-Ih correction for both end blankets to conform to the Fermi engineering design. This corresponds to a correction of approximately -0.1 kg U^{235} in the engineering-core critical mass.

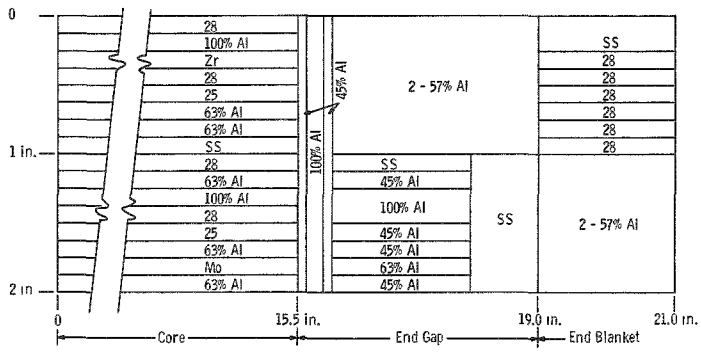

Fig. 61. Staggered Loading to Eliminate End-gap Streaming Channel, Core Drawer

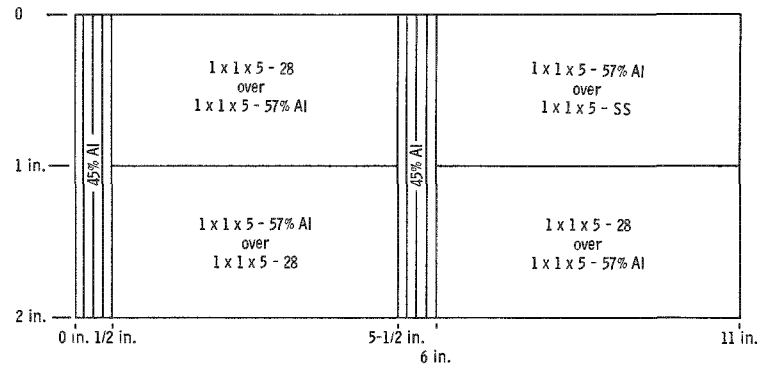

Fig. 62. Staggered Loading to Eliminate Axial End-blanket Streaming Channel, Back Blanket Drawer

G. Variation of Core Length

Axial Extension of Core. The design length of the Fermi reactor is 30.950 in. This includes a $\frac{1}{2}$-in. tapered section at both ends of the fuel pins, resulting from the addition of a swaged zirconium end cap. A core, 30.6 in. long and uniform in composition, was selected as best to mock up this geometry in ZPR-III. However, to better evaluate the reactivity effect of the additional length of the Fermi core, the engineering-core mockup was lengthened by adding $\frac{1}{2}$-in. of core material to the 15.5-in. core section. This extension was made with the 4.0-in. end-gap section in place, thereby increasing the core section in this half to 16.0 in. and reducing the end gap to 3.5 in. The axial blanket remained constant, with 1.5 in. of depleted uranium in the back of the front drawers. The drawer loading for the above conditions are shown in Fig. 63. This change

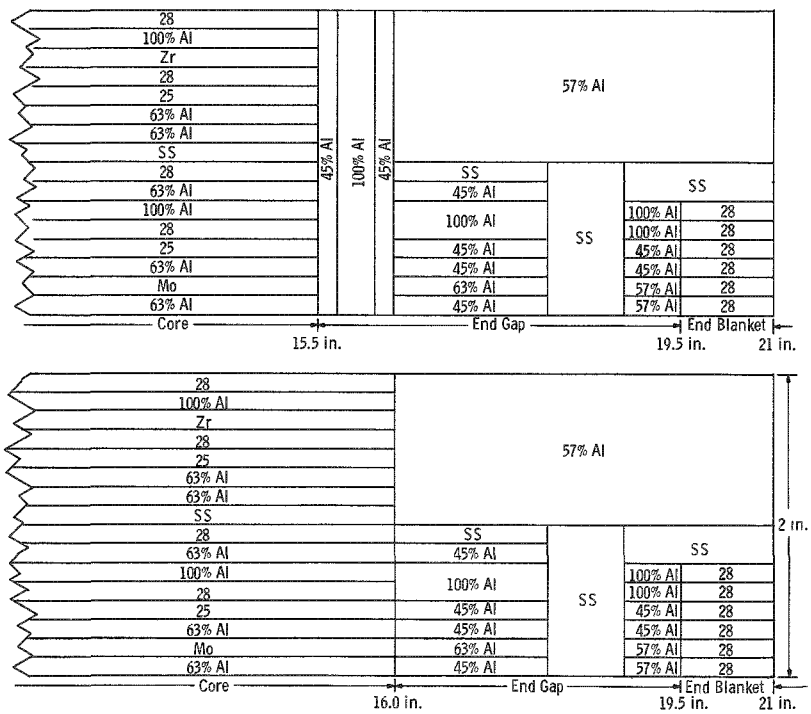

Fig. 63

Comparison of 15.5-in. and 16.0-in. Core Loadings in Half No. 1

over the entire end of the core in Half No.1, including partial drawers, resulted in a reactivity increase of 122.2 Ih. This reactivity change resulted from the addition of 7.2 kg U^{235} and 22.2 kg U^{238} together with the corresponding quantities of Al, Mo, Zr, and stainless steel, and the removal of 8.1 kg of aluminum in reducing the gap length. The negligible effect of increasing the gap length from 3.5 in. to 4.0 in. removes the need for gap correction.

Axial Fuel Shimming, Constant Mass. The axial expansion of the uranium fuel pins in the Fermi reactor was simulated in the ZPR-III engineering-core loading by inserting $\frac{1}{32}$-in. aluminum shims between the butting ends of the enriched and depleted uranium pieces along the length of the columns. This produced an elongation of the fuel material with no change in uranium content of the core and a minimum addition of aluminum. The average density of uranium in the core was lowered, but the local density obviously remained constant.

The core drawers were rearranged to form $\frac{1}{4}$-in. columns of uranium, and the drawer spring was moved from the back of the drawer to the core-end gap interface to prevent movement of the end gap and end blanket when the shims were inserted. A reference run established the reactivity of this configuration. Aluminum shims, $\frac{1}{4}$ x 2 x $\frac{1}{32}$-in., were then placed at 5-in. intervals along the axial columns to represent the expansion of fuel. Figure 64 shows a typical drawer with the shims inserted. Shims were placed only in drawers of Half No. 2 with nine shims per drawer as shown. About two-thirds of the edge drawers contained shims.

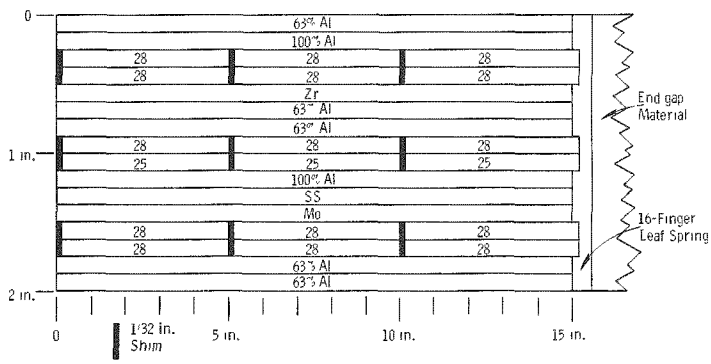

Fig. 64

Location of Shims and Spring Gap in a Typical Core Drawer for Shim Experiment

Insertion of the shims resulted in a net reactivity loss of 32.3 Ih. The shims represented an addition of 0.807 kg aluminum. With the worth of aluminum as 4.24 Ih/kg as determined from the partial drawer substitution experiments with the clean core (see V,E,2 and Table IX), the aluminum correction is 3.42 Ih. Therefore, the net expansion effect resulted in a reactivity loss of 35.7 Ih over approximately half the core.

H. Precise Positioning of Mockup Safety Rod Channels

As noted in the description of the engineering-core assembly, the control and safety rod channels were loaded into ZPR-III in slightly off-design, but compensating positions, as shown in Fig. 29. The largest deviation from design location occurred for the four corner channels loaded in M,N-13,-19 and R,S-14,-18 (see Fig. 27). The other mockup channels were self-compensating within experimental error.

To determine the correction for the accurate placement of the above corner channels, two of these channels were correctly positioned in Half No. 2 in 2M,N-13,-14 and 2R,S-13,-14, as shown in Fig. 65. Moving the first mockup channel in toward the center from 2M,N-13 to 2M,N-13,-14 decreased the reactivity 10.6 Ih. The second channel produced a reactivity gain of 3.8 Ih when moved from 2R,S-14 to 2R,S-13,-14, for a net loss of 7 Ih for the correct positioning of two of the eight, corner half-channels. The total for the correct positioning of these channels in the mockup would then be -27.2 Ih, or a correction of +0.52 kg U^{235} on the engineering-core critical mass.

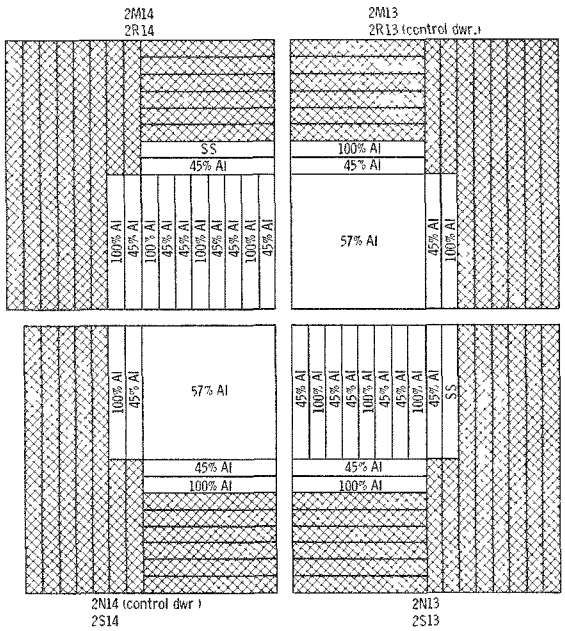

Fig. 65. Correct Positioning of Fermi Mockup Safety Rod Channel

I. Worths of Fermi Fuel Subassemblies

Four different Fermi fuel subassemblies were mocked up in ZPR-III, and careful attention was paid with regard to location, cross section, volume, and total mass. The worth of the central fuel subassembly was found relative to aluminum in a mocked-up, sodium-filled channel. The worths of the three fuel subassemblies at the edge of the core were found relative to a blanket subassembly mockup. The location of these subassemblies is shown in Fig. 66.

Central Fuel Subassembly. The worth of the central fuel subassembly was of interest because it represents the maximum amount of reactivity that can be added by inserting a fuel subassembly into the core during loading operations. Since the empty channel would be filled with sodium, the fuel subassembly was mocked up with a loading similar to the aluminum-filled safety and control rod channels.

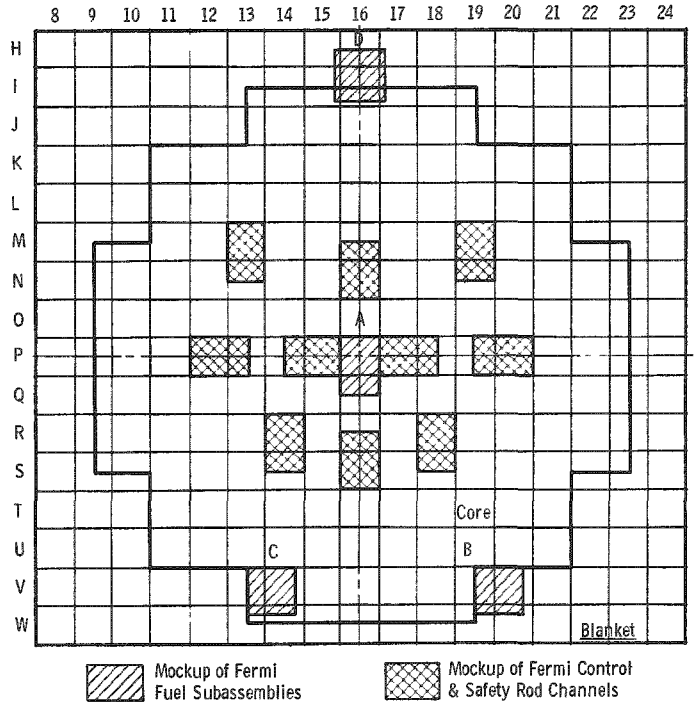

Fig. 66

Location of Fermi Fuel Subassemblies Mocked Up in ZPR-III for Worth Determinations

Figure 67 shows the top view of the P-16 drawer and the top 1-in. of the Q-16 drawer used to mock up the core section of the central fuel subassembly. Since it was not possible to use full-length columns of all materials, some columns contained several materials. The materials were distributed as uniformly as possible along the length of the core. The end gaps and axial blanket regions were also simulated in a similar manner.

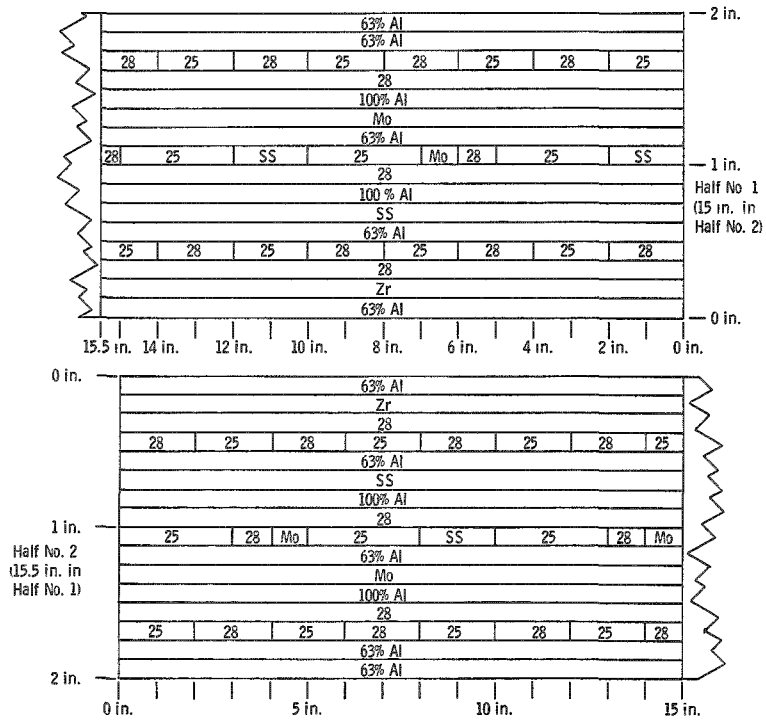

Fig. 67

Drawer Loadings for Central Fermi Fuel Subassembly Mockup (P-16 and Top 1 in. of Q-16)

In Table XXIX are compared the amounts of material in the Fermi fuel subassembly with the amounts actually used in the ZPR-III mockups. The amounts of stainless steel and zirconium differ because a subassembly with a stainless steel rather than a zirconium fuel-support grid was used as the model. However, the worths of stainless steel and zirconium are very nearly the same, so no appreciable error should result.

Table XXIX

COMPARISON OF FERMI FUEL AND BLANKET SUBASSEMBLIES WITH MOCKED-UP SUBASSEMBLIES IN ZPR-III

Fuel Subassembly	Length (in.)	Cross-Sectional Area (in.^{2})	Materials (kg)					
			U^{235}	U^{238}	SS	Mo	Zr	Al
Fermi	30.95	7.25	4.978	14.077	3.882	2.173	1.418	-
P & Q16	30.58	7.13	4.932	14.071	4.192	2.027	1.147	2.512
H & I15, 16 & 17	31.08	7.42	4.954	13.884	4.150	2.158	1.203	2.451
V & W13 & 14 (19 & 20)	31.08	7.42	5.003	14.025	4.028	2.126	1.225	2.407

Blanket Subassembly	Length (in.)	Cross-Sectional Area (in.^{2})	Materials (kg)			
			Depleted U	SS	Mo	Al
Fermi	1	7.25	1.009	0.177	0.026	-
ZPR-III Mockup	1	7.42	0.993	0.163	0.030	0.049

The worth of the central fuel subassembly displacing sodium in the form of low-density aluminum was measured in two ways. The normal method of using positive period measurements by means of fuel additions to compensate for the reactivity loss gave a worth of 345.0 Ih. The method of using subcritical multiplication count rates gave a worth of 347.5 ± 10 Ih. These measurements were made by stepwise withdrawal of the simulated subassembly and replacement with low-density aluminum to represent sodium. Reactivity measurements were made for each step.

Fuel Subassemblies at the Core Edge. The worths of fuel subassemblies at the edge of the core were measured. The subassembly mockup in V,W-13,-14 represents the last fuel subassembly to be added to the 91-subassembly array. The other two mockups in H,I-15,-16,-17 and V,W-19,-20 represent two fuel subassemblies in the row of interchangeable blanket subassemblies surrounding the core. A comparison between the mocked-up and Fermi blanket subassembly is shown on a per-inch basis in Table XXIX. Table XXX shows the results of the substitutions.

Figure 68 shows the portions of drawers H,I-15,-16,-17 which contained the subassembly mockup. Figure 69 shows the portions of drawers V,W-13,-14 and V,W-19,-20 which contained the mockup. The core materials were distributed in a manner similar to that used in the central fuel subassembly.

Table XXX

WORTH OF FERMI FUEL VS. RADIAL BLANKET SUBASSEMBLIES AS MOCKED UP IN ZPR-III

Location	Average Radius (in.)	Worth (Ih)
V,W-13,-14 (C)	14.50	125.2
V,W-19,-20 (B)	15.70	98.1
H,I-15,-16,-17 (D)	16.16	90.4

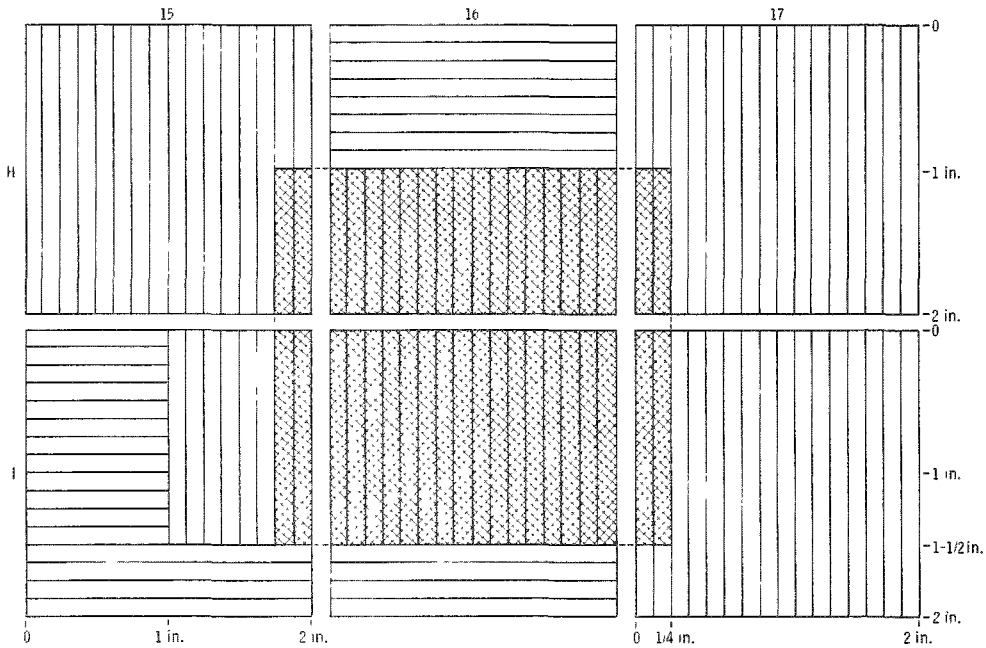

Fig. 68. Core-Edge Subassembly Mockup in ZPR-III (H,I-15,-16,-17)

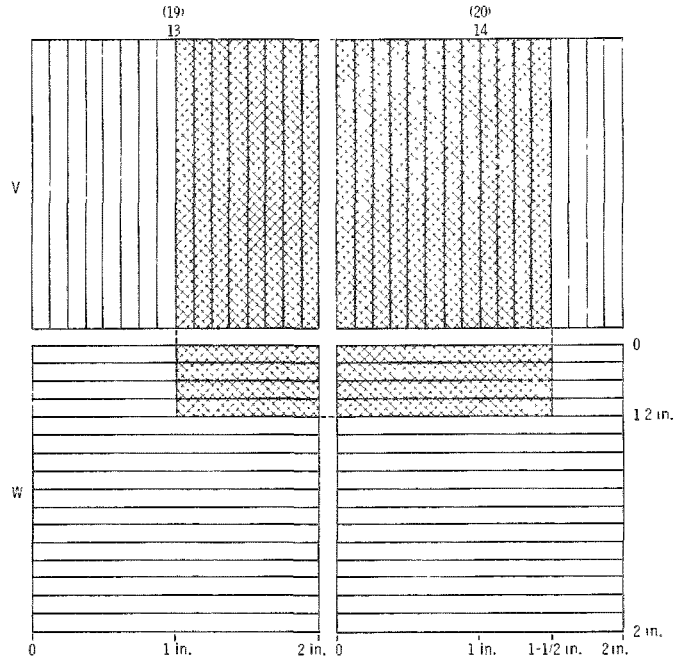

Fig. 69.

Core-Edge Subassembly Mockup in ZPR-III (V, W-13,-14 and V,W-19,-20)

J. Fermi Control and Safety Rod Worths

The purpose of this series of experiments was to determine the B^{10} enrichment necessary to provide a reactivity effect of 0.00316 $\Delta k/k$, or 46 cents (142.6 Ih), in each of the two central shim-control rods and 0.00687 $\Delta k/k$, or \$1.00 (310 Ih), in each of the eight outer safety rods. In addition to determining the enrichment necessary for an individual rod, it was necessary to investigate the shadow or coupling effects of one shim-control rod on the other, as well as the shadow effects between adjacent safety rods with the shim-control rods in place. The detailed engineering designs and the ZPR-III mockups of both the shim-control and safety rods are shown in Figs. 72 through 75.

The experiments consisted, first, of locating both identical boron carbide shim-control rods in their respective channels in the fully withdrawn position at the core-end blanket interface, and then stepping first one rod and then the other rod into the core. This provided the uncoupled worth of the first rod and the shadowed or coupled worth of the second. The worth of each rod was then just half the total of these two measurements. The effect of a change in the B^{10} enrichment was also measured. The reactivity measurements were made by means of supercritical period determinations accompanied by the addition or removal of distributed seeded drawers to remain within the operating reactivity range of the critical assembly.

The shim-control rods were both withdrawn to the Fermi nominal operating position (extending from 7 to 17 in. from the interface in Half No. 1) and remained in this position throughout the measurements of safety rod worth. The measurements of safety rod worth were conducted by stepwise insertion of one of the safety rods to obtain the uncoupled worth. A second rod was then inserted, twice removed from the first rod, to obtain its uncoupled worth. Shadowing or coupling between alternate rods was assumed to be negligible. A third rod was inserted between the first two to obtain the coupled worth. The first and second rods were then covered on either side by the appropriate fully inserted safety rods and the coupled worth of each was obtained in two separate series of stepwise withdrawals. As the coupling effect between the individual rods increased, the B^{10} enrichment of the rods was increased to retain the total desired negative reactivity in the rods by replacing the small ($\frac{1}{4} \times \frac{1}{2} \times 2$-in.) pieces of natural boron carbide with identical pieces of 90%-enriched B^{10} carbide. The effect of these incremental enrichments are noted to facilitate the final adjustment of the B^{10} enrichment in the Fermi reactor safety rods.

Shim-Control Rods. For the purposes of this set of experiments, the rod channels in the Fermi engineering core mockup were relocated as shown in Fig. 70 to obtain better correspondence between the engineering design and the ZPR-III mockup. This also allowed accurate positioning of

the boron carbide with respect to the engineering design. Figure 71 shows a cross section of the loading for a typical sodium-filled rod channel. Figures 72 and 73 show the detailed loadings for a typical position of the shim-control rod mockup. Weights and volume per cent compositions are given in Table XXXI. For reference, the rod position is indicated by the distance between the forward end of the rod ($\frac{1}{4}$-in. stainless steel) and the assembly interface which, for this case, was $\frac{1}{4}$-in. below the Fermi core midplane. Positive numbers indicate the position in Half No. 1 (upper portion of core, 15.5 in.) and negative numbers indicate the position in Half No. 2 (lower portion of core, 15.0 in.).

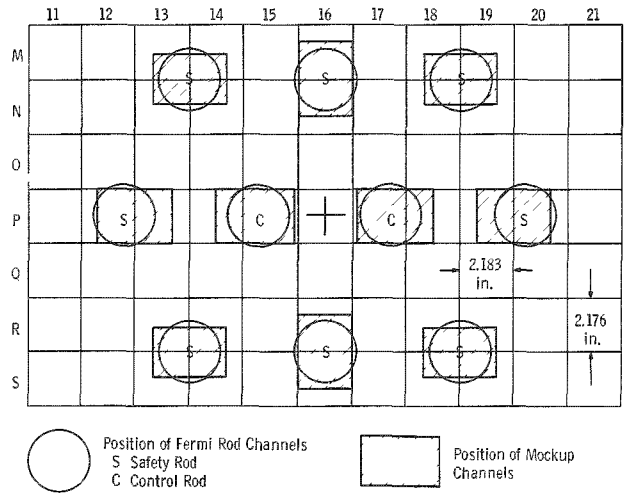

Fig. 70

Mockup of Fermi Rod Channels in ZPR-III for Rod Worth Measurements

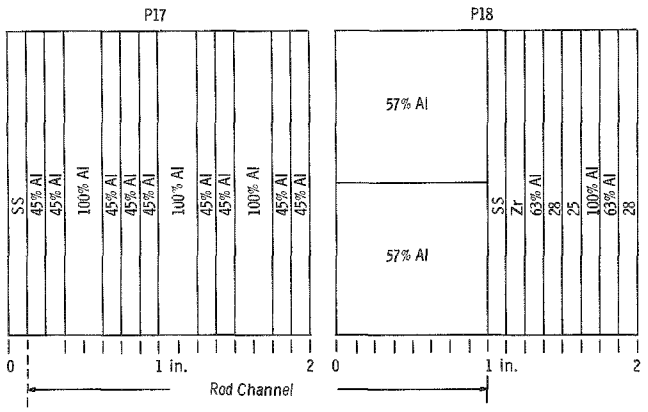

Fig. 71. Cross Section of Mockup Sodium-filled Rod Channel

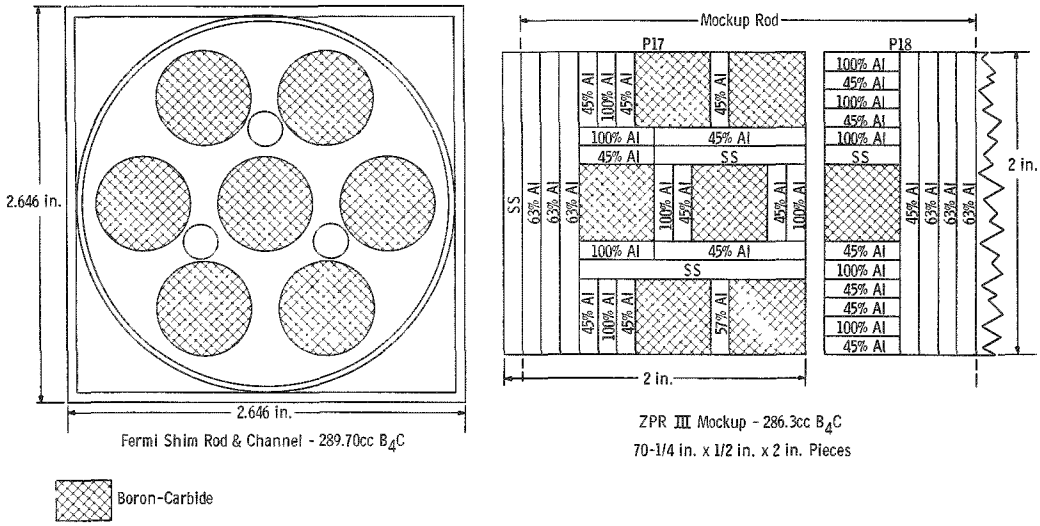

Fig. 72. Comparison of Cross Sections of Fermi and ZPR-III Mockup Shim Rods

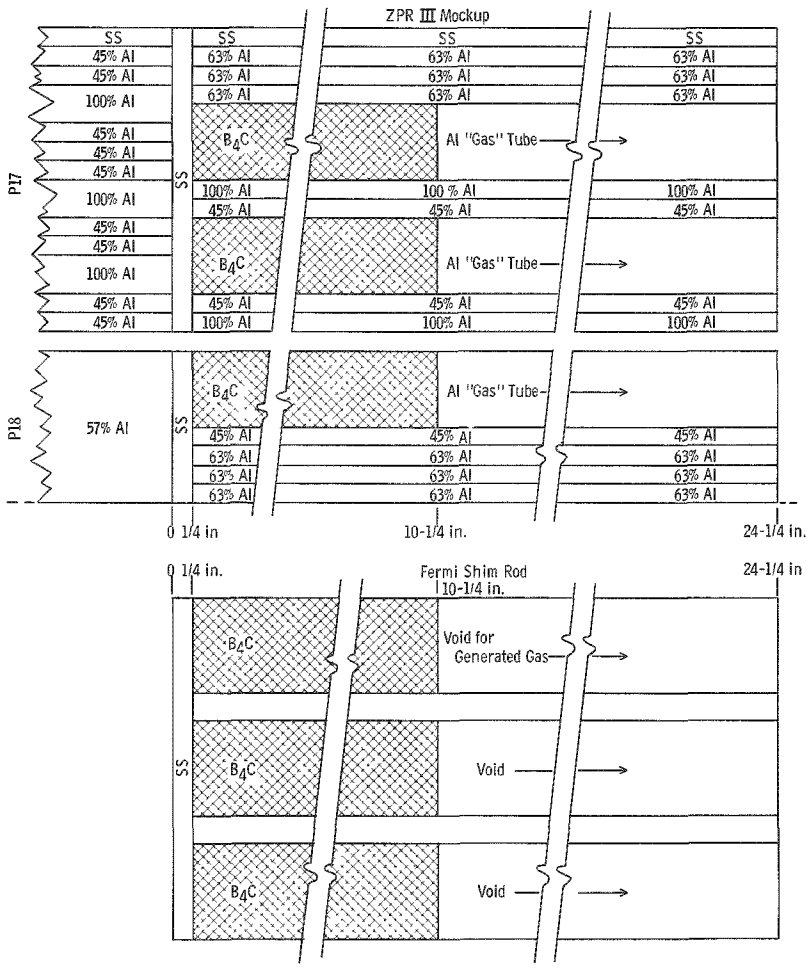

Fig. 73. Axial Cross Sections of Fermi and ZPR-III Mockup Shim Rods

Table XXXI

WEIGHTS AND VOLUME PER CENT COMPOSITION OF MOCKUP SHIM-CONTROL RODS IN ZPR-III

		B_4C[1]		Al		SS[2]	
	Vol (cc)	Wt(g)	v/o	Wt(g)	v/o	Wt(g)	v/o
10-in. Poison Section	1120.9	620.8	22.2	968.8	32.0	466.1	5.3
14-in. Gas Void Section	1569.2	-	-	1662.0	39.2	652.5	5.3

(1) Natural Boron Carbide

(2) Does not include stainless steel in drawer and matrix tube.

It should be noted that the 10.0-in. boron carbide section is followed by a 14-in. mockup gas-void section formed by loading hollow $\frac{1}{2}$ x $\frac{1}{2}$-in.-cross section aluminum tubes (3.12 g/in.) in the same geometry as the boron carbide. The weights, composition, and dimensions of the boron carbide pieces utilized in the loading are given in Table XXXII.

Table XXXII

WEIGHTS, COMPOSITIONS,* AND DIMENSIONS OF BORON CARBIDE PIECES UTILIZED FOR MOCKUP RODS

	Natural	Enriched		Natural	Enriched
B^{10} (a/o)	19.2	90.7	SiO_2 (w/o)	0.04	0.36
$\frac{1}{4}$ x $\frac{1}{2}$ x 2-in. (g B_4C)	8.87	8.01	Fe	0.20	0.24
$\frac{1}{4}$ x $\frac{1}{2}$ x 3-in. (g B_4C)	13.15	12.41	Al	0.13	$\leq$ 0.50
Boron (w/o)	76.98	69.34	Ni	$\leq$ 0.10	$\leq$ 0.10
Carbon	22.56	27.68	Cr	$\leq$ 0.50	0.38

*Letter, F. B. Huke, Norton Company to R. A. Wood, Power Reactor Development Company, dated October 12, 1959.

The following summarizes and tabulates the experimental data:

A total of 70 $\frac{1}{4}$ x $\frac{1}{2}$ x 2-in. pieces of boron carbide were loaded in each rod mockup.

Each rod mockup contained 5 pieces B^{10}-enriched B_4C and 65 pieces natural B_4C.

First rod inserted from infinity to $16\frac{3}{4}$-in. in Half No. 1 (17 in. from interface to front of $\frac{1}{4}$-in. stainless steel). = -12 Ih

Second rod inserted at $16\frac{3}{4}$-in. = - 9 Ih

The 5 B^{10}-enriched B_4C pieces in each rod removed and replaced with natural B_4C. = +2.9 Ih

1. Uncoupled Worth of Shim-Control Rod in P-14,-15

Natural B_4C mockup rod in P-14,-15 inserted stepwise with natural B_4C mockup rod in P-17,-18 remaining at $16\frac{3}{4}$ in.:

Rod Position (in.)	B_4C Position (in.)	ΔIh	Total Ih
$16\frac{3}{4}$	17	0	0
$14\frac{3}{4}$	15	-4.0	-4.0
$12\frac{3}{4}$	13	-8.2	-12.2
$10\frac{3}{4}$	11	-12.4	-24.6
$8\frac{3}{4}$	9	-17.3	-41.9
$4\frac{3}{4}$	5	-25.8	-84.9
$2\frac{3}{4}$	3	-24.3	-109.2
$\frac{3}{4}$	1	-22.3	-131.5
$-2\frac{1}{4}$	-2	-21.5	-153.0
$-4\frac{1}{4}$	-4	-6.8	-159.8
$-6\frac{1}{4}$	-6	+0.5	-159.3

2. Coupled Worth of Shim-Control Rod in P-17,-18

Natural B_4C mockup rod in P-17,-18 inserted stepwise with first natural B_4C mockup rod in P-14,-15 at $-5\frac{1}{4}$ in. (B_4C 5 in. either side of assembly interface):

Rod Position (in.)	B_4C Position (in.)	ΔIh	Total Ih
$16\frac{3}{4}$	17	0	0
$12\frac{3}{4}$	13	-12.8	-12.8
$8\frac{3}{4}$	9	-28.7	-41.5

Rod Position (in.)	B_4C Position (in.)	ΔIh	Total Ih
$6\frac{3}{4}$	7	-20.2	-61.7
$4\frac{3}{4}$	5	-22.6	-84.3
$2\frac{3}{4}$	3	-23.6	-107.9
$\frac{3}{4}$	1	-20.1	-128.0
$-2\frac{1}{4}$	-2	-20.1	-148.1
$-5\frac{1}{4}$	-5	-4.4	-152.5

Average coupled worth of natural B_4C rod from $16\frac{3}{4}$ in. to $-5\frac{1}{4}$ in. interpolating worth of rod in P-14,-15 = -156.3 Ih

Replaced 5 $\frac{1}{4} \times \frac{1}{2}$ x 2-in. pieces of natural B_4C along 10-in. length of mockup rod in P-14,-15 with equal volume of enriched B_4C. Both rods at $-5\frac{1}{4}$ in. = -26.7 Ih
or -5.34 Ih/piece

As above for mockup rod in P-17,-18 with enriched B_4C in P-14,-15 = -27.3 Ih
or -5.46 Ih/piece

Average value for replacing natural B_4C with enriched B_4C in both rods at fully inserted position. = -5.40 Ih/piece

Safety Rods. The locations of the mockup safety rod channels utilized in these measurements may be seen by referring to Fig. 70. Figures 74 through 77 illustrate the manner in which the mocked-up safety rods were loaded to simulate the design dimensions and compositions. The composition (in v/o) over the various mocked-up safety rods remained constant with variations only in the B^{10} enrichment and the material distribution over the various matrix channels necessary to obtain the correct geometry. The weights and compositions (in v/o) for a mocked-up safety rod are listed in Table XXXIII.

A particular point in question in this series was a possible positive reactivity effect of the hollow stainless steel ram at the forward end of the safety rod upon initial insertion of the rod into the core. This region of insertion was investigated in detail. A small positive effect, 1.7 Ih, was observed for the safety rod containing natural boron carbide. However, this was not seen in subsequent measurements using enriched B^{10} carbide.

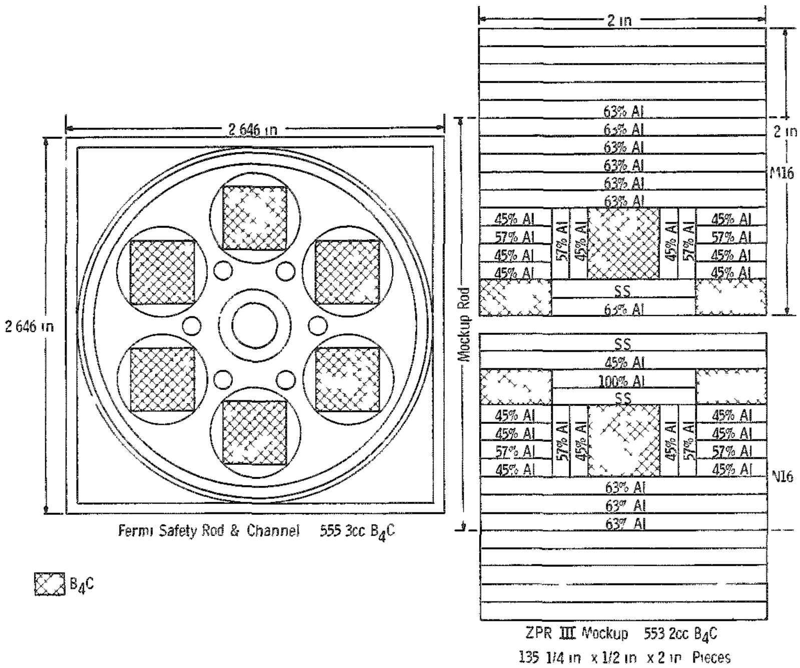

Fig. 74

Comparison of Cross Sections of Fermi and ZPR-III Mockup Safety Rods (M,N-16)

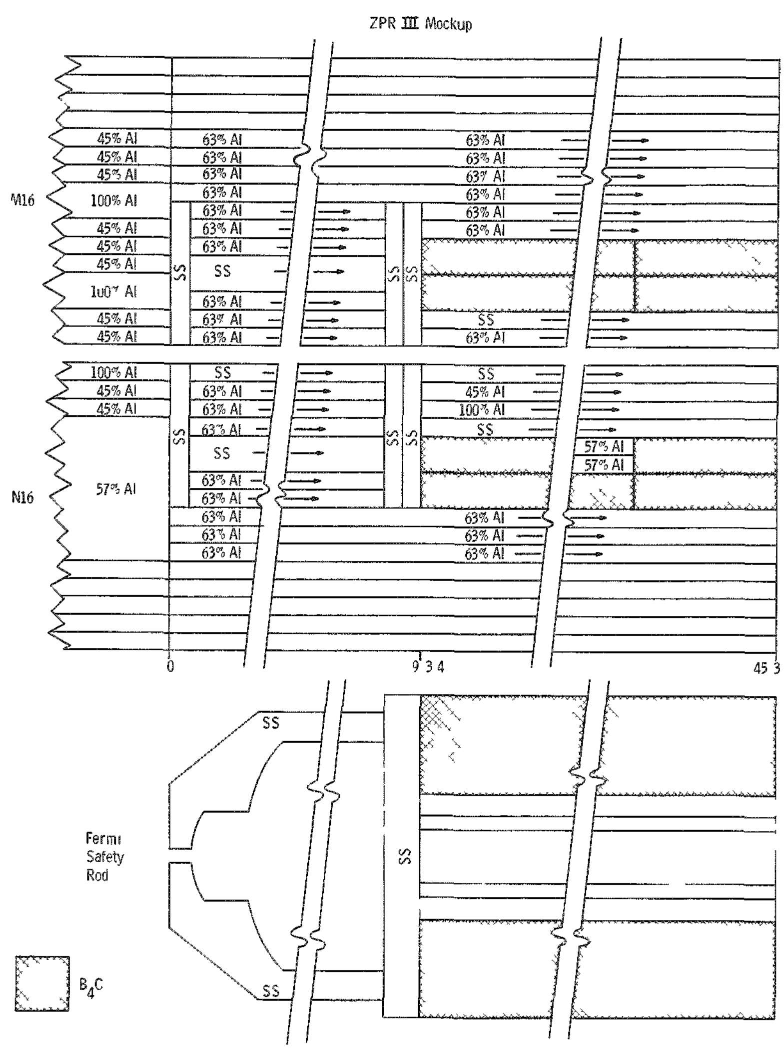

Fig. 75

Axial Cross Sections of Fermi and ZPR-III Mockup Safety Rods (M,N-16)

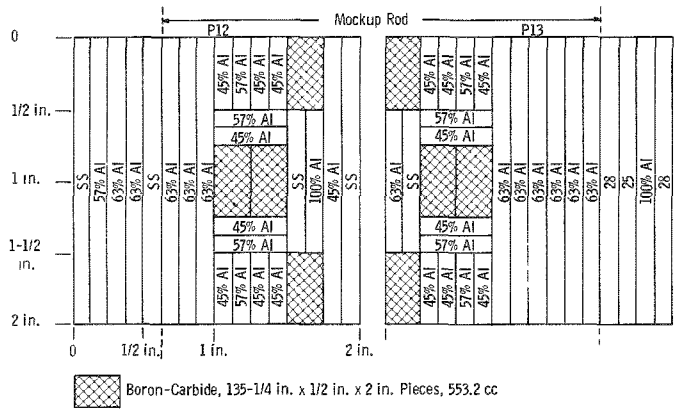

Fig. 76

Cross Section of ZPR-III Mockup Safety Rod (P-12,-13)

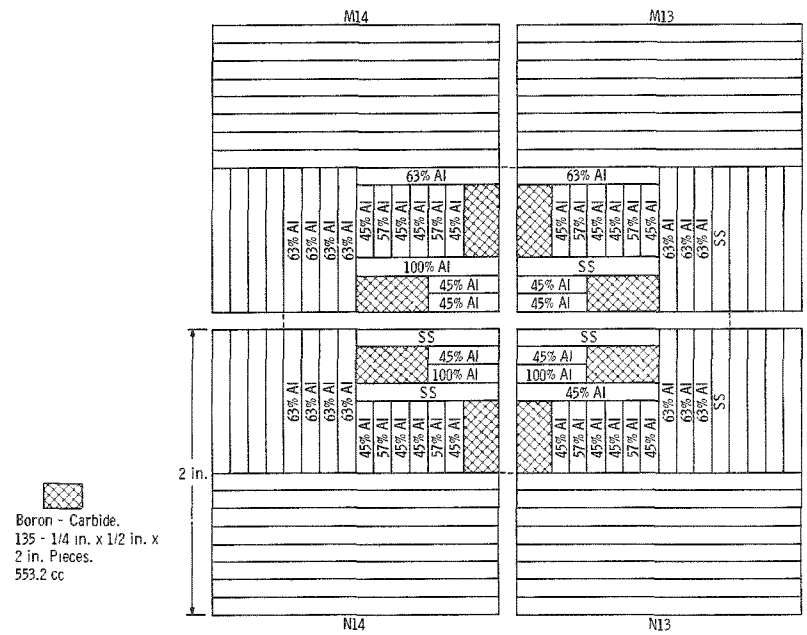

Fig. 77

Cross Section of ZPR-III Mockup Safety Rod (M,N-13,-14)

Table XXXIII

WEIGHTS AND VOLUME PER CENT COMPOSITION OF MOCKUP SAFETY RODS IN ZPR-III

		B_4C[1]		Al		SS[2]	
	Vol (cc)	Wt(g)	v/o	Wt(g)	v/o	Wt(g)	v/o
Safety Rod Ram							
0 - $\frac{1}{4}$ in.	28.0	-	-	11.9	15.7	128.4	58.4
$\frac{1}{4}$ - $9\frac{1}{4}$ in.	1008.8	-	-	1096.7	40.3	1435.6	18.1
$9\frac{1}{4}$ - $9\frac{3}{4}$ in.	56.0	-	-	23.7	15.7	256.8	58.4
36-in. Poison Section	4035.1	1197.2	11.9	3806.6	34.9	2240.4	7.1

(1) Natural Boron Carbide

(2) Does not include stainless steel in drawer and matrix tube.

The reference for the safety rod position was again chosen at the assembly interface with distances measured to the front of the ram and to the front of the B_4C as indicated. The safety rods are normally fully withdrawn from the upper axial end blanket (Half No. 1) during operation of the Fermi reactor. Only that portion of the boron carbide residing within the core and end blanket was mocked up during the stepwise insertions.

The following summarizes and tabulates the experimental data:

1. Uncoupled Worth of Safety Rod in M,N-16

When fully inserted, this rod contains 135 $\frac{1}{4}$ x $\frac{1}{2}$ x 2-in. pieces of boron carbide along 36-in. length.

Both natural B_4C shim-control rods positioned at nominal operating position ($6\frac{3}{4}$ in. from interface).

Safety rod initially consists entirely of natural B_4C.

Ram Position (in.)	B_4C Position (in.)	Length of B_4C (in)	ΔIh	Total Ih
$21\frac{1}{2}$	-	0	0	0
$17\frac{1}{4}$	$27\frac{1}{4}$	4	0	0
$13\frac{1}{4}$	$23\frac{1}{4}$	8	+1.7	+1.7
$9\frac{1}{4}$	19	12	-1.7	0
$5\frac{1}{4}$	15	16	-5.7	-5.7
$1\frac{1}{4}$	11	20	-12.7	-18.4
$-2\frac{3}{4}$	7	24	-21.9	-40.3
$-6\frac{3}{4}$	3	28	-30.2	-70.5
$-9\frac{3}{4}$	0	31	-24.9	-95.4
$-12\frac{3}{4}$	-3	34	-24.0	-119.4
$-16\frac{3}{4}$	-7	36	-27.6	-147.0
$-20\frac{3}{4}$	-11	36	-19.0	-166.0
$-27\frac{3}{4}$	-18	36	-11.2	-177.2

Replaced natural B_4C with B^{10} enriched B_4C in fully inserted rod in M,N-16:

	ΔIh	Ih/piece
9 $\frac{1}{4}$ x $\frac{1}{2}$ x 2-in. pieces in last 6 in. on either end of rod (12 in. to 18 in. from interface).	-12.4	-1.388
6 $\frac{1}{4}$ x $\frac{1}{2}$ x 2-in. pieces (8 to 12 in.)	-26.9	-4.485

	ΔIh	Ih/piece
6 $\frac{1}{4}$ x $\frac{1}{2}$ x 2-in. pieces (4 to 8 in.)	-27.5	-4.583
3 $\frac{1}{4}$ x $\frac{1}{2}$ x 2-in. pieces (2 to 4 in.)	-16.2	-5.40
3 $\frac{1}{4}$ x $\frac{1}{2}$ x 2-in. pieces (0 to 2 in.)	-15.9	-5.30
9 $\frac{1}{4}$ x $\frac{1}{2}$ x 2-in. pieces uniformly distributed over 36-in. length of rod	-28.7	-3.19

Total uncoupled worth of enriched mockup safety rod in M,N-16:

36 $\frac{1}{4}$ x $\frac{1}{2}$ x 2-in. pieces $B_4^{10}C$
99 $\frac{1}{4}$ x $\frac{1}{2}$ x 2-in. pieces B_4C } = -304.8 Ih

2. Uncoupled Worth of Safety Rod in P-12,-13

Above enriched safety rod fully inserted in M,N-16.

Both natural B_4C shim-control rods in nominal operating position ($6\frac{3}{4}$ in. from interface).

Final enrichment of previous rod used for this insertion at P-12,-13:

36 $\frac{1}{4}$ x $\frac{1}{2}$ x 2-in. pieces $B_4^{10}C$

99 $\frac{1}{4}$ x $\frac{1}{2}$ x 2-in. pieces B_4C

Ram Position (in.)	B_4C Position (in.)	Length of B_4C (in.)	ΔIh	Total Ih
+21 $\frac{1}{2}$	-	-	0	0
+ $\frac{1}{4}$	10	21	-32 6	-32.6
-2 $\frac{3}{4}$	7	24	-22.2	-54.8
-6 $\frac{3}{4}$	3	28	-39.8	-94.6
-8 $\frac{3}{4}$	1	30	-22.6	-117.2
-13 $\frac{3}{4}$	-4	35	-52.6	-169.8
-17 $\frac{3}{4}$	-8	36	-33.4	-203.2
-27 $\frac{3}{4}$	-18	36	-27.6	-230.8

Replaced natural B_4C with B^{10} enriched B_4C in fully inserted rod in P-12,-13:

	Δ Ih	Ih/piece
12 $\frac{1}{4}$ x $\frac{1}{2}$ x 2-in. pieces 0 to 18 in. in Half No. 2	-31.0	-2.58
13 $\frac{1}{4}$ x $\frac{1}{2}$ x 2-in. pieces 0 to 18 in. in Half No. 1	-30.2	-2.32

Total uncoupled worth of safety rod in P-12,-13:

60 $\frac{1}{4}$ x $\frac{1}{2}$ x 2-in. pieces $B_4^{10}C$
75 $\frac{1}{4}$ x $\frac{1}{2}$ x 2-in. pieces B_4C
} = -291.9 Ih.

3. Coupled Worth of Safety Rod in M,N-13,-14

The two rods (P-12,-13 and M,N-16) adjacent to this position fully inserted with above final enrichment.

Both natural B_4C shim-control rods at nominal operating position ($6\frac{3}{4}$ in. from interface).

Final enrichment of preceding rod used here:

60 $\frac{1}{4}$ x $\frac{1}{2}$ x 2-in. pieces $B_4^{10}C$
75 $\frac{1}{4}$ x $\frac{1}{2}$ x 2-in. pieces B_4C

Ram Position (in.)	B_4C Position (in.)	Length of B_4C (in.)	Δ Ih	Total Ih
$21\frac{1}{2}$	-	0	0	0
$13\frac{1}{4}$	23	8	0	0
$1\frac{1}{4}$	11	20	-27.9	-27.9
$-2\frac{3}{4}$	7	24	-31.4	-59.3
$-6\frac{3}{4}$	3	28	-44.0	-103.3
$-11\frac{3}{4}$	-2	33	-60.6	-163.9
$-17\frac{3}{4}$	-8	36	-63.5	-227.4
$-27\frac{3}{4}$	-18	36	-38.8	-226.2

Replaced natural B_4C with B^{10} enriched B_4C in fully inserted rod in M,N-13,-14.

	ΔIh	Ih/piece
13 $\frac{1}{4}$ x $\frac{1}{2}$ x 2-in. pieces of $B_4^{10}C$		
0 to 18 in. in Half No. 1	-26.7	-2.05
11 $\frac{1}{4}$ x $\frac{1}{2}$ x 2-in. pieces of $B_4^{10}C$		
0 to 18 in. in Half No. 2	-23.0	-2.09

Total coupled worth of safety rod in M,N-13,-14

84 $\frac{1}{4}$ x $\frac{1}{2}$ x 2-in. pieces $B_4^{10}C$
51 $\frac{1}{4}$ x $\frac{1}{2}$ x 2-in. pieces B_4C } = -315.8 Ih

4. Coupled Worth of Safety Rod in M,N-16

The two adjacent safety rods, M,N-13,-14 and M,N-18,-19 fully inserted and each contain:

84 $\frac{1}{4}$ x $\frac{1}{2}$ x 2-in. pieces $B_4^{10}C$

51 $\frac{1}{4}$ x $\frac{1}{2}$ x 2-in. pieces B_4C

Both natural B_4C shim-control rods at nominal operating position ($6\frac{3}{4}$ in. from interface). M,N-16 initially fully inserted with:

36 $\frac{1}{4}$ x $\frac{1}{2}$ x 2-in. pieces $B_4^{10}C$

99 $\frac{1}{4}$ x $\frac{1}{2}$ x 2-in. pieces B_4C

Replaced natural B_4C with B^{10} enriched B_4C in fully inserted rod in M,N-16:

9 $\frac{1}{4}$ x $\frac{1}{2}$ x 2-in. pieces distributed uniformly along rod = -23.8 Ih
or -2.65 Ih/piece

For stepwise withdrawal, rod now contains:

45 $\frac{1}{4}$ x $\frac{1}{2}$ x 2-in. pieces $B_4^{10}C$

90 $\frac{1}{4}$ x $\frac{1}{2}$ x 2-in. pieces B_4C

Rod Position (in.)	B_4C Position (in.)	Length of B_4C (in.)	Δ Ih	Total Ih
$-27\frac{3}{4}$	-18	36	0	0
$-19\frac{3}{4}$	-10	36	22.1	22.1
$-15\frac{3}{4}$	-6	36	32.9	55.0
$-11\frac{3}{4}$	-2	33	45.5	100.5
$-6\frac{3}{4}$	+3	28	63.0	163.5
$-2\frac{3}{4}$	+7	24	43.4	206.9
$+1\frac{1}{4}$	+11	20	34.2	241.1
$+21\frac{1}{2}$	-	0	29.8	270.9

Total coupled worth of safety rod in M,N-16:

$$\left.\begin{array}{l} 45\ \frac{1}{4} \times \frac{1}{2} \times 2\text{-in. pieces } B_4^{10}C \\ 90\ \frac{1}{4} \times \frac{1}{2} \times 2\text{-in. pieces } B_4C \end{array}\right\} = -270.9 \text{ Ih}$$

5. Coupled Worth of Safety Rod in P-12,-13

The two adjacent safety rods M,N-13,-14 and R,S-13,-14 fully inserted and each contain:

$84\ \frac{1}{4} \times \frac{1}{2} \times 2$-in. pieces $B_4^{10}C$

$51\ \frac{1}{4} \times \frac{1}{2} \times 2$-in. pieces B_4C

Both natural B_4C shim-control rods at nominal operation position ($6\ \frac{3}{4}$ in. from interface). P-12,-13 initially fully inserted with:

$60\ \frac{1}{4} \times \frac{1}{2} \times 2$-in. pieces $B_4^{10}C$

$75\ \frac{1}{4} \times \frac{1}{2} \times 2$-in. pieces B_4C

Replaced natural B_4C with B^{10} enriched B_4C in fully inserted rod in P-12,-13:

$24\ \frac{1}{4} \times \frac{1}{2} \times 2$-in. pieces $B_4^{10}C$ distributed uniformly along rod = -45.7 Ih

or -1.905 Ih/piece

For stepwise withdrawal, rod now contains:

84 $\frac{1}{4}$ x $\frac{1}{2}$ x 2-in. pieces $B_4^{10}C$

51 $\frac{1}{4}$ x $\frac{1}{2}$ x 2-in. pieces B_4C

Rod Position (in.)	B_4C Position (in.)	Length of B_4C (in.)	ΔIh	Total Ih
-27$\frac{3}{4}$	-18	36	0	0
-19$\frac{3}{4}$	-10	36	+19.7	+19.7
-15$\frac{3}{4}$	-6	36	34.4	54.1
-11$\frac{3}{4}$	-2	33	49.5	103.6
-6$\frac{3}{4}$	+3	28	67.1	170.7
-2$\frac{3}{4}$	+7	24	50.1	220.8
+1$\frac{1}{4}$	+11	20	36.1	256.9
+21$\frac{1}{2}$	-	0	31.4	288.3

Total coupled worth of safety rod in P-12,-13:

84 $\frac{1}{4}$ x $\frac{1}{2}$ x 2-in. pieces $B_4^{10}C$
51 $\frac{1}{4}$ x $\frac{1}{2}$ x 2-in. pieces B_4C
} = - 288.3 Ih

VII. OSCILLATOR ROD REACTIVITY WAVE SHAPE AND TOTAL WORTH

A. Rotating Poison Rod

An eccentric B^{10} carbide oscillator rod was fabricated to simulate the dimensions and composition of the oscillator rod to be installed in the Fermi reactor. Figure 78 shows the cross section and dimensions of the oscillator rod mockup. Aluminum was used to simulate the sodium in the cooling channels of the actual rod. The enriched B^{10} carbide to be used in the operating rod in the Fermi reactor was supplied for this experiment. The oscillator rod mockup contained 468.6 g of B_4C (including impurities), 5.30 kg stainless steel, and 0.94 kg aluminum. The stainless steel jacket weighed 1.67 kg. An analysis of the boron carbide is given in Table XXXIV.

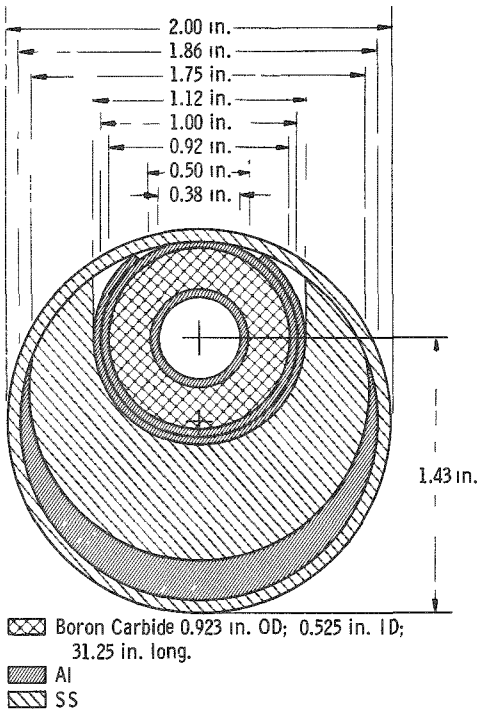

Fig. 78. Fermi Oscillator Rod Mockup

Table XXXIV

ANALYSIS* OF ENRICHED BORON CARBIDE FOR FERMI OSCILLATOR ROD

B^{10} (a/o)	92.0	Fe_2O_3(w o)	0.20
Boron (w/o)	61.66	Al_2O_3	1.34
Carbon	20.76	TiO_2	0.28
W	14.70	CaO	0.05
SiO_2	0.81	MgO	0.05

*Letter, F. B. Huke, Norton Co. to R. A. Wood, Power Reactor Development Co., dated June 15, 1959.

The objectives of the experiment in ZPR-III were:

1. to determine the reactivity effect of the oscillator rod versus sodium in an outer safety rod channel (P-12,-13 or P-19,-20); and

2. to determine the wave shape and peak-to-peak worth of this rod at the position of the safety rod channel in the Fermi core.

Unfortunately, the late delivery of the boron carbide at ZPR-III prevented the inclusion of this experiment in the Fermi engineering-core mockup. Consequently, to better simulate the engineering core conditions in a subsequent repeat of the clean-core assembly, the shim-control channels were mocked up in P-14,-15 and P-17,-18, together with the two natural boron carbide shim-control rods at the nominal operating position, i.e., extending from 7 to 17 in. from the interface in Half No. 1. The wave shape and peak-to-peak worth of the full oscillator rod were

also obtained with the mocked-up shim-control rods fully inserted. The safety rod channel was mocked up initially in P-13 (6.55-in. average radius) and subsequently in P-12 (8.73-in. average radius) to bracket the 8.08-in. radial dimension of the Fermi safety rod channel. This channel mockup (2 x 2 in.) contained 50.56 v/o aluminum, or 106.22 g Al per axial in. of channel, to simulate sodium. The remaining safety channels were not mocked up. The total worth of the oscillator rod versus the aluminum-filled channel was found to be -206.8 Ih in P-12 and -260.5 Ih in P-13 with the 2 shim-control rods at the nominal operating position.

The wave shape and peak-to-peak worth of the oscillator rod was determined by statically positioning the rod with a remotely controlled drive motor and noting the period of the reactor. The angular position of the rod with reference to an arbitrary zero was indicated by a selsyn motor-generator hookup. The position accuracy of the selsyn indicator is estimated to be within ±1 degree and the error of the reactivity measurement to be within ±0.2 Ih.

The data obtained for the oscillator rod in channel P-12 are given in Table XXXV and plotted in Fig. 79. Table XXXVI lists the data resulting from the measurements in P-13. These data are plotted in Fig. 80. All measurements are summarized in Table XXXVII.

Table XXXV

FULLY LOADED OSCILLATOR ROD IN P-12

A. Shim-control rods at 7-17 in. from assembly interface in Half No. 1		B. Shim-control rods 5 in. either side of assembly interface	
Angular Position (degrees)	Δk/k (Ih)	Angular Position (degrees)	Δk/k (Ih)
104.0	39.4	150.0	38.1
150.0	36.2	193.5	30.5
196.0	28.7	240.0	22.8
240.5	20.5	284.0	19.5
288.5	17.1	330.0	22.4
331.5	20.4	12.5	29.7
13.5	27.9	59.0	37.4
60.5	36.1	105.5	40.6
105.5	39.7	148.5	38.1
151.0	36.6	239.0	22.9
197.0	28.3		

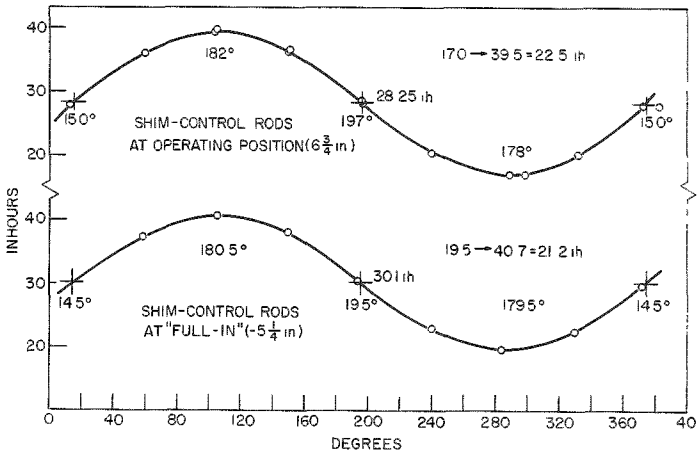

Fig. 79

Wave Shape of Full Oscillator Rod in P-12

Table XXXVI

FULLY LOADED OSCILLATOR ROD IN P-13

A. Shim-control rods at 7-17 in. from assembly interface in Half No. 1

Angular Position (degrees)	Δk/k (Ih)
114.0	38.8
152.0	35.8
199.5	29.6
246.5	24.1
288.5	22.3
336.5	25.9
21.0	32.3
64.0	37.2
109.0	39.3
155.5	36.0

B. Shim-control rods 5 in. either side of assembly interface

Angular Position (degrees)	Δk/k (Ih)
110.5	30.2
152.0	27.7
198.5	22.4
246.5	16.8
291.0	15.5
335.5	18.8
17.0	24.1
62.5	29.0
112.5	30.6
155.0	28.7

Fig. 80

Wave Shape of Full Oscillator Rod in P-13

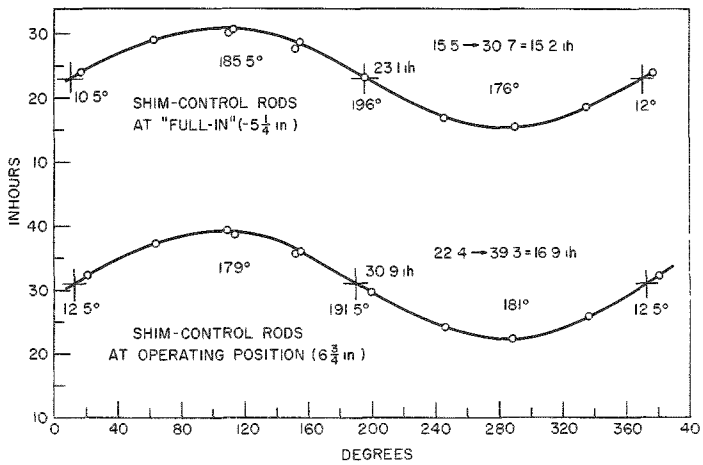

Table XXXVII

PEAK-TO-PEAK WORTH OF FULL OSCILLATOR ROD

Full Oscillator Rod at:	$\Delta k/k$ (Ih) (Shims at Operating Position)	$\Delta k/k$ (Ih) (Shims Full-In)
P-12 (8.73 in.)	22.5	21.2
P-13 (6.55 in.)	16.9	15.2
Design Location (8.08 in.)	~20.8	~19.4

An additional measurement of rod worth and wave shape was made with a reduced length of B^{10} carbide. This was done by removing approximately $9\frac{1}{4}$ in. of B^{10} carbide from either end of the $31\frac{1}{4}$ in. rod, leaving $12\frac{3}{4}$ in. of B^{10} carbide centered about the midplane of the core. This produced a peak-to-peak worth of 10.0 Ih in P-13 and 12.8 Ih in P-12. Both measurements were made with the shim-control rods in the nominal operating position only, (7-17 in. in Half No. 1). This would indicate a worth of 12.0 Ih at the design position for this length of 90% enriched B^{10} carbide. The detailed wave-shape data for this partial rod are given in Table XXXVIII and plotted in Fig. 81.

Table XXXVIII

PARTIAL OSCILLATOR ROD IN P-12
(Shim-control rods at 7-17 in. from assembly interface in Half No. 1)

Angular Position (degrees)	$\Delta k/k$ (Ih)	Angular Position (degrees)	$\Delta k/k$ (Ih)
108.5	39.9	338.0	28.5
151.0	38.7	24.0	33.5
202.0	33.7	68.5	37.7
244.5	29.3	108.0	39.5
288.0	27.3	243.0	28.5

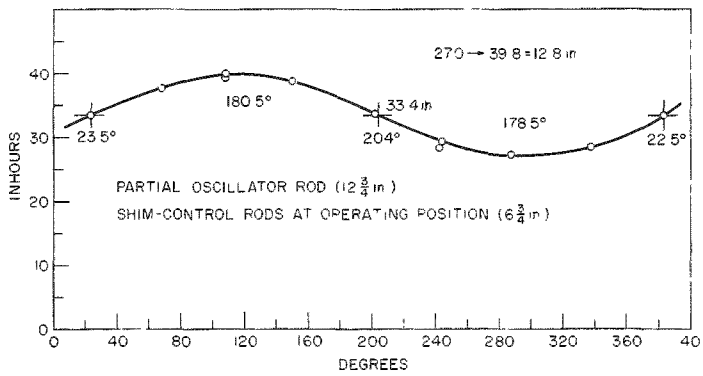

Fig. 81

Wave Shape of Partially Loaded Oscillator Rod in P-12

B. Streaming Oscillator Rod

The possibility of utilizing a neutron-streaming-type oscillator rod was suggested by APDA.(6) This oscillator rod would be constructed somewhat like a semicircular variable electrical condenser which would vary neutron leakage or streaming by alternately opening and meshing the plates. This mechanism was simulated by first emptying that portion ($\frac{2}{3}$) of the mocked-up safety channels which occurred in R-14, thus providing a through-hole or void in this channel in both the core and end blankets. It was believed that this position would give the maximum difference in streaming worth and be equivalent to the safety rod channel nearest to the core center occurring at R,S-16.

The open position of the mechanism was simulated by loading the 21-in. core drawer in each half with 2 x 2 x $\frac{1}{4}$-in. pieces of stainless steel loaded transversely and spaced $\frac{1}{4}$-in. apart by means of two 2 x $\frac{1}{2}$ x $\frac{1}{8}$-in., 45%-density aluminum pieces, as shown in Fig. 82. This represented the most reactive situation. The back drawers were omitted from each half in this channel, providing a 2-in.-square void channel on both ends of the 42-in. oscillator section. The least reactive or meshed position was simulated by reloading the same material in both drawers such that the stainless steel formed a solid axial section 1 x 2 in. in cross section along one side of the drawer. The aluminum spacers were loaded along the bottom $\frac{1}{2}$ in. of the remainder of the drawer. A cross section of this closed or meshed loading is also shown in Fig. 82. In this case, a continuous axial void with cross-sectional dimensions of 1 by 1.5 in. was produced through the core and both end blankets.

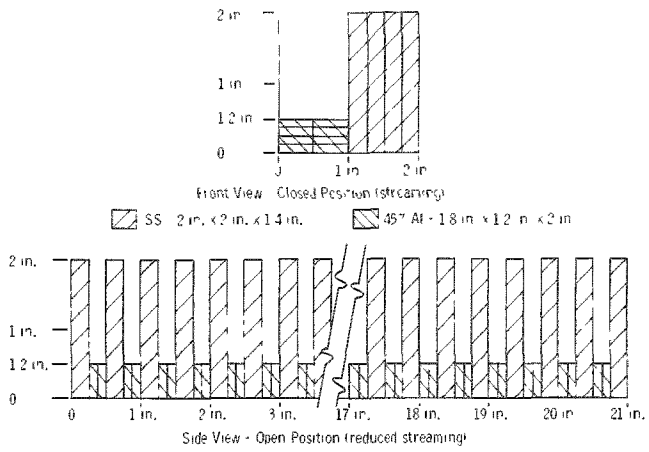

Fig. 82. Mockup Streaming Oscillator

The reactivity difference observed between the above two conditions for one matrix channel (R-14) was 6.6 Ih.

VIII. APPLICATION OF CRITICAL EXPERIMENT DATA

A. Clean-core Experiments

The clean-core critical studies of the Fermi Core A program have provided extensive data for the verification of analytical techniques for dilute fast reactor systems. The utilization of a homogenized cylindrical core and a uniform blanket composition provides a simplified geometry for analysis and was therefore used for the major portion of the Fermi Core A program. Typical applications of the data are as follows:

1. Verification of cross-section sets and analytical methods for critical-mass and flux-distribution calculations.
2. Application of distributed reactivity coefficient data to compensate for minor differences between the engineering-core loading in ZPR-III and the final Fermi Core A design.
3. Application of central reactivity coefficient data to evaluate regional versus perturbation-type calculations.
4. Application of the fuel-bunching measurements to evaluate the validity of using $\frac{1}{8}$-in.-thick plates of highly enriched and depleted uranium to represent a relatively homogeneous array of lower enrichment fuel.
5. Application of distributed reactivity coefficient data to obtain the parameters contributing to the net isothermal temperature coefficient.
6. The sodium-substitution test data provided additional information concerning the validity of an aluminum representation of sodium for fast critical studies. Test results also indicated the need for more extensive sodium loadings to define adequately the distributed and local density coefficients of sodium.

B. Engineering-core Experiments

The engineering-core critical studies of the Fermi Core A program were intended to provide data for specific characteristics of the final Fermi design and to investigate any major differences between the homogenized clean core and the geometrically detailed engineering core. The primary purpose of the engineering-core assembly was to obtain critical mass, i.e., fuel enrichment, and control rod worth, with the remaining portion of the engineering-core studies devoted to incidental effects. The analyses of both the clean-core and engineering-core critical studies have been reported in detail by others.[3,18,19,20] Typical design and operating characteristics obtained from the engineering core data are as follows:

1. Fuel enrichment required for criticality of the Fermi design core under operating conditions of temperature and burnup.
2. Boron-10 enrichment required in the control and safety rods to provide the desired reactivity control.
3. The worth of a design Fermi fuel subassembly at the core center and at various locations at the core edge.
4. The power distribution throughout the core and at the inner edge of the radial blanket where high-temperatures result from the reduced coolant flow of the blanket.
5. The fuel-expansion effect contributing to the net isothermal temperature coefficient was determined with the engineering-core assembly with the axial core-blanket end gap included.
6. The total and peak-to-peak worth of the enriched boron-10 carbide oscillator rod at its operating position.
7. The reactivity effect of neutron leakage through the sodium-filled flow channels in the axial end blankets.

IX. REFERENCES

1. AEC Contract AT(11-1)-476.

2. APDA-124, Enrico Fermi Atomic Power Plant, (Jan 1959).

3. Enrico Fermi Atomic Power Plant, Technical Information and Hazards Summary Report, Power Reactor Development Company, Vols. 1-6 (June 1961).

4. R. O. Brittan, B. Cerutti, H. V. Lichtenberger, J. K. Long, R. L. McVean, M. Novick, R. Rice, and F. W. Thalgott, Hazard Evaluation Report on the Fast Reactor Zero Power Experiment ZPR-III, ANL-6408 (Oct 1961).

5. B. C. Cerutti, H. V. Lichtenberger, D. Okrent, R. E. Rice, and F. W. Thalgott, ZPR-III, Argonne's Fast Critical Facility, Nuclear Sci. and Engineering, 1(2), 126-134 (1956).

6. J. K. Long, W. B. Loewenstein, C. E. Branyan, G. S. Brunson, F. S. Kirn, D. Okrent, R. E. Rice, and F. W. Thalgott, Fast Neutron Power Reactor Studies with ZPR-III, Proceedings of the Second United Nations International Conference on the Peaceful Uses of Atomic Energy, Geneva, Switzerland. 12, 119 (1958).

7. E. L. Alexanderson, The Critical Experiment for the Enrico Fermi Reactor, APDA Technical Memorandum No. 15 (June 16, 1958).

8. Specifications of Meltdown Configurations for ZPR-III, APDA Memorandum, R. B. Nicholson to W. J. McCarthy (Sept 21, 1959).

9. W. Gemmell, Studies of Two Fast Reactor Critical Assemblies Based on Meltdown Configurations, Trans. Am. Nuclear Soc., 3, 335 (Dec 1960).

10. Enrico Fermi Atomic Power Plant, Technical Information and Hazards Summary Report, Power Reactor Development Company, Vol. 7 (Sept 1961).

11. D. M. O'Shea, D. Okrent, and J. M. Chaumont, Some Calculations Pertaining to Fast Reactor Safety (Feb 1962).

12. F. S. Kirn, An Absolute Fission Counter, presented at the ANS Winter Meeting, Oct 28, 1957.

13. W. G. Davey and R. N. Curran, An Experimental Investigation of Some Sources of Error in the Measurement of Absolute Fission Ratios in Fast Reactors, ANL-6468 (Nov 1961).

14. W. Y. Kato, F. S. Kirn, and W. C. Redman, Measurement of the Conversion Ratio for a Fast Breeder Reactor, Published in "Reactor Operational Problems," Vol. II, page 196, Pergamon Press (1957).

15. W. C. Redman and J. H. Roberts, Some Current Techniques of Fast Neutron Spectrum Measurements, Proceedings of the Second United Nations International Conference on the Peaceful Uses of Atomic Energy, Geneva, Switzerland, 12, 72 (1958).

16. G. S. Brunson, F. S. Kirn and W. B. Loewenstein, Fission Ratios and Distributions in Fast Critical Assemblies, presented at the ANS Winter Meeting, Oct 28, 1957.

17. G. S. Brunson, R. Curran, S. G. Kaufmann, J. McMahon and L. Pahis, Measuring the Prompt Period of a Reactor, Nucleonics, 15, 132 (Nov 1957).

18. Fuel Enrichment, APDA Memorandum, E. L. Alexanderson to O. E. Homeister, December 9, 1958.

19. E. L. Alexanderson, E. Garelis, and J. B. Nims, Critical Experiment Calculations for the Enrico Fermi Reactor, presented at the ANS Winter Meeting, December 8-10, 1958.

20. E. Garelis, Fuel Enrichment for the Enrico Fermi Reactor, APDA-131, (May 12, 1959).

ACKNOWLEDGMENTS

The conduct of the critical studies program for Fermi Core A resulted from the cooperative efforts of many people. Major experiments in the program were planned and coordinated by Argonne National Laboratory and other assigned personnel under the direction of F. W. Thalgott. Portions of the program were conducted under the supervision of G. S. Brunson, F. S. Kirn, H. Lawroski, and R. A. Porter of the Idaho Division of ANL, D. T. Eggen of Atomics International, and R. L. McVean, who was assigned along with the author to the Idaho Division of ANL by the Atomic Power Development Associates, Inc. for this program. The requirements for the experimental program were originally established by E. L. Alexanderson of APDA in cooperation with ANL personnel, and were continuously reviewed and revised during the conduct of the program by APDA personnel under the direction of W. J. McCarthy.

The author is deeply indebted to J. K. Long for his critical review and comments on this report and to M. Novick and F. W. Thalgott who contributed to the timely and successful completion of this experimental program by their encouragement and splendid cooperation. Many others at both APDA and ANL contributed to this program through helpful discussions, technical assistance and the procurement of materials.